DESIGN AND CONSTRUCTION OF A FLOW SYSTEM FOR CONTROLLED BIOFILM GROWTH AND ELECTROCHEMICAL MONITORING

by

DAOYUAN YANG

(Under the Direction of José I. Reyes De Corcuera)

ABSTRACT

A flow system was built to monitor biofilm growth on the inner surface of stainless steel tubes in a wide range of time intervals with adjustable initial microbial populations. Biofilm formation was detected by total plate counting (TPC) and electrochemical impedance spectroscopy (EIS) methods. The system was tested using *Pseudomonas putida* biofilms. Bacteria suspensions were flowing through the system continuously and maintained at 5.1 +/- 0.3 log CFU/ml for the entire duration of the experiment period. Biofilm was detected after 16 h by TPC, while impedance started to decrease at 28 h when biofilm populations were greater than 2.3 $\times 10^5$ CFU/swab. The regression equation for the corrected Z_{real} (Z_{rc}) versus log biofilm colony counts (C, $5.2 < C < 7.0$) was $Z_{rc} = -23.3\ C + 100.9$ with $R^2 = 0.772$.

INDEX WORDS: Biofilm, Flow system, Electrochemical impedance spectroscopy

DESIGN AND CONSTRUCTION OF A FLOW SYSTEM FOR CONTROLLED BIOFILM GROWTH AND ELECTROCHEMICAL MONITORING

by

DAOYUAN YANG

B.E., Ocean University of China, China, 2013

A Thesis Submitted to the Graduate Faculty of The University of Georgia in Partial Fulfillment of the Requirements for the Degree

MASTER OF SCIENCE

ATHENS, GEORGIA

2015

DESIGN AND CONSTRUCTION OF A FLOW SYSTEM FOR CONTROLLED BIOFILM GROWTH AND ELECTROCHEMICAL MONITORING

by

DAOYUAN YANG

Major Professor:	José I. Reyes De Corcuera
Committee:	Mark A. Harrison
	Ronald B. Pegg

Electronic Version Approved:

Suzanne Barbour
Dean of the Graduate School
The University of Georgia
August 2015

ACKNOWLEDGEMENTS

I would like to give my greatest gratitude to my major professor, Dr. Reyes, for the great guidance and support he has given. Dr. Reyes is the most enthusiastic, energetic, and hard-working person I have ever seen. He also has a sense of humor and tons of smart ideas. I am so lucky to be his student. I would also like to express my gratitude to my committee members, Dr. Harrison, and Dr. Pegg, for their great support and extensive contributions.

I would like to extend my gratitude to Gwen N Hirsch, for her help in microbiology labs. I am also grateful for all the help from Dr. Garcia and my lab mates. At last, I would like to thank my parents, Yinqiu Lu, and Ming Yang from the bottom of my heart. Their love and support makes everything possible.

TABLE OF CONTENTS

Page

LIST OF TABLES

Page

LIST OF FIGURES

Page

CHAPTER 1

LITERATURE REVIEW

1.1. Introduction

Biofilms form when multiple microbial cells adhere to each other and attach to a surface. It is formed as a sequence of several steps: initial attachment, irreversible attachment, early development of biofilm architecture, maturation and dispersion (Srey et al., 2013). Compared with planktonic cells, microorganisms within a biofilm show stronger resistance to antimicrobials, biocides and host defense mechanisms due to a protective environment (Pulcini, 2001). Extracellular polymeric substances (EPS) synthesized by the microorganisms in the biofilm are believed to be the substance having the function of promoting attachment, forming and maintaining biofilm structure and enhancing its resistance to disinfectants (Czaczyk and Myszka, 2007).

Biofilms can be used as bioreactors in fermentations of economic relevance (Saravanan and Sreekrishnan, 2006). However, when made of pathogenic bacteria, they constitute a hazard to the food industry, potentially causing illness, death, and economic loss. In the USA alone, it is reported that 48 million people suffer from foodborne illnesses annually with 2,612 deaths (Scallan et al., 2011). According to the U.S. National Institutes of Health (NIH) and the Centers for Disease Control and Prevention (CDC), 65% of the microbial diseases are related to biofilms (Potera, 1999). In addition to pathogenic bacteria, biofilms cost industry $15 billion every year mainly by impairing equipment, reducing heat transfer, clogging water filters, and inducing corrosion (Meerpoel et al., 2002).

The great impact that biofilms have in the food industry has been well reviewed in the past ten years (Shi and Zhu, 2009; Simões et al., 2010; Srey et al., 2013). Pathogenic bacteria such as *Salmonella* spp. and *Listeria monocytogenes* are capable of forming biofilms on different kinds of surfaces (Stepanović et al., 2004).

Biofilm control strategies have been researched for years and systematic reviews are well documented (Jahid and Ha, 2012; Simões et al., 2010; Srey et al., 2013; Van Houdt and Michiels, 2010). Generally, these strategies could be divided into the following categories: cleaning and disinfection; chemical-based control such as sodium hypochlorite, hydrogen peroxide, ozone, or peracetic acid; physical methods such as ionizing radiation, ultrasonication, atmospheric plasma inactivation; and novel green approaches like enzymes, phages and bioregulation. Combined methods are recommended to build multiple synergistic hurdles with higher efficiency and reduced energy consumption (Srey et al., 2013). In addition, when eliminating biofilms, the key step is to eliminate the EPS or the biofilm matrix, not the microorganisms themselves. This is because EPS acts like a "house", offering nutrients and protection, to the biofilm (Flemming et al., 2007). Only if the EPS is destroyed first can the biofilm be eliminated thoroughly.

Compared to biofilm controlling strategies, biofilm detection methods require more research and modification. Based on the biofilm forming steps, biofilm forms from spot to spot instead of forming uniformly in the whole system, for example, in a pipeline or conveyor in a food processing plant. This increases the biofilm detection difficulty and the cleaning cost for industries. In view of the need to better control biofilms, in this paper, biofilm detection strategies are reviewed with emphasis on electrochemical impedance spectroscopy (EIS) methods.

1.2. Biofilm Detection Strategies

Detecting biofilm formation has been a difficult challenge to researchers for years. Several biofilm monitoring methods have been developed and most of them have been well reviewed (Janknecht and Melo, 2003).

In the food industry, rapid detection of biofilm formation is essential to reduce the risk of food contamination. Detection methods, including total plate count (TPC), contact plates and dipstick techniques, are regarded as standard and reliable practices (Chmielewski and Frank, 2003). However, these methods are time-consuming and labor-intensive. To confirm the identity of one microorganism, conventional methods often have steps like pre-enrichment, selective enrichment, plating onto the selective media, presumptive identification and biochemical identification (Swaminathan and Feng, 1994). These steps extend analysis time to 5-7 days, which cannot meet the current food safety requirement of early stage detection (Yang and Bashir, 2008). Furthermore, some bacteria have the ability to enter a viable but non-culturable state, which cannot be easily cultivated by conventional cultivation methods (Linke et al., 2010). Therefore, many novel detection strategies are under research and some rapid detection products are produced.

1.2.1. Molecular Biology Methods

Real-time PCR is a modification to the traditional PCR technique, which uses fluorescent tags to monitor the target sequence amplification in real-time, resulting in precise quantification of specific nucleic acids in a mixture with a very low starting concentration (Fraga et al., 2008). Using real-time PCR, *Listeria monocytogenes* growing in a biofilm can be detected as low as 6×10^2 CFU/cm^2 (Guilbaud et al., 2005), and *Helicobactor pylori* in a biofilm is possible to be detected in less than 10 genomic units (Linke et al., 2010). In addition, detection of

Staphylococcus epidermidis biofilm formation, detection of mycobacteria, *Escherichia coli* and antibiotic-resistant bacteria in biofilms from drinking and wastewater distribution systems using PCR-related methods have been reported (Arciola et al., 2006; Juhna et al., 2007; Schwartz et al., 1998; Schwartz et al., 2003).

Furthermore, combined with vortexing and sonication for the purpose of disrupting biofilms, real-time PCR is a sensitive method to detect bacteria adhered to bone cement (Kobayashi et al., 2009). Nevertheless, one major disadvantage of the PCR method is that it is difficult and unreliable to distinguish live and dead cells, which may not accurately detect the existence of a health hazard (Linke et al., 2010).

1.2.2. Acoustic Methods

Ultrasonic Time Domain Reflectometry (UTDR) is a novel biofilm and biofouling detection method. Among the few published papers, UTDR has the ability to detect *Pseudomonas aeruginosa* biofilm on certain kinds of surfaces like flat sheet polyethersulfone ultrafiltration and thin film composite polyamide in real time (Sim et al., 2013). UTDR is based on the principle that different parameters will be given by different ultrasound waves when it encounters various media. Ultrasonic Frequency Domain Reflectometry (UFDR) is a modification to the UTDR technique. It replaces the time domain with frequency domain to acquire more sensitive detecting ability. Using UFDR, Kujundzic et al. (2007) successfully monitored *Pseudomonas aeruginosa* biofilm development on three different surfaces (dense polycarbonate, polyamide nanofiltration composite membranes, and fully porous polyvinylidene fluoride microfiltration membranes). However, these technologies have limitations. Only limited numbers of surfaces have been tested with these methods, and the resolution of the ultrasound signal is often low. Distinguishing acoustic properties between a biofouling layer and the surface or adjacent solution is often

difficult; thus a specific cell or an acoustic enhancer is needed at the same time. Finally, now these methods can only be used in the laboratory due to the complicated ultrasound system (Sim et al., 2013).

Quartz Crystal Microbalance (QCM) is a method that can be used to detect biofilm thickness by observing frequency change when reacting with solution compounds (Reipa et al., 2006). With advantages of being real-time, on-site, and non-destructive, QCM can be used to monitor the *Pseudomonas aeruginosa* biofilm thickness for several days (Reipa et al., 2006). Grown in the QCM device, the biofilm's colony count can be correlated to the QCM frequency in a 20-h period experiment (Schofield et al., 2007). Chen et al. (2010) also used QCM to detect the biofilm early attachment process and found a lag time before early biofilm formation.

1.2.3. Optical Methods

Scanning confocal laser microscopy (SCLM) is a useful tool for routinely imaging fluorescently labeled biological specimens (Paddock, 1999). However, SCLM instruments are not practical in industry for real-time monitoring due to the cost and current equipment configuration.

With similar functions, episcopic differential interference contrast (EDIC) solves the problem of high cost and failure to observe motile bacteria, which are the limitations of SCLM (Keevil, 2003). *Salmonella* biofilm growth was tracked with EDIC by presenting complex three-dimensional aggregations (Warner et al., 2008). SCLM and EDIC methods do have the ability to monitor biofilm development, but to date they are still restricted to use in a laboratory by well-trained technicians.

Combining SCLM and Raman microscopy (RM), Wagner et al. (2009) observed the EPS matrix composition change (from polysaccharides to proteins) when biofilms grow older. When

adding ^{13}C Nuclear Magnetic Resonance (NMR) to the SCLM test, Garny et al. (2010) successfully characterized the biofilm structures, composition and growth phases.

1.2.4. Commercial Biofilm Detection Products

Currently, some products can be found on the market for biofilm detection. One is called "BioFinder" produced by ITRAM HIGIENE Company (Barcelona, Spain). This product has the ability to detect biofilms and microorganisms in 30 s. If a biofilm exists, the surface would form a large quantity of bubbles after using this solution (ITRAMHIGIENE). However, this product is based on bubble evolution upon addition of hydrogen peroxide that may not be suitable for surfaces such as those found in the poultry industry where other residues containing calalase also react with hydrogen peroxide besides the biofilm.

Another product is called "Biofilm detection kit" produced by REALCO Company (Ottignies-Louvain-la-Neuve, Belgium). This enzyme-based kit consists of coloration reactive and cleaning reactive components. It takes approximately 10 min to finish the detection. The result is positive when a blue coloring is produced (REALCO).

In addition, there is a biofilm monitor called "BioSense" produced by Pi Company (Norcross, GA, USA)(PI). The principle of this product is to apply a potential between electrodes on a probe, causing microorganisms to settle on the probe surface before settling on the pipe surface. The controller then collects the signal released by biofilm's biological activities and gives a warning before a biofilm really forms on the pipe or vessel surfaces. These ready-to-use products give the food industry more options to detect biofilms.

1.2.5. Impedance Methods

Impedance microbiology is the detection method that keeps drawing attention for its greatly shortened detection time. Similar to resistance, impedance is a measure of the circuit's ability to

resist the electrical current flow. In general, microbial growth can alter the electrical impedance of a culture medium or a reaction solution (Yang and Bashir, 2008). Particularly, bacteria can change impedance in six different ways: generation of redox substances; biofilm attachment on the electrodes; charge transfer through bacterial attachment activities; existence of bacteria close to electrodes; and protein absorption onto the electrodes (Ward et al., 2014).

Electrochemical impedance spectroscopy is an impedance technique measuring the signal generated by applying small amplitude wave perturbations to an electrochemical system through a large frequency range (Lu et al., 2013). Compared with other methods, EIS has the advantage of being real-time, on-site, and easy to operate. Furthermore, small amplitude can barely influence the bacteria (Kim et al., 2011). Therefore, EIS can be used for detection or as a monitoring method both for bacteria in suspension and in biofilms.

1.2.5.1. EIS Theory

According to Ohm's law, resistance R is expressed as the ratio of voltage E and current I shown as equation 1. In this case, the circuit consists only one ideal resistor.

$$R \equiv \frac{E}{I} \tag{1}$$

When it comes to electrochemical impedance, the impedance is measured by applying an AC potential to an electrochemical cell. Assuming it is a linear or pseudo-linear system, the current and the potential are two sinusoids with the same frequency but having a shifted phase (Orazem and Tribollet, 2011). Now the potential and current are expressed as equation 2 and 3, respectively.

$$E_t = E_0 \sin(\omega t) \tag{2}$$

$$I_t = I_0 \sin(\omega t + \phi) \tag{3}$$

E_t and I_t are the potential and current at time t; E_0 and I_0 are the signal amplitude; ω is the radial frequency; and ϕ is the phase shift.

Similar to Ohm's law, the impedance can be expressed as the ratio of E_t and I_t.

$$Z = \frac{E_t}{I_t} = \frac{E_0 \sin(\omega t)}{I_0 \sin(\omega t + \phi)} = Z_0 \frac{\sin(\omega t)}{\sin(\omega t + \phi)} \quad (4)$$

Equation 4 can be represented as a complex number shown in equation 5.

$$Z(\omega) = \frac{E}{I} = Z_0 \exp(j\phi) = Z_0(\cos\phi + j\sin\phi) \quad (5)$$

The graph of the real part of equation 5 on the X-axis and the imaginary part on the Y-axis is called a "Nyquist plot". In a Nyquist plot, the data's frequency decreases from left to right, but the frequency for each point is unknown. Hence, there is another graph, the "Bode plot" that plots the absolute impedance value and phase-shift against the logarithm of frequency.

Figure 1.1 shows a typical Nyquist plot for an electrochemical cell. Nyquist plots may have other shapes depending on the nature of the electroactive species and the electrodes used in the electrochemical cell.

In Figure 1.1 the semicircle (high frequency range) is related to the electron-transfer-limited process (kinetically controlled region), while the straight line (low frequency range) stands for the diffusion-limited processes (diffusion-controlled region) (Randviir and Banks, 2013; Yang and Bashir, 2008). When the imaginary component ($Z_0 j\sin\phi$ or Z_{imag}) is zero, the intercept to the x-axis may stand for the electrolyte solution resistance (R_s). The diameter of the Nyquist plot semicircle represents the electron transfer resistance (R_{et}) (Lu et al., 2013).

Together with the Nyquist plot, an equivalent electric circuit model is often built to better explain the EIS data. An equivalent circuit consists of different kinds of elements and these elements can be placed in series or in parallel. Common electrical elements consist of electrolyte resistance, double layer capacitance, charge transfer resistance, etc. Electrolyte resistance is the

resistance within the solution between the electrodes. Double layer capacitance (C_{dl}) is the tiny capacitance that results from the accumulation of charged ions on the surface of the electrodes when a potential is applied between the electrodes. Charge transfer resistance occurs during electrochemical reactions, such as the electron/ion exchange process when metal is dissolving into the electrolyte (Orazem and Tribollet, 2011).

Many simple equivalent circuit models have already been built to help interpret EIS data. One common example is the simplified Randles cell. It consists of a solution resistance, a double layer capacitance, and a charge transfer resistance. The equivalent circuit elements of a simplified Randles cell are shown in Figure 1.2. Randles cell is often used as the basic model, that can be modified to fit complex electrochemical systems. The correlated Nyquist plot for a typical simplified Randles cell is always a semicircle (Orazem and Tribollet, 2011).

When interpreting the data to monitor bacteria in suspension or biofilm, one or more electrical elements may be involved in the impedance change. In addition, since parameters like C_{dl}, R_{et} are quite flexible under different conditions (temperature, ionic concentration, electrodes properties, etc.), each experiment requires its own specific data analysis.

1.2.5.2. EIS Applied to Bacterial Suspension

EIS has been widely used with different electrodes to detect various pathogens in suspension. Yang and Bashir (2008) have already reviewed relevant research in detail and Paredes et al. (2014b) also did a summary including some recent research. Table 1.1 lists some of the most relevant studies that report the use of EIS to detect pathogens in suspension. Table 1.1 also summarizes the reported performance of the determinations in terms of detection limit, determination time and the element of the equivalent circuit identified as measured. Pure cultures were most commonly used. Milk (Dong et al., 2013) and beef (Nandakumar et al., 2008) samples

have also been tested. Many strategies have been used to improve EIS detection sensitivity, including employing new electrodes, immobilizing antibodies onto the electrodes, capturing or concentrating bacteria cells, etc.

Conventional electrodes have relatively large surface areas that may lead to some shortcomings when used to detect bacteria. Low mass transport rates result in long measurement time, which will cause electrochemical potential drift or, if the potential is too high electrodes can react with substances in solution, thus modifying the electrochemical properties of the solution (Lu et al., 2013). Larger surface area typically increases the cost of the electrodes as well.

By reducing the electrode surface area, microelectrodes or microchips are introduced and Interdigitated Array Microelectrode (IDAM) is the most commonly used one. Compared to the conventional electrodes, IDAM has improved signal-to-noise ratio, rapid reaction time, and low ohmic drop (Varshney and Li, 2008). IDAM can also be combined with dielectrophoresis (DEP) or immobilized antibodies to further enhance the sensitivity (Varshney and Li, 2008).

For the purpose of detecting specific microorganisms or lowering the detection limit, antibodies are employed in the EIS test. They can be immobilized through two different ways: covalently through amide bond formation or non-covalently by Neutravidin/Biotin conjugation (Barreiros dos Santos et al., 2009). In most cases, antibodies are immobilized directly onto the electrodes (Dong et al., 2013; Ruan et al., 2002; Yang et al., 2004a), while they can also be functionalized onto some nanoparticles instead. With the help of a magnetic field, nanoparticles and the attached targeted bacteria can be captured within the effective distance to the electrodes (Varshney et al., 2007). Thanks to the antibodies, the detection limit can be lowered to around 10^2 CFU/ml without the need for enrichment (Dong et al., 2013; Nandakumar et al., 2008).

Barreiros dos Santos et al. (2013) even reported that they successfully made the *E. coli* O157: H7 detection limit as low as 2 CFU/ml by employing anti-*E. coli* antibodies.

For pathogen detection in suspension using EIS, most of the researchers used impedance change or electron transfer resistance as their analytical parameter and the frequency at which impedance changed the most can vary considerably among reports. Low frequency has been commonly used when solution conductivity is high while high frequency worked better in relatively low conductivity. For example, maximal change was observed at 10 Hz in high conductivity Lennox broth (Nandakumar et al., 2008) while at 1 MHz in low conductivity yeast-peptone-lactose-TMAO medium (Varshney and Li, 2008).

1.2.5.3. EIS Applied to Biofilm Detection

Researchers have applied EIS to detect biofilms since the 1990s. Some researchers shared similar equivalent circuits to analyze their results (Hernández-Gayosso et al., 2004; Kim et al., 2012; Kim et al., 2011; Muñoz-Berbel et al., 2008; Munoz-Berbel et al., 2008; Muñoz-Berbel et al., 2007), some tried to distinguish different biofilms (Dheilly et al., 2008; Paredes et al., 2013), and some developed a biofilm detecting flow system (Bayoudh et al., 2008; Ben-Yoav et al., 2011; Pires et al., 2013).

Details and recent studies of biofilm detection using EIS are discussed in the following section. Summaries of some research reports are shown in Table 1.2.

1.2.5.3.1. Commonly Used Equivalent Circuit

Equivalent circuits are conceptually developed based on the knowledge and understanding of the electrochemical cell and conditions of the specific experiment. Since all electrode and electrolyte solutions share elements in common, development of equivalent circuits often starts

with a standard template and is modified afterwards to model the observed response. Below are two common equivalent circuits.

Figure 1.2 is the simplified Randle cell used by Hernández-Gayosso et al. (2004), Kim et al. (2012) and Kim et al. (2011) to model biofilm detection.

Kim et al. (2012) used silicon wafer interdigitated array (IDA) electrodes and EIS to detect *Pseudomonas aeroginosa* biofilm attachment process. In the one-hour test, double layer capacitance made the greatest contribution and scanning electron microscopy was used for verification at the same time. It was observed that double layer capacitance had a big decrease, which was in accordance with the biofilm attachment activity.

Kim et al. (2011) used platinum disk electrodes with EIS to monitor biofilm attachment and growth activity. They also chose *Pseudomonas aeroginosa* as the model bacterium. However, they did experiments for a longer time (72 h) to get the whole picture of all biofilm growth stages. They found that the double layer capacitance decreased sharply after inoculation and then remained constant, which may account for the attachment and maturation process for the biofilm.

Both Kim et al. (2012) and Kim et al. (2011) reported that the R_s stayed stable and R_{et} can be ignored because R_{et} accounts for leakage current which was insignificant to the experiments. As for the decrease of constant phase element (CPE), they both explained that the electrode area was influenced or blocked by the adhered bacteria or bacterial materials. Constant phase element is often used to replace C_{dl} when the capacitor is not ideal.

$$C_{dl} = \frac{\varepsilon A}{d} \tag{6}$$

Double layer capacitance is defined as equation 6, where ε is the permittivity of the electrolyte, A is the electrode surface and d is the double layer thickness. Kim et al. (2012) explained that the parameters other than A did not change because, upon application of a

potential, the double layer formed instantaneously in immediate contact with the electrode while the biofilm formed at a greater distance from the electrode surface than the double layer. Kim et al. (2011) did EIS experiments in fresh medium every time to keep the other parameters constant.

Hernández-Gayosso et al. (2004) also used the same equivalent circuit. For the purpose of testing the stainless steel corrosion rate caused by sulfate reducing bacteria, they used EIS to measure the bacteria taken from a gas pipeline and biofilm was detected based on the observation of increased resistance.

X. Muñoz-Berbel (2007, 2008), with his research group, did three different experiments using EIS with platinum or gold electrodes to monitor biofilm growth focusing on its pre-attachment, attachment and entire growth process, respectively. In the first two studies, they used the same equivalent circuit as shown in Figure 1.3 A for *E. coli* biofilm, and for the third one, they developed another circuit shown as Figure 1.3 B for *P. putida* biofilm.

They found that the double layer capacitance was sensitive to the biofilm attachment process (Muñoz-Berbel et al., 2007), which was also true with low concentration bacterial concentration (Munoz-Berbel et al., 2008). However, the biofilm capacitance, instead of double layer capacitance, was more sensitive when researching biofilm growth and degradation (Muñoz-Berbel et al., 2008). In their short-time studies (1 min and 40 min), they stored the certain diluted bacterial suspension at 4 ^{o}C before measurement. Concentration of bacteria was not controlled during the six-day experiment.

For the two attachment tests, reference electrode capacitance (C_{ref}) was ignored for its small magnitude and R_s remained constant all the time. The only important parameter, CPE, increased a little at first then decreased afterwards for both experiments (Munoz-Berbel et al., 2008;

Muñoz-Berbel et al., 2007). The same phenomenon can be observed for the third study. X. Muñoz-Berbel et al. (2008) explained that the adhered bacteria at the pre-attachment stage likely decreased the Debye length at the electrode double layer, which accounted for the CPE increase. For the decrease of CPE afterwards, they explained that the total capacitance measured was the sum of the bare electrode capacitance (C_{pt}) and the bacterial capacitance ($C_{bacteria}$). Also, C_{pt} was usually higher than 100 μF, which was much greater than $C_{bacteria}$ (usually below one picoFarad). Based on equation 6, when bacteria attached the electrodes, the coverage percentage of the bare electrodes decreased, resulting in the decrease of CPE.

Unlike the biofilm attachment, biofilm capacitance ($C_{biofilm}$) was found to be most sensitive to the biofilm growth and maturation. The biofilm capacitance increased as the biofilm grew and stayed stable as the biofilm matured. Then, $C_{biofilm}$ had a decline when bacteriophage was introduced to eliminate the biofilm.

X. Muñoz-Berbel et al. (2007, 2008) provided evidence that different stages of biofilms could be distinguished using EIS methods. They also proposed a potential EIS method for detecting bacteriophages through biofilm infection. However, more data or more frequent sampling is needed to have a better understanding of the correlation between EIS parameters and biofilm growth and to elucidate whether these findings can be observed for different bacteria and in different media.

1.2.5.3.2. Attempts to Distinguish Different Kinds of Biofilms

Although EIS is non-specific, researchers have attempted to distinguish different kinds of biofilms or at least trying to see the different EIS performance by various biofilms. Examples are the work done by Paredes et al. (2013), Dheilly et al. (2008) and Bayoudh et al. (2008).

Paredes et al. (2013) performed the experiment in 96-well microtiter plates commonly used in microbiological assays. Interdigitated microelectrodes were combined with EIS to monitor the biofilms growth by two strains of *S. aureus*, ATCC 29213 and CEIT001, and two strains of *S. epidermidis*, ATCC 35984 and CUN 19. In this test, impedance was explained using serial resistance (R_{serial}) and serial capacitance (C_{serial}). The parameters were observed to be most sensitive at low frequency and R_{serial} was the more sensitive one. It increased at first and then had a drop and then remained stable. In the 30-h experiment, R_{serial} curves were explained to correlate different biofilm growth stages, and two different initial concentrations (10^5 CFU/ml and 10^7 CFU/ml) were used. In this experiment, four strains of bacteria had the similar impedance curves and impedance behavior, which cannot be distinguished based on the results.

Bayoudh et al. (2008) used EIS to detect *Pseudomonas stutzeri* and *Staphylococcus epidermidis* biofilm growth on a semicircular indium tin oxide plate (ITO). They chose ITO for its stability in aqueous solution, optical transparency and conductive properties. During the 2-h experiment, impedance for both kinds of biofilm decreased due to the bacterial adhesion. Particularly, the impedance decrease was the combination of charge transfer resistance decrease and double layer capacitance increase. The difference for these two bacteria was that the adhesion of *P. stutzeri* was detected earlier than *S. epidermidis*. *P. stutzeri* had a bigger charge exchange between bacterial and electrode surfaces than *S. epidermidis*, which donated more charge, resulting in a faster and more firm adhesion.

Dheilly et al. (2008) used EIS to explore the difference when Gram-positive and Gram-negative bacterial strains form biofilms on a metal surface (stainless steel 304). *Pseudomonas aeruginosa* and *Bacillus subtilis* were chosen as the Gram-positive and Gram-negative bacteria, respectively. Both of the bacteria had electron transfer resistance increase after one week.

However, the resistance had a decrease after two weeks for *P. aeruginosa* while resistance remained stable for *B. subtilis*. This can be explained that *P. aeruginosa* entered the detachment stage after two weeks while *B. subtilis* did not. This explanation was consistent with the optical results, which showed weaker biofilm forming ability of *B. subtilis*. Their results were not enough to prove that EIS can distinguish biofilms formed by different strains of bacteria, but they thought the possibility still existed if a curve of biofilm thickness could be established for each single strain to act as a calibration.

The outcome of these three studies showed that impedance curves or patterns could be used to explain biofilm growth stages. Different bacteria may have similar curves while possessing their specific impedance values. However, none of these tests tried to distinguish a single bacteria or biofilm from cocultures. These three studies have an important weakness in that the conductivity or capacitance of the medium during the comparison was not controlled to be the same.

Changes in EIS are caused not only from biofilm formation but also by changes in impedance of the bacterial suspension due to bacterial metabolism and growth. Therefore, it is better to use fresh medium for every measurement. However, changing medium also has influence when the biofilm has grown to some extent. Introducing a flow system with fresh medium flowing all the time is one possible solution.

1.2.5.3.3. Flow Systems Adopted

Three studies developed some flow systems and used EIS to monitor the biofilm growth condition inside. The reason they adopted a flow system, instead of simply immersing the electrodes into a bacterial suspension, was that they thought bacterial adhesion kinetics was of

vital importance, and it could only be well studied under controlled hydrodynamic conditions (Bayoudh et al., 2008).

Bayoudh et al. (2008) used a pump to let the bacterial suspension flow through the chamber for two hours and the bacteria could be detected by EIS when attaching to the ITO surface. Optical methods were performed at the same time to verify the results.

Ben-Yoav et al. (2011) also used ITO electrodes and a flow system to monitor biofilm growth by EIS. Optical methods were also used for verification. However, unlike Bayoudh et al. (2008), they used the seeding and growth strategy to grow *E. coli* biofilm. Seeding means that the bacterial suspension was pumped for a short period of time (approximately 30 min) to allow the bacteria to attach the surface. Growth means sterilized medium instead of bacterial suspension was used to let the biofilm grow after the seeding stage. In that study, impedance parameters, biomaterial capacitance and biomaterial resistance, were used to explain biofilm growth. At the biofilm attachment stage, the increase of bacterial cell density caused the increase of capacitance, while higher density of resistance components resulted in the increase of resistance. At the biofilm growth stage, the biofilm thickness increase contributed to the decrease of capacitance and the increase of resistance. At the biofilm maturation stage, a stable biofilm thickness maintained a steady capacitance value.

Pires et al. (2013) developed a flow system including a reference channel to study the influence of medium. They also used an amperometric sensor to monitor biofilm respiratory activity in combination with EIS. Seeding and growth strategy was also adopted in this experiment. The idea of this flow system is shown in Figure 1.4. Only sterilized medium was allowed to go through the reference channel during the entire experiment. The reference channel was placed upstream to avoid contamination.

In this experiment, only the attachment stage of the biofilm was monitored (impedance increase), for the reason that test time was limited to let the biofilm mature. However, more importantly, biocides were used to test whether alive/dead cells could be detected using EIS. When biocides were added, the respiratory activity decreased for cell death or injury. However, the EIS results still remained stable suggesting that EIS cannot distinguish alive/dead cells when the biomass on the electrode surface does not change much. On the contrary, Paredes et al. (2014a) thought distinguishing live/dead cells was possible because impedimetric response can be affected by alive/dead ratio. If the membrane of a cell is damaged, the electrical response generated by the cell is different. No capacitance effect should be detected if the dead/alive ratio is high. Therefore, whether the live/dead cells can be detected greatly depends on the capacitance or conductivity of the medium and the biofilm growth stages.

1.2.5.3.4. Medium Impedance Change

Few studies using EIS to monitor biofilm considered the influence of medium impedance change. Two studies that did consider medium impedance are described below.

Pires et al. (2013) (Figure 1.4) used the flow system as mentioned above to differentiate the control channel and the measurement channel. The control channel only allowed sterilized medium through. Kim et al. (2011) took the electrodes out of the bacterial suspension and put it in the fresh sterilized medium every time doing the EIS measurement.

Unlike the above two studies, Paredes et al. (2012) realized the medium impedance influence but only used it as a theory to explain their results. In their experiment, impedance decreased at first and then a small increase was observed before a stable stage emerged. They explained the small increase was the result of the stationary and death phase occurring in the cultures in the suspension.

In some cases like metal corrosion monitoring, microbial induced corrosion (MIC) is the combined result of biofilm and plancktonic microorganisms activities (Hernández-Gayosso et al., 2004). Medium impedance influence should be considered. Nevertheless, they did not test the medium impedance change in their experiment.

1.3. Summary

Currently, in multiple industries, there is a need to detect biofilm in real-time; thus many detection methods are under research and development. Electrochemical methods are receiving increased attention for their possibilities of *in-situ*, real-time and online monitoring as well as convenient installation and operation (Kim et al., 2011). In particular, EIS has a great potential for bacteria and biofilm detection. By measuring the electrochemical signals, EIS has the advantage of not injuring the bacterial cell or the environment (Kim et al., 2012; Kim et al., 2011). Using EIS to detect or monitor biofilm is being researched. Below is a summary of some conclusions from these studies.

The formation of a biofilm produces changes in the impedance spectrum. All of the biofilm growth stages can be monitored and explained by changing patterns in impedance parameters. Biofilms generated by at least 7 different bacterial strains have been tested and many have similar impedance behaviors. In most cases, low frequency has proven to be the most suitable setting for EIS to monitor biofilm. From the various equivalent circuits developed, biofilm resistance, solution resistance, electron-transfer resistance, biofilm capacitance and double-layer capacitance have been used to explain the impedance change as biofilms grow.

1.4. Research Needs

1. For better understanding the biofilm impedance change, different biofilm growth surfaces need to be tested. For the EIS studies in the past 10 years, the biofilm is usually simply allowed

to grow directly onto the EIS electrodes. Other surfaces are seldom used. Although a very common material in industry, stainless steel has only been used in two studies. No studies have examined the inner surface of a stainless steel tube as a biofilm growth surface.

2. A long-term biofilm formation study is needed to elucidate the impedance change when cells start to detach from the biofilm. Although different stages of biofilm growth have been tried, researchers mostly focus on the biofilm attachment process. The correlation between biofilm natural detachment stage and impedance change has never been reported.

3. For a long-term biofilm growth experiment, a well-controlled bacterial suspension concentration is necessary to project an expected biofilm growth speed. In current studies, concentrations of bacterial suspension used to form a biofilm cannot be ensured constant during the experiment. When testing the influence by different concentrations of bacterial suspensions on biofilm formation, the usual method is to make dilutions on the spot and store at 4 ^{o}C before measurement. These concentrations are assumed to be constant if the experiment period is not long. However, using low temperature is not practical for long-term experiment controlled or monitored by electrical equipment.

4. A better way to monitor medium impedance change needs to be developed. Medium conductivity is not stable due to bacterial activities, such as producing highly charged substances, cells membrane breakage, etc. In order to measure biofilm impedance change, medium impedance change has to be considered.

5. A flow system with a larger scale needs to be developed for better understanding the biofilm impedance change in larger systems. Current flow systems developed are all of a very small scale.

6. It is necessary to build up a certain impedance-changing pattern to indicate biofilm existence or growth stages. It is valuable to predict biofilm growth with the same impedance-changing pattern every time in the same conditions.

7. Biofilm detection limit by EIS has to be lowered to match industrial needs. If we can detect biofilm forming with a better detection limit, this method is more valuable in the industry to prevent biofilm forming in the first place.

Based on the literature review, we hypothesize that a flow system controls biofilm growth well. We also hypothesize that biofilm impedance is different from solution impedance. Biofilm from single cultures specifically correlates to EIS. If this hypothesis is supported by experimental data, we can further hypothesize that EIS data of biofilms from mixtures of microorganisms may correlate to the data for biofilms of the individual microorganisms.

Therefore, the objective of this research is to design, construct, and test a flow system for controlled biofilm growth and electrochemical monitoring.

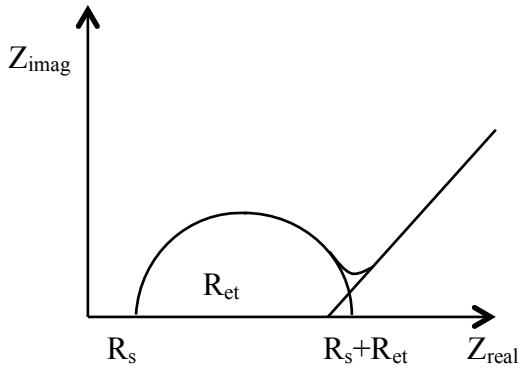

Figure 1.1. A typical Nyquist plot (Z_{imag} vs. Z_{real}). R_s: resistance of electrolyte; R_{et}: electron transfer resistance (Modified from Ruan et al., 2002).

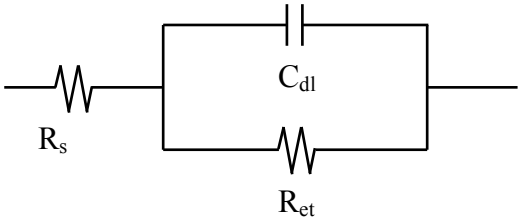

Figure 1.2. Simplified Randles Cell. R_s: solution resistance; C_{dl}: double layer capacitor; R_{et}: Electron Transfer Resistance (Modified from Orazem and Tribollet, 2011).

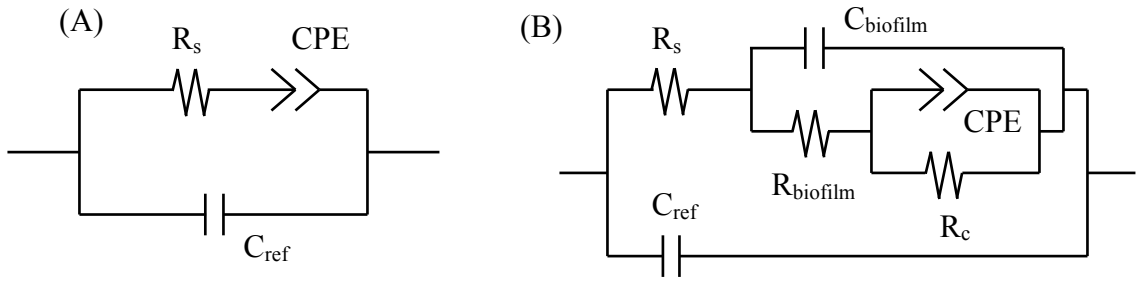

Figure 1.3. Modified equivalent circuit model examples. (A) R_s refers to solution resistance; CPE refers to constant phase element; C_{ref} refers to reference electrode capacitance (Modified from Muñoz-Berbel et al. 2007, 2008). (B) R_s refers to solution resistance; C_{ref} refers to reference electrode capacitance; $C_{biofilm}$ refers to biofilm capacitance; $R_{biofilm}$ refers to biofilm resistance; CPE refers to constant phase element; R_{et} refers to electron-transfer resistance (Modified from Muñoz-Berbel et al. 2008).

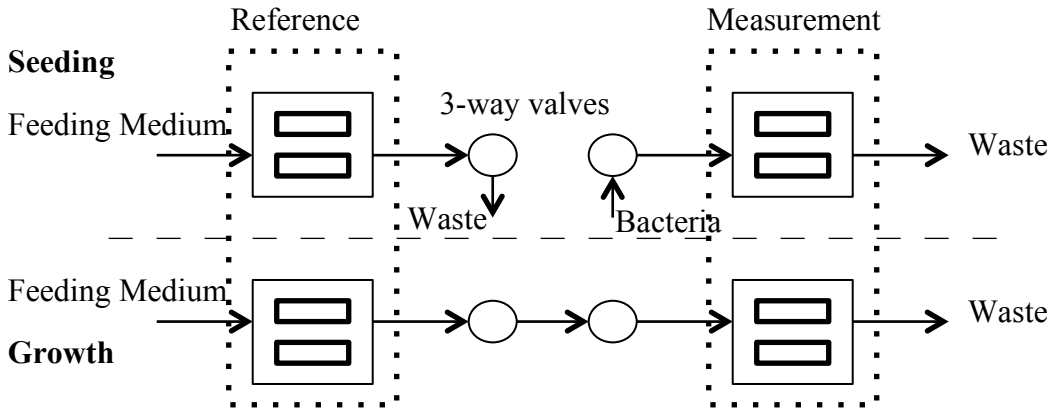

Figure 1.4. Flow system layout using seeding and growth strategy for biofilm growth. The bars in the square stand for electrodes (Modified from Pires et al. 2013).

Table 1.1. Research summary of pathogen detection in suspension by EIS

Electrode	Microorganism	Detection Limit (CFU/ml)	Detection Time	Frequency (Hz)	Parameter	Relative Change	Note	Reference
Conventional Redox Electrode	*Salmonella* Typhimurium	5×10^2	6 min	10	Impedance	NA	Faradaic Impedance; Antibody Immobilized	Nandakumar et al. (2008)
	E. coli O157:H7	2	NA	1 – 100 k	R_{et}	NA	Faradaic Impedance; Antibody Immobilized	Barreiros dos Santos et al. (2013)
Interdigitated Array Microelectrode (IDAM)	*E. coli* O157:H7	10^6	NA	1 – 100 k	R_{et}	NA	Faradaic Impedance; Antibody Immobilized	Yang et al. (2004a)
	E. coli O157:H7	1.6×10^2	35 min	16 k	Normalized Impedance Change	61%	Faradaic Impedance; Antibody Immobilized	Varshney et al. (2007)
	E. coli O157:H7	8.0×10^0	14.7 h	1M	Normalized Impedance Change	30.5%	Double IDAM	Varshney and Li (2008)
	Salmonella Typhimurium	$10^2 – 10^4$	2.17 – 9.33 h	10	Impedance	36%		Yang et al. (2004b)

	Salmonella Typhimurium	3.5×10^6	NA	1k	Impedance	NA	Tested in Deionized (DI) Water	Yang (2008)
Modified Glassy Carbon Electrode	*Salmonella* Typhimurium	5×10^2	NA	$10^{-1} - 10^5$	R_{et}	NA	Faradaic Impedance; Antibody Immobilized	Dong et al. (2013)
Indium Tin Oxide (ITO) Electrode Chips	*E. coli* O157:H7	6×10^3	NA	1 – 100 k	R_{et}	NA	Faradaic Impedance; Antibody Immobilized	Ruan et al. (2002)
Microwire	*E. coli K12*	10^3	NA	0.1 – 10,000	R_{et}	NA	Faradaic Impedance; Antibody Immobilized	Lu et al. (2013)

Table 1.2. Research summary of biofilm detection by EIS

Electrode	Microorganism	Bacteria concentration	Electrolyte Solution	Detection Limit	Experiment Time	Frequency	Parameter	Note	Reference
Indium-tin-oxide-coated electrodes	*E. coli*	NA	LB medium	NA	91 h	100 mHz to 400 kHz	Capacitance, resistance	Flow system; optical microscopy combined	Bayoudh et al. (2008)
Semiconducting indium tin oxide plate	*P. stutzeri, Staphylococcus epidermidis*	10^7 to 10^8 cells/ml	PBS	NA	2 h	10 mHz to 100 kHz	Capacitance, resistance	Flow system	Ben-Yoav et al. (2011)
Planar gold electrode	*P. aeruginosa*	10^8 CFU/ml	NA	NA	120 h	NA	Impedance	Flow system; Optical microscopy and amperometric combined	Pires et al. (2013)
Interdigitated array microelectrode	*Staphylococcus aureus; Staphylococcus epidermidis*	10^5 CFU/ml and 10^7 CFU/ml	TSB	10^4 CFU/cm^2	20 h	100 kHz to 10 Hz	Equivalent serial resistance	96-well plate	Paredes et al. (2013)
Reference: saturated calomel electrode; Counter: a graphite electrode; Working: the grids and coupons.	*B. subtilis* *P. aeruginosa*	NA	LB	NA	240 h	NA	Electron-transfer resistance	Scanning electron microscopy (SEM) combined	Dheilly et al. (2008)
Platinum and gold electrodes	*P. putida;*	NA	AB minimal medium	NA	6 d	10 Hz to 100 kHz	Capacitance	Optical microscopy combined	Muñoz-Berbel et al. (2008)

	E. coli								
Platinum	*E. coli*	10^9 CFU/ml	AB minimal medium	NA	40 min	10 Hz to 100 kHz	Double layer capacitance	Fluorescence microscopy combined	Muñoz-Berbel et al. (2007)
Platinum disk	*P. aeruginosa*	10^8 CFU/ml	TSB	NA	72 h	1 Hz to 100 Hz	Double layer capacitance	Image analysis combined	Kim et al. (2011)
Interdigitated array electrode	*P. aeruginosa*	10^8 CFU/ml	1/10 TSB	NA	1 h	100 Hz	Double layer capacitance	Scanning electron microscopy combined	Kim et al. (2012)

CHAPTER 2

MATERIALS AND METHODS

2.1. Introduction

Though EIS has been introduced to detect or monitor bacterial suspensions or biofilms for several years, few studies have tested this technology in flow systems. Those who used flow systems mainly adopted them for controlled hydrodynamic conditions or microscopy examination availability (Bayoudh et al., 2008; Ben-Yoav et al., 2011). Their flow systems were very small. For example, one chamber was as big as a key (major radius =10.5 mm × minor radius =1.5 mm × height = 3 or 8 mm) (Ben-Yoav et al., 2011) and the others were similar.

No well-controlled flow system exists in a larger scale and is capable of continuously adjusting the initial bacterial populations. The first objective of this study was to design and build a prototype flow system to monitor biofilm growth in a wide range of time intervals (from minutes to days) with adjustable initial microbial populations. This system was expected to better mimic industrial conditions (using flow system and stainless steel tubes) and to better understand biofilm growth dynamics (manipulating growth conditions). The second objective was to use EIS and TPC to monitor *P. putida* biofilm growth in the system. This was to test the system's ability for EIS monitoring and to look for any correlation between biofilm growth and EIS data.

2.2. Flow System Design and Construction

2.2.1. Design Bases

The basic design concept is to continually pump bacterial suspensions through tubes made of stainless steel 316, a material commonly used in the food industry for contact with foods. As

time passes, bacteria have the ability to attach to the tube inner surface and form a biofilm. As the biofilm grows, the impedance of the system changes based on the hypothesis that the biofilm impedance is different than the impedance of the solution. Because the impedance of the bacterial suspension may change as result of growth or nutrient depletion, EIS measurements of the suspensions must be made in the absence of the biofilm. For example, the metabolism of substrates during microorganisms growth can convert uncharged substances to highly charged substances to alter conductivity (Yang, 2008). For this purpose, a system with a biofilm cell and a reference cell was designed. In the first cell, the bacterial suspension flows constantly (except when impedance measurements are done) during the entire experiment. In the reference cell, bacterial suspension flows only prior to impedance measurements and is otherwise kept clean to avoid biofilm formation. Each measurement cell consists of two stainless steel 316 seamless tubes (2 cm long × 18 mm outside diameter × 1.0 mm wall thickness) that serve as work and counter electrodes and an Ag/AgCl reference electrode. As for the controlled bacterial concentration, the design takes advantage of the fact that *Pseudomonas putida* counts can remain in the range of 10^8 CFU/ml to 10^9 CFU/ml (stationary phase) in 1/10 TSB for about two weeks. Other microorganisms such as *Listeria* spp. (Zwietering et al., 1990) also have the ability to maintain a certain concentration for a period of time if proper temperature and medium are provided. The reason choosing *Pseudomonas* is because of its strong biofilm forming ability. Prototype evolution is detailed in the following sections.

2.2.2. Prototype 1

The first prototype is shown in Figure 2.1. An autoclavable 500 ml plastic water bottles (Fisher Scientific, Suwanee, GA), 6.4 mm × 11.1 mm and 3.2 mm × 6.4 mm platinum silicone tubes (Cole Parmer, Vernon Hills, IL) and luer-lock nylon connectors (Cole Parmer, Vernon

Hills, IL) were used for their sterilization capability. A KDS 200 syringe pump (KD Scientific, Holliston, MA) was used to continuously withdraw and infuse the bacterial suspension through the system. Two-way and three-way (3.2 mm × 6.4 mm) pinch valves (Cole Parmer, Vernon Hills, IL) were used to control fluid direction because they did not directly contact the liquid.

This first prototype worked well pumping bacteria through the system and changing the fluid directions as controlled by a 2014 version LabVIEW program (National Instrument, Austin, TX). Electrochemical impedance measurements were done using Reference 600TM (Gamry, Warminster, PA). However, tubes placed horizontally trapped bubbles that insulated the reference electrode and caused a potentiostat potential overload error or resulted in unstable drifting data.

2.2.3. Prototype 2

To solve the bubble entrapment problem, the system was rearranged vertically as shown in Figure 2.2. Tubing was also rearranged in two loops to produce an upward flow through the stainless steel tubes that were microbiologically sampled to obtain plate counts.

2.2.4. Prototype 3

For either prototype 1 or prototype 2, the bacterial suspension went back into the system after passing through the reference cell (see Figure 2.1 A). After the reference cell test finished, the cell was washed and filled with sterilized deionized water to minimize the potential for biofilm growth. However, it had the possibility of system contamination when washing the tubes because a portion of the tube was exposed to air all the time. Hence, the tube that connected the reference cell outlet to the biofilm cell outlet was removed to prevent the reference cell solution from flowing back into the system. Prototype 3 is shown in Figure 2.3.

Prototype 3 was the first practical flow system that allowed collection of experimental data. Figures 2.4 and 2.5 are results for a 108-h and a 128-h test, respectively. *Pseudomonas putida* had the initial concentration 10^8 CFU/ml and the flow rate was 40 ml/min. Biofilm microbial counts in the tube sample were above 2.6×10^4 CFU/swab even from the very beginning, and this number continued to increase rapidly to more than 10^6 CFU/swab within 24 h. Reaching such large counts in a very short period of time did not allow detection of any change using the EIS method. With the biofilm results in Figure 2.5, the EIS result is shown in Figure 2.6. Figure 2.6 A shows the Nyquist plots and Figure 2.6 B is the change of the Z_{real} with 1 kHz frequency where Z_{imag} is the lowest, both for biofilm cell and reference cell.

No obvious impedance change was observed from these plots, indicating impedance changed too quickly to monitor any biofilm development. The most severe problem prototype 3 had was that the biofilm grew too fast, mainly because the original bacteria concentration was too high (~10^8 CFU/ml). Furthermore, Figure 2.5 indicates that the biofilm also grew to a large number (~10^5 CFU/swab) in reference cell, which was supposed to be clean and free of any biofilm.

2.2.5. Prototype 4

To solve this problem, we designed a continuous dilution system that injected 3.33 μl/min original bacterial suspension and 33.33 ml/min peptone water and mixed both streams to achieve a 10,000 times dilution. The resulting bacterial concentration through the system was approximately 10^4 CFU/ml. To ensure the peptone water was free of bacteria, a disposable in-line liquid filter (Cole Parmer, Vernon Hills, IL), 0.3 μm, was also included at the system outlet, shown in Figure 2.7. However, the filter quickly clogged and eventually broke after

approximately 16 h of continuous flow. In addition the filter resulted in a pressure increase in the system, which caused backflow to the syringe every time the valve was changing directions.

For accomplishing the dilution, a check valve was used to ensure the small volume (10 μl) of bacterial suspension could enter the bigger tube without being pushed back by pressure. An inline static mixer (Cole Parmer, Vernon Hills, IL) was also incorporated to mix the two fluids well before the fluid passed through the biofilm cell. The positions of the check valve and inline mixer are shown in Figure 2.7 C. To ensure adequate mixing, 4, 8 or 12 mixing elements were tested by putting them in series in three different tubes in the same system controlled by three-way valves. Mixing uniformity increases with the number of mixing elements. Mixed bacterial suspensions went through each mixer one by one and samples were taken every 30 s for each mixer. Comparison result is shown in Table 2.1. The 12-element inline mixer was able to provide stable mixed concentration as determined by repeatable microbial counts when sampling immediately downstream from the static mixer.

To completely eliminate the potential contamination of the reference cell in experiments with prototype 4, we used a sterilized reference cell every time before testing. With this new procedure, the electrodes should be replaced every time. Since working and reference electrodes' locations are critical to accurate and reproducible data collection, they must be placed at the same position every time. Hence, a new connector, which allowed for easier electrode changing, was included in prototype 4, shown in Figure 2.8. The data reproducibility for the two different connector types is shown in Table 2.2.

When the reference electrode is placed at the inner surface of the connector (shown in Figure 2.8 A), the data shows the best stability and is easy to control. Results of testing the reference electrode insert depth are shown in Table 2.2. A mark was made on the electrode to

precisely indicate how deep it should be inserted into the connector. Also, the working electrode should be as close to the reference electrode as possible to minimize ohmic drop effect. Using 1/10 tryptic soy broth (TSB), an increase of 69 kΩ/mm was measured in an experiment correlating Z_{real} (where Z_{imag} was the minimum) with the distance between working and reference electrodes. The new connector showed a stable result 186.4 +/- 4.3 kΩ with 2.2% Coefficient of Variation by mounting and dismounting the electrodes 3 times using peptone water in a series of experiments, indicating that the influence of distance "a" between tubes to the reference electrode is acceptable.

2.2.6. Prototype 5

Prototype 4 successfully diluted the original ~10^8 CFU/ml bacterial suspension to ~10^4 CFU/ml, but because prototype 4 failed to operate continuously for the entire duration of the experiments, the filter was discarded and a 20 L container of peptone water was used instead. The peptone needed for the entire 72-h experiment was 72 L. All fluids were pumped through the system only once and then collected as waste. Every twelve hours, the peptone water carboy was changed and the waste bucket had to be autoclaved. Every time before changing the peptone carboy, pumping was stopped, was changed, and the new carboy spigot was treated with 70% ethanol to lower contamination possibility. Figure 2.9 shows the updated prototype 5.

2.2.7. Prototype 6

For prototypes 1 to 5 we used a wooden board to support all the components of the system. Wood was a convenient material for prototyping; however, it was difficult and time-consuming to assemble and disassemble tubes every time (approximately 1 h) experimenting with only one board. The wooden board was also difficult to clean or sanitize, especially when occasional spills occurred. The whole board had to be autoclaved and it would eventually degrade. Therefore, a

1.6-mm thick stainless steel 304 plate was used for a new supporting board. This prototype was strong enough to hold tubes and the bacteria bottle, while not too heavy or big to carry and autoclave without need to disassemble most of its components. Holders were attached to the board to secure the tubes. Stainless steel supporting boards and the entire working system are shown in Figure 2.10.

The new prototype comprised two boards, a "tubing" board and a "holding" board. The "holding" board (Figure 2.10 B, C) held all valves and data acquisition box that cannot be autoclaved. The "tubing" board held all tubes and the bacterial bottle that need to be sterilized for each experiment. This design made it much easier and faster (less than 5 min) to separate the parts that needed autoclaving and greatly reduced the possibility of spilling while disassembling.

2.2.8. Summary of the Best Prototype

Prototype 6 had a flow rate range for media from 54.6×10^{-3} ml/min to 83.3 ml/min with two 50 ml syringes using a KDS 200 syringe pump (KD Scientific, Holliston, MA), while a range for bacterial suspension from 57.4×10^{-3} ml/min to 59.6 µl/min with one 50-µl syringe using a Legato 111 syringe pump (KD Scientific, Holliston, MA). Therefore in theory, the maximum dilution fold is $\frac{83.3 \text{ ml}}{57.4 \times 10^{-3} \text{ ml}} = 1.5 \times 10^{6}$.

2.2.9. Summary

A summary for prototype evolution is shown in Table 2.3.

2.2.10. LabVIEW Programming

The LabVIEW program was written to automatically operate the syringe pumps and pinch valves continually while running the experiment. This made it possible to run a one-week experiment and change the flow between biofilm cell and reference cell regularly and reliably. Two sequence structure LabVIEW programs were used, one for the operation of prototype 3 and

the other for the operation of prototype 5. One event structure LabVIEW program was used for prototype 6. Figure 2.11 shows the sequence of steps that the program controls.

2.2.10.1. Sequence Structure

Figure 2.12 shows LabVIEW programs for Prototype 3 and Prototype 5 based on the sequence structure. Sequence structure is easy to build but unable to change the order sequence while running. For example, when running the Prototype 3 program, "RUN REFERENCE CELL" cannot be operated again after the button has been clicked. Clicking the next button is essential to redo the same task. The program for Prototype 5 is modified on the basis of the program for Prototype 3. A "PREPUMPING" command was added to fill the bacterial syringe in order to be ready for diluting. "EMPTY REFERENCE CELL" was deleted because reference cell was changed every time when using Prototype 6.

2.2.10.2. Event Structure

For easier operation, the event structure was designed to replace the sequence structure. This allowed the operator to click the same button several times to operate the same commands. In addition, syringe parameters, running time (h) or number of times running can be examined and adjusted. Figure 2.13 shows the event structure, the control panel and some examples. The intact LabVIEW program can be found in Appendix A.

2.3. Biofilm Monitoring

2.3.1. Bacterial Strain Culture Preparation

Pseudomonas putida was inoculated from frozen beads from the collection in the University of Georgia Food Science microbiology labs. One bead was thawed and inoculated into a 9-ml TSB tube to grow overnight at 28 ^{o}C. Tryptic soy agar (TSA) plates were streaked with the *Pseudomonas* suspension and incubated at 28 ^{o}C overnight to make cultures. Cultures were

stored at 4 ^{o}C and renewed every three months. A loop of bacteria from the prepared culture was transferred into 200 ml 1/10 TSB and incubated at 28 ^{o}C with agitation (160 rpm, G24 Environment Incubator Shaker, New Brunswick Scientific, Enfield, CT) for 24 h.

2.3.2. Stainless Steel Tube Preparation

Stainless steel 316 seamless tubing, 18-mm outside diameter × 1.0-mm wall thickness (Swagelok, Alpharetta, GA) was cut into 2-cm long pieces. Prior to use, all these tubes were thoroughly washed with the method modified from the biofilm attachment study by Kim et al. (2006). Tubes were sonicated in the 1.9-L ultrasonic bath (Fisher Scientific Company LLC, Suwanee, GA) in 15% phosphoric acid solution and 2% sodium hydroxide solution at 55 ^{o}C for 1 h successively. Deionized water was used for rinsing after each sonication. For minimizing EIS data drifting, tube pieces were also treated by chemical passivation (Standard, 2005). They were sonicated in 25% nitric acid at 55 ^{o}C for 25 min and fully rinsed with deionized water. Washed stainless steel tubes were dried and assembled in series with 6.4 mm × 11.1 mm and 3.2 mm × 6.4 mm platinum silicon tubes (Cole Parmer, Vernon Hills, IL) before autoclaving.

2.3.3. Biofilm Forming Experiments and EIS Measurements

The flow system was connected to the peptone carboy and filled up with sterilized peptone using a syringe pump before infusing bacteria. Then the *Pseudomonas putida* was transferred to the bottle attached to the "tubing" board with a disposable 5-ml pipette.

Two 50-ml plastic syringes (Fisher Scientific Company LLC, Suwanee, GA) and one 50-µl glass syringe (Hamilton, Reno, NV) were used simultaneously as described in Chapter 2 to make a controlled 10,000-fold dilution, by mixing the streams of peptone and bacterial suspension using a flow rate of 33.33 ml/min and 5 µl/min, respectively. Considering the very small volume of bacterial suspension that was injected with every stroke of the pump, a priming step had to be

ran first to fill the 50 µl syringe and made the bacteria suspension reach the mixing point. A check valve was placed at the end of the bacteria tube and right before the mixing point to prevent the backflow of bacterial suspension. Peptone water was chosen to dilute the bacterial suspension for it can barely lower bacterial counts while keeps the counts number the same level by offering some nutrient source for a short time. However, since peptone water used in this study only spent 3 min in the system, other cheaper salt solutions can be tested and used in future experiments.

The whole experiment was performed in triplicate at room temperature (23 ^{o}C) for 72 h. TPC and EIS methods were applied every 4 h to monitor biofilm growth, in conventional microbiological and electrochemical impedance methods. The peptone solution and waste bucket were changed every 12 h. A detailed experiment timeline is shown in Appendix B.

For EIS, two stainless steel tubes, placed exactly in the same position on opposite sides of the reference electrode holding connector, worked as the working electrode and counter electrode, respectively. The reference electrode used was a 60 mm Ag/AgCl electrode (Pine Research Instrumentation, Durham, NC) and was inserted into the connector to a certain depth every time. These three electrodes were connected to a potentiostat model Reference 600^{TM} (Gamry, Warminster, PA) and potential-controlled tests were performed on biofilm cell and reference cell. A 100 mV AC voltage was applied to the cell over a frequency ranging from 0.1 Hz to 1 MHz. 100 mV was chosen by comparing different AC voltages including 10 mV, 20 mV, 50 mV, 100 mV and 250 mV. One MHz is the highest frequency for the equipment and frequency lower than 0.1 mV takes too long (more than 5 min) to finish one test. No bubble should exist in the cells during the potential-controlled tests. The reference cell was changed with a sterilized clean one every time before measurement.

For the TPC method, one piece of stainless steel tube was sampled right after each EIS test. The outside of the tube to be sampled was sprayed with 70% ethanol to lower the risk of contamination. Before sampling, the system was emptied by withdrawing liquid back to the 50 ml plastic syringes after flushing the entire system with 200 ml sterilized peptone. The biofilm was recovered using the specific swabbing procedure designed for this study. Each stainless steel tube sample was placed vertically on a piece of sterilized cotton. Virtually all the liquid (cell suspension) hanging to the tube wall was removed by vigorously tapping it three times against the cotton piece. This was done to ensure that microbial counts correspond to the biofilm and not to cell suspension residue. A sterile cotton tip (Fisher Scientific Company LLC, Suwanee, GA) was used to swab the tube inner surface three times in every eight directions. The stainless steel tube and the swabbing direction are shown in Figure 2.14. The original bacteria suspension and diluted suspension were also sampled every 4 h. All samples were plated on TSA and incubated at 28 ^{o}C overnight before counting.

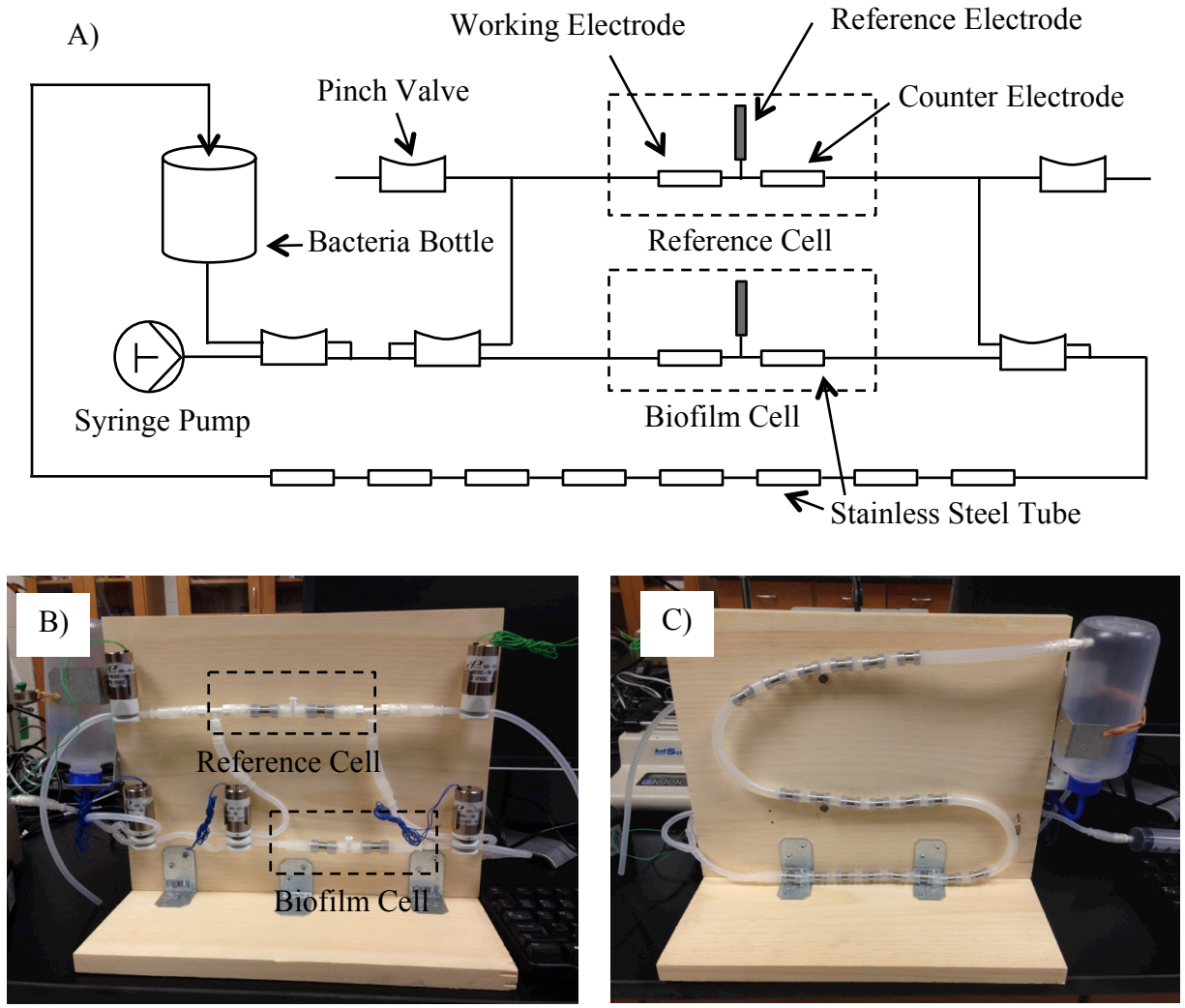

Figure 2.1. Prototype 1, two cells design with tubes placed horizontally. A: Flow system layout. B: Front side of the system board. C: Reverse side of the system board.

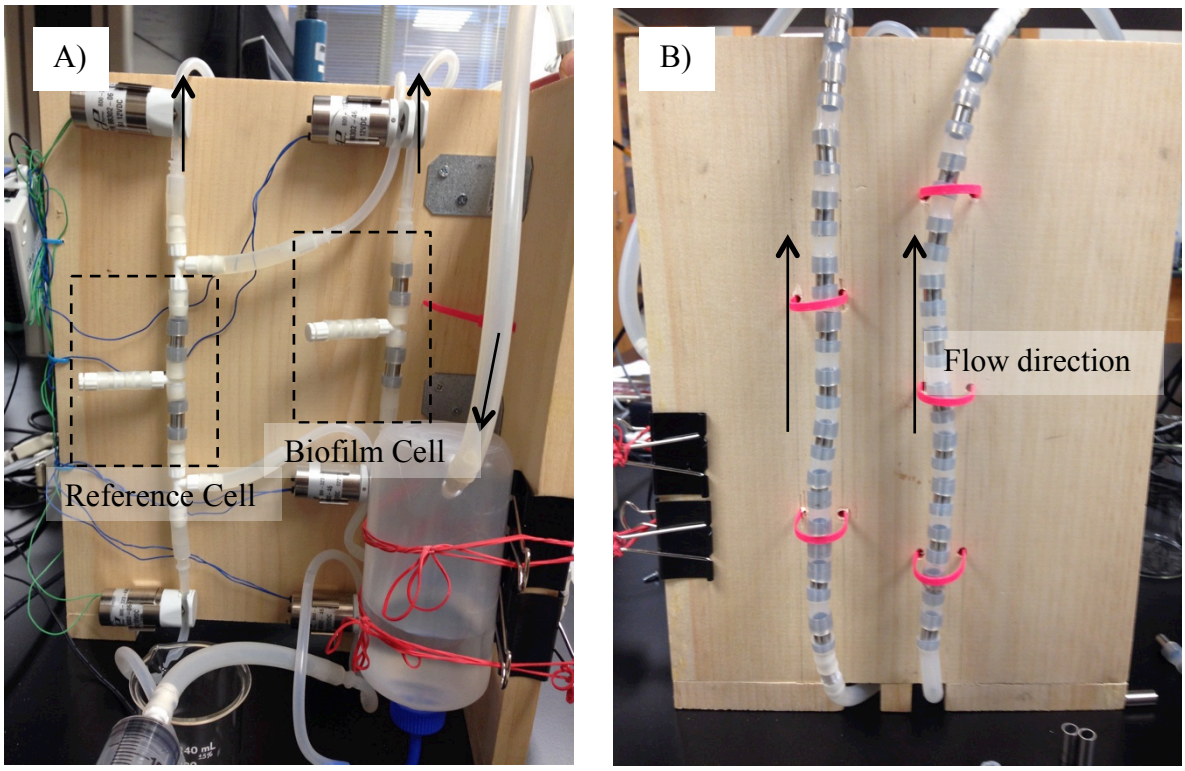

Figure 2.2. Prototype 2, system placed vertically to remove bubbles. A: Front side of the system board. B: Reverse side of the system board. Arrows indicate the fluid direction.

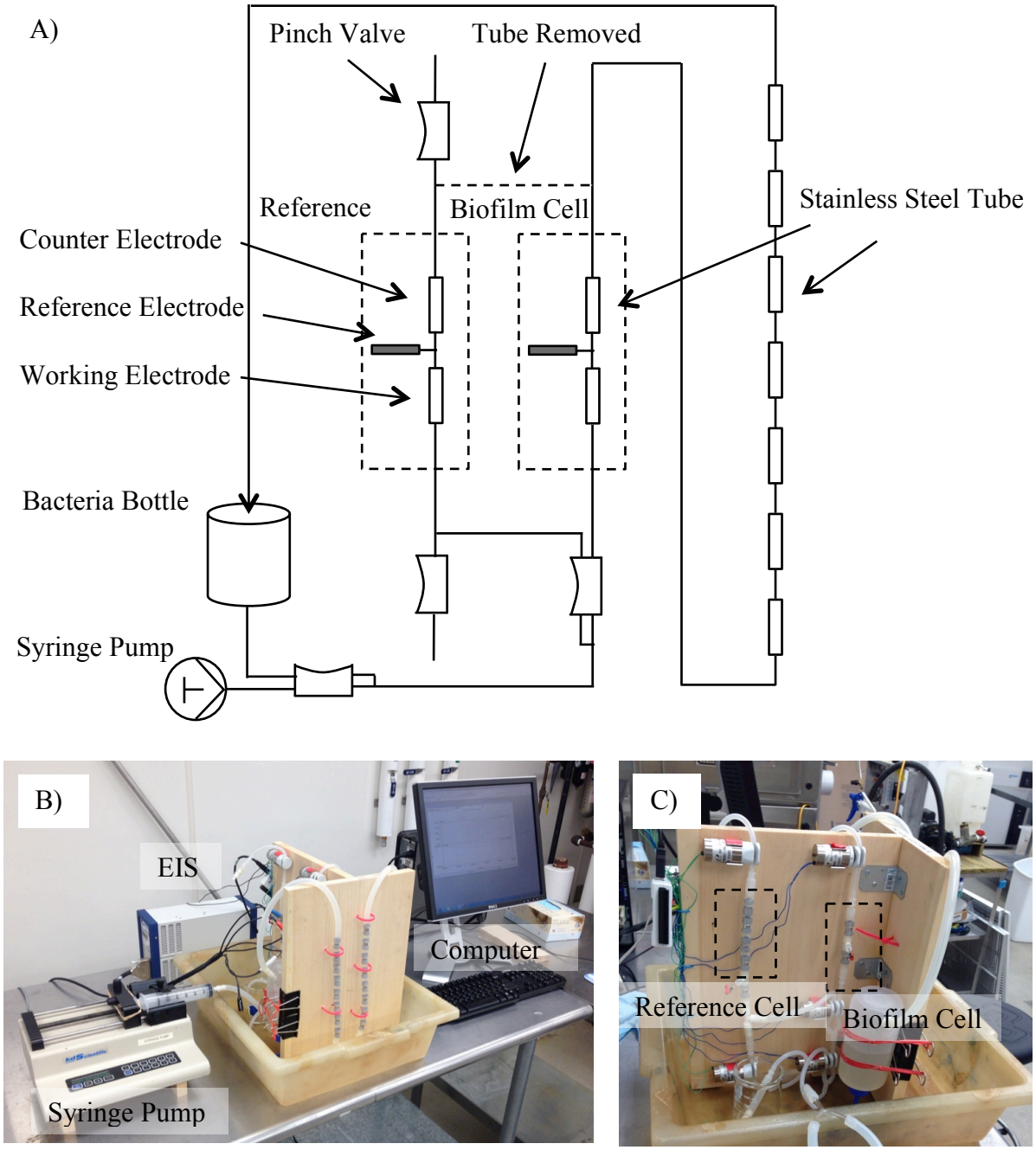

Figure 2.3. Prototype 3, with reference fluid collected as waste. First prototype used to collect experimental data. A: Flow system layout, similar to prototype 1, only deleted one piece of tube. B: Whole system looks. C: Biofilm cell and reference cell positions on board.

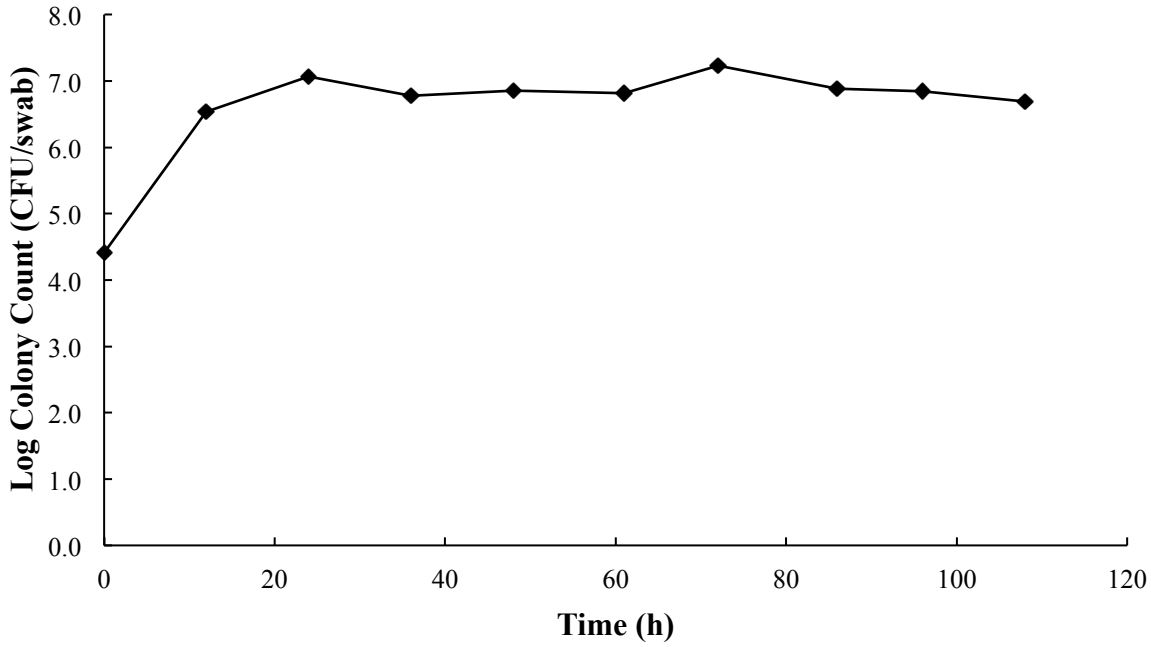

Figure 2.4. *P. putida* biofilm microbial counts using prototype 3 for 0 - 108 h with sampling every 12 h.

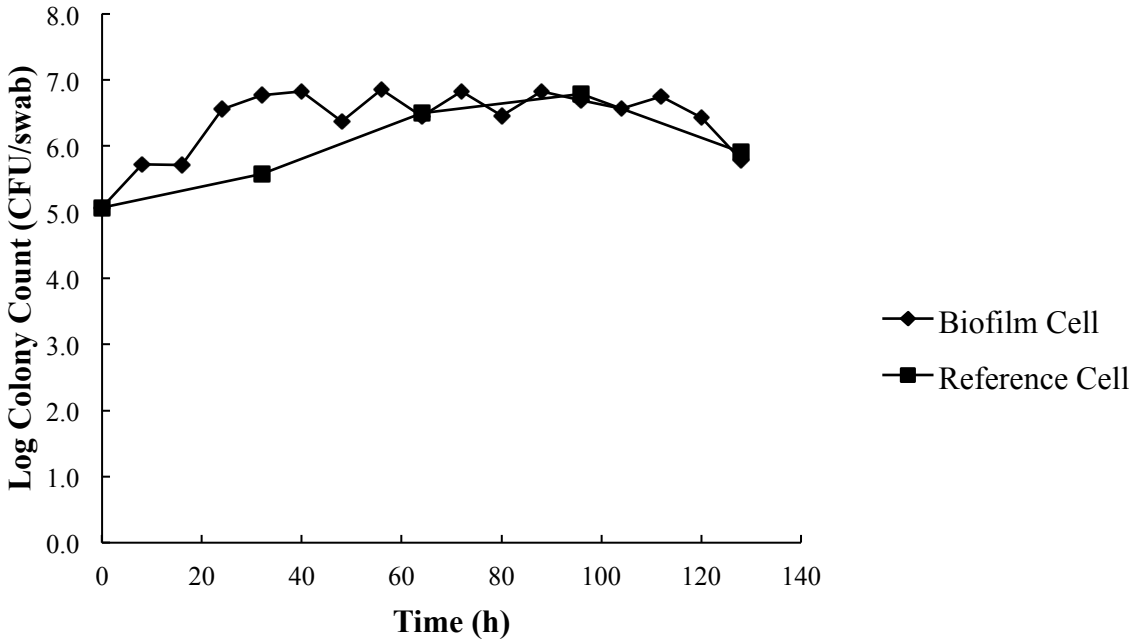

Figure 2.5. *P. putida* biofilm microbial counts using prototype 3 for 0 - 128 h with sampling every 8 h.

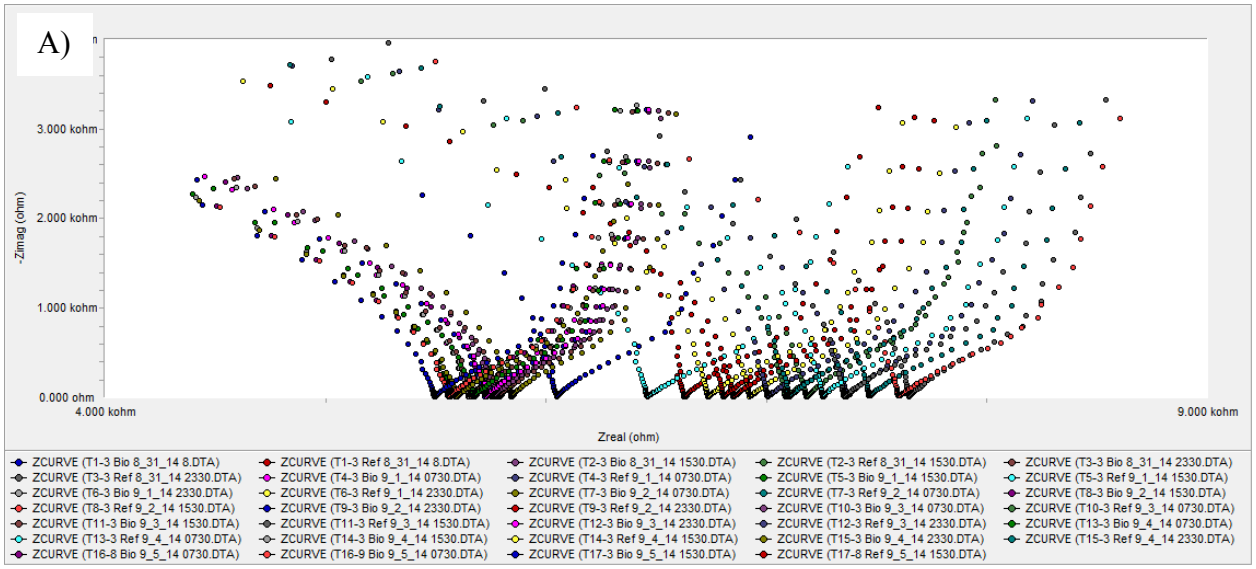

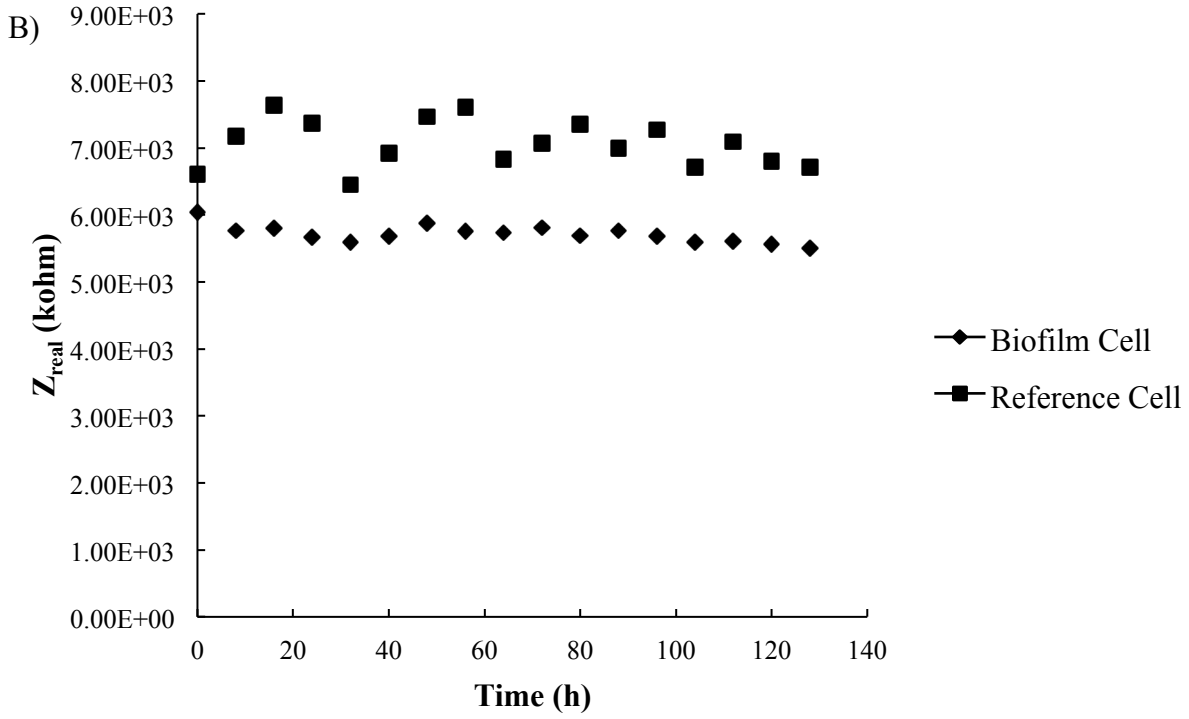

Figure 2.6. Electrochemical impedance spectroscopy during the growth of *P. putida* biofilm for 128 h using prototype 3. A: Nyquist plots for biofilm cell and reference cell. B: Impedance change of biofilm cell and reference cell.

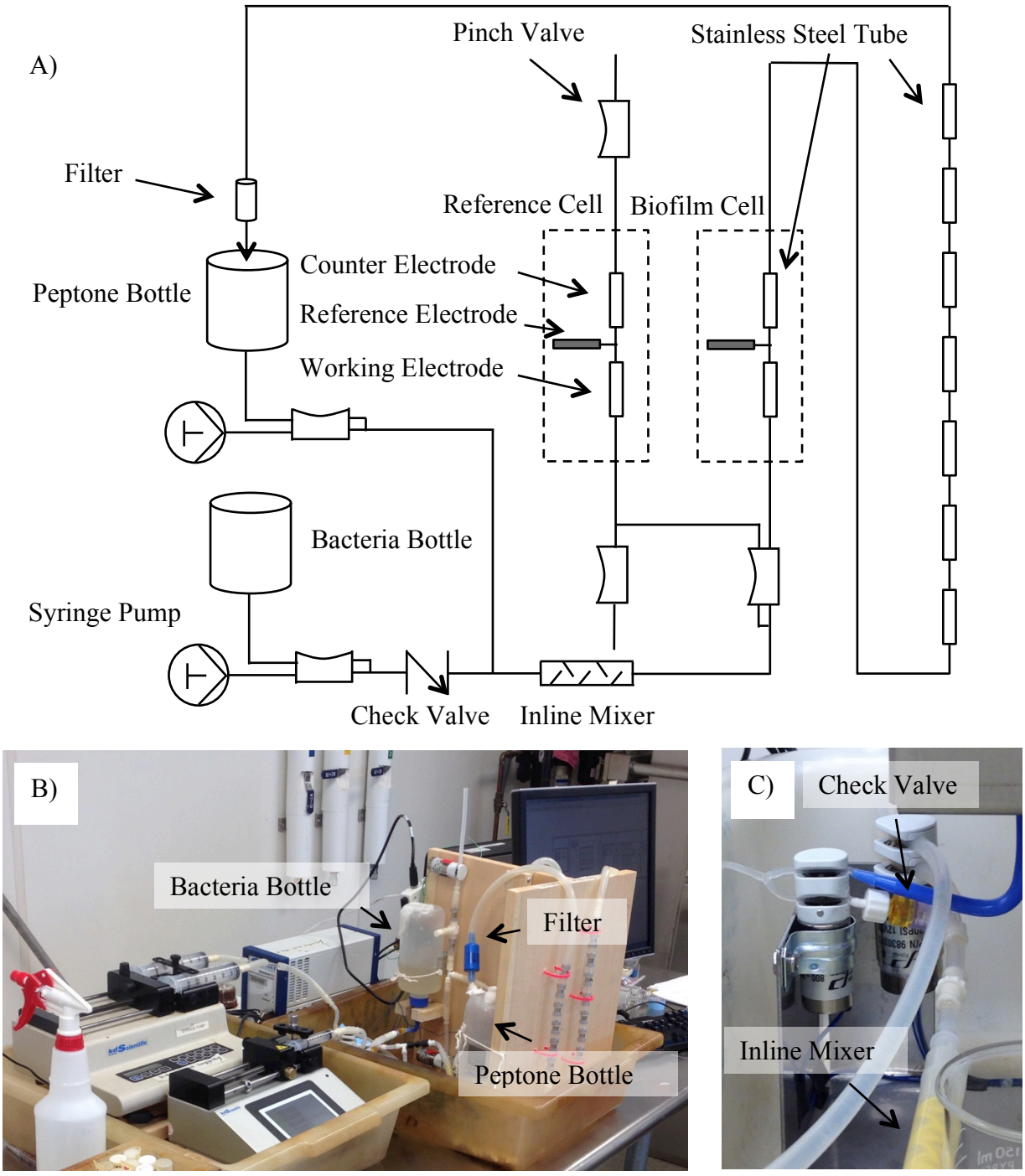

Figure 2.7. Prototype 4, including continuous dilution and mixing to slow down the growth rate of biofilm. A: Flow system layout, two bottles system. B: Whole system looks. C: Valves used to control the mixing operation.

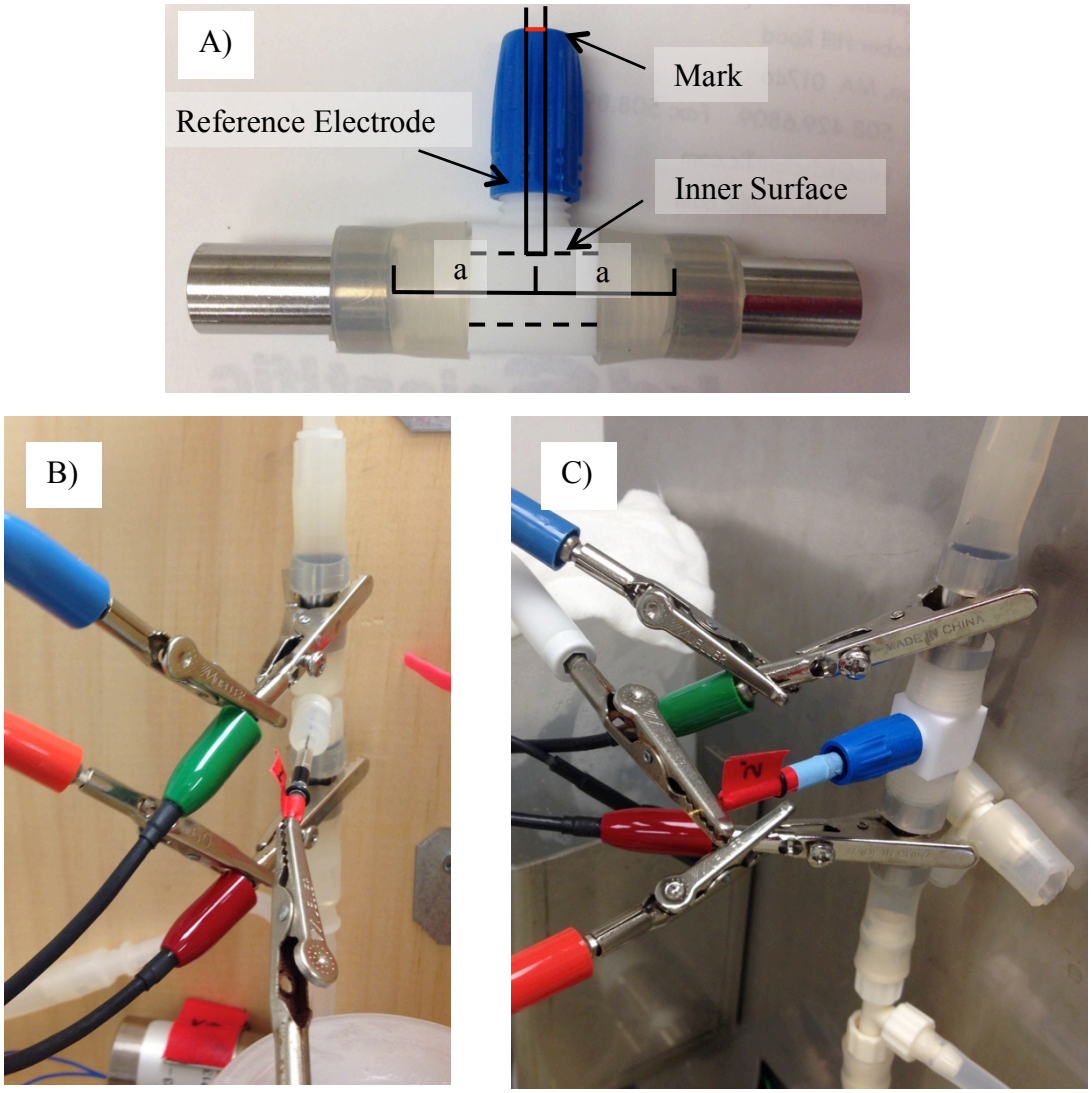

Figure 2.8. Types of connectors used for electrodes holding. A: New connector. B: Connector used in Prototype 1, 2, 3, connected with electrodes. C: New connector connected with electrodes.

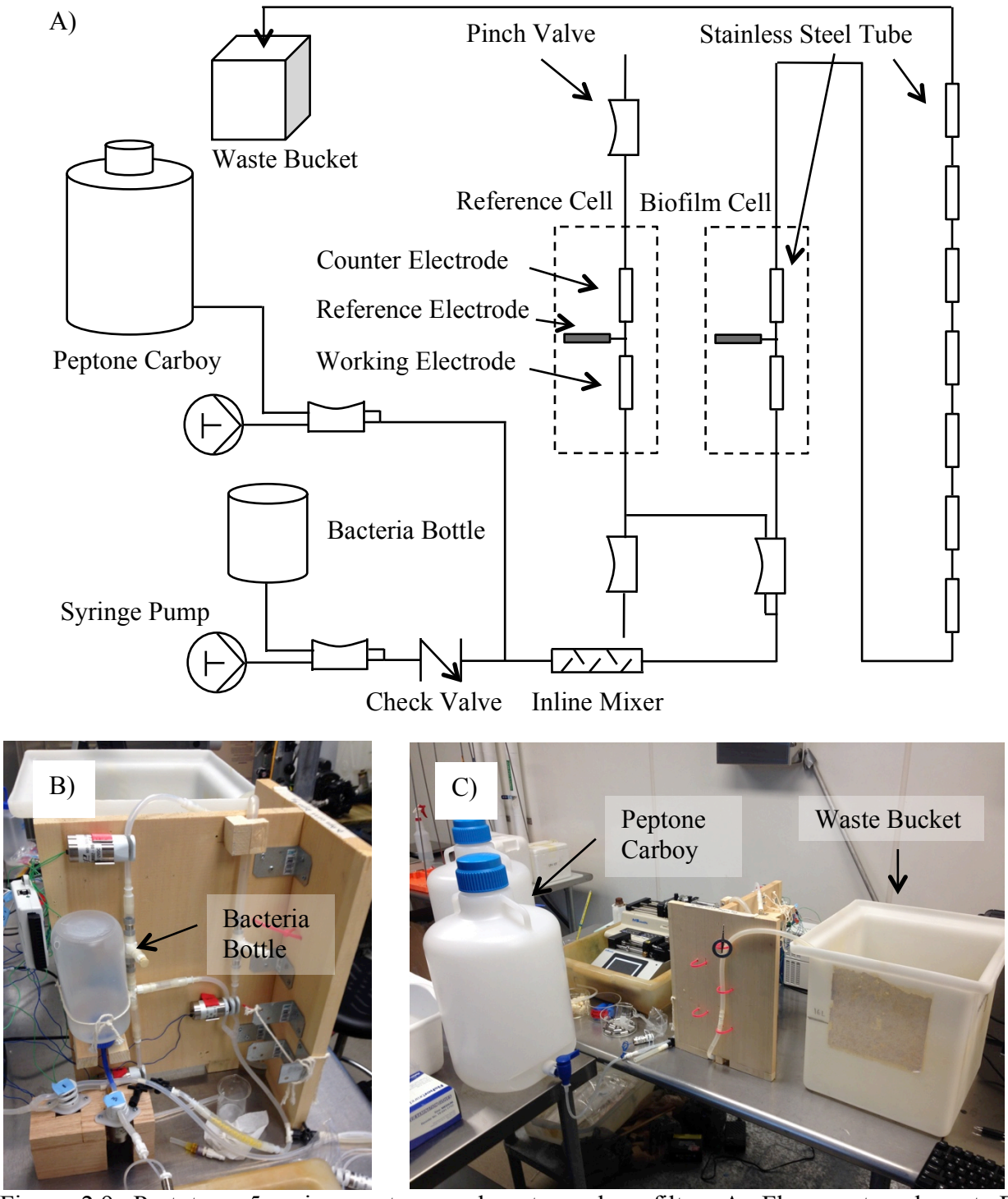

Figure 2.9. Prototype 5, using peptone carboy to replace filter. A: Flow system layout. B: Bacteria bottle side of the supporting board. Peptone bottle was removed. C: The whole system, peptone carboy and waste bucket were included.

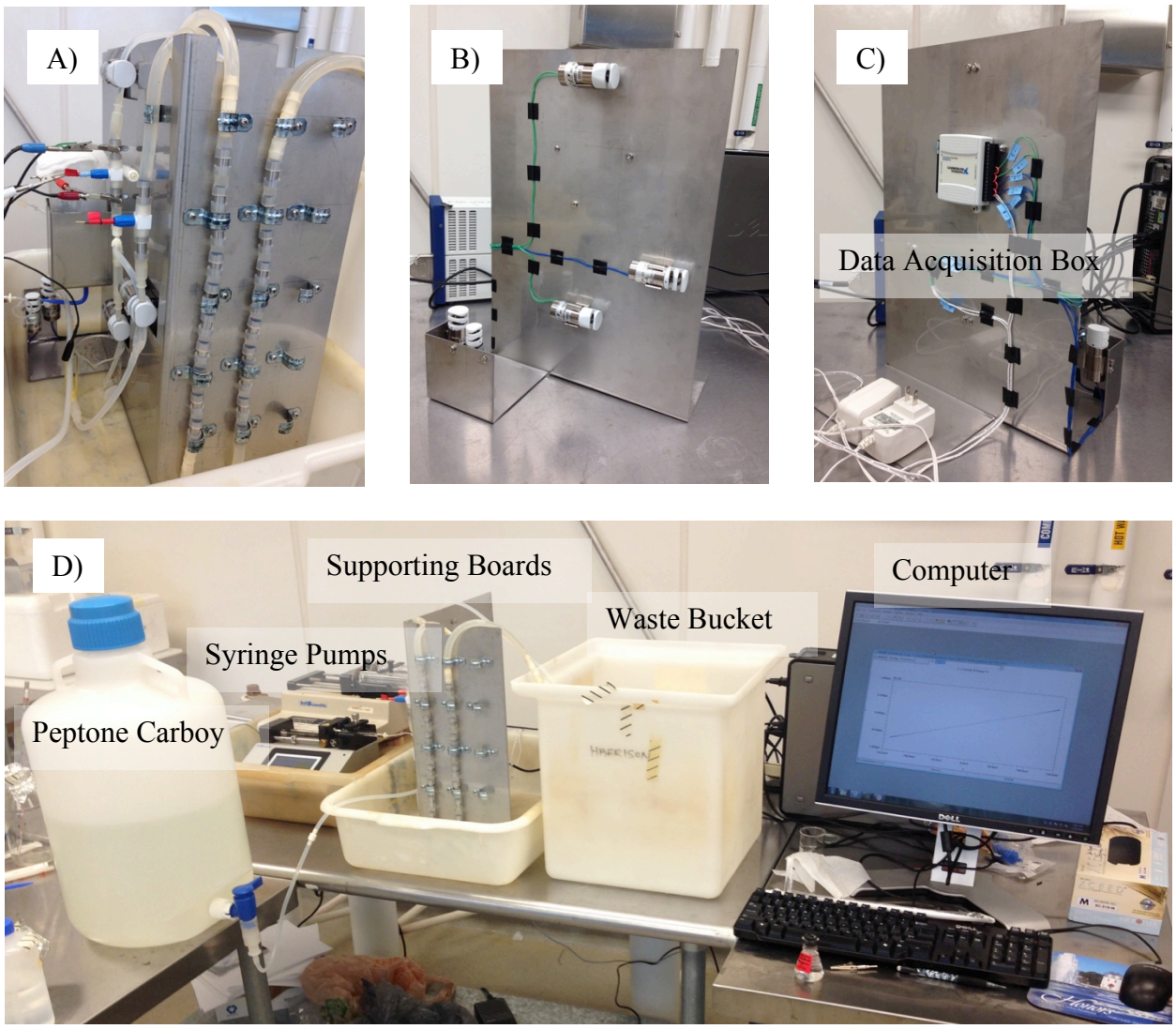

Figure 2.10. Prototype 6, stainless steel 304 supporting boards, comprising a "tubing" board and a "holding" board. A: Assembled boards with tubes on. B: Front side of the "Holding" board. C: Reverse side of the "Holding" board. D: Complete system assembly.

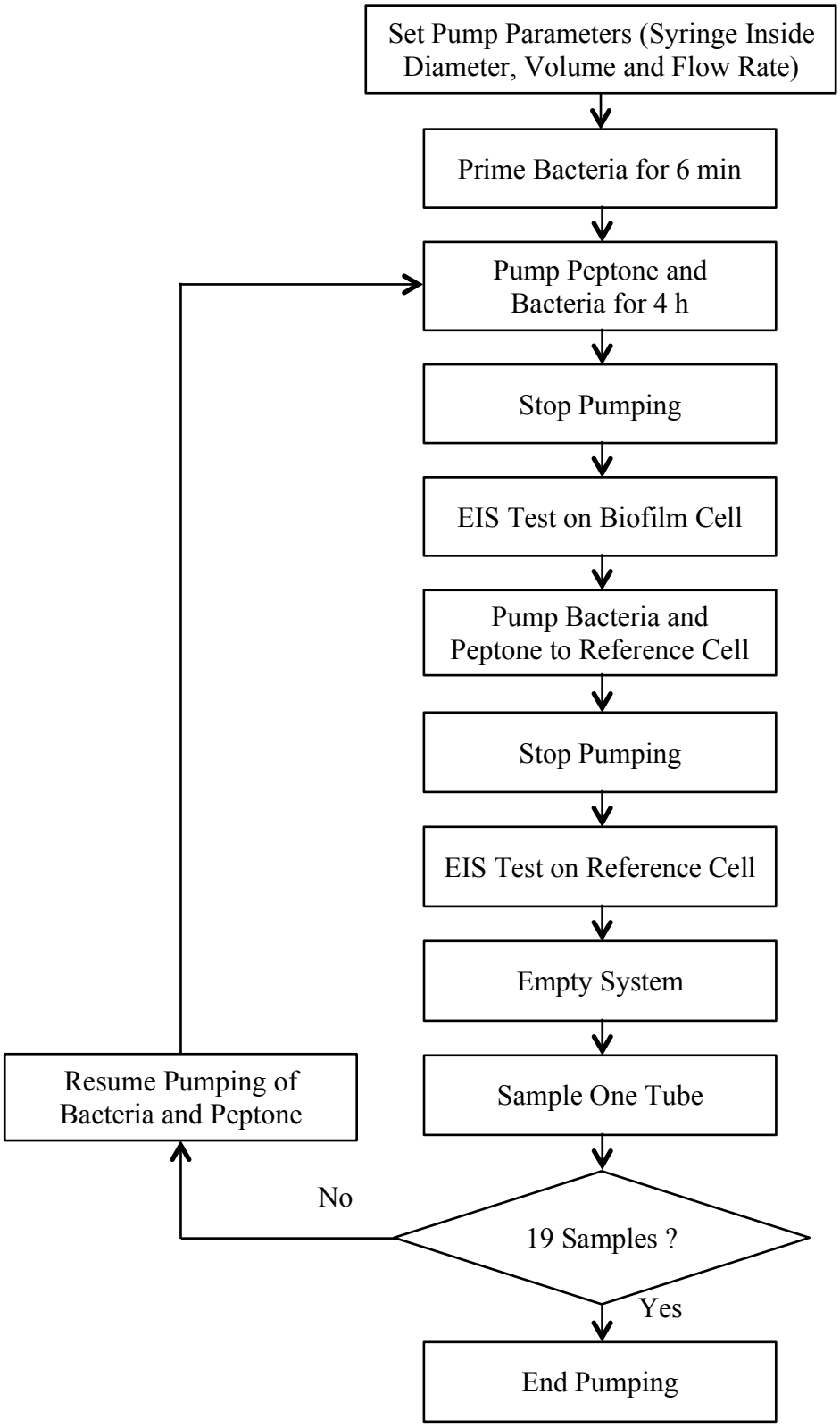

Figure 2.11. Sequence of steps for automatic control system.

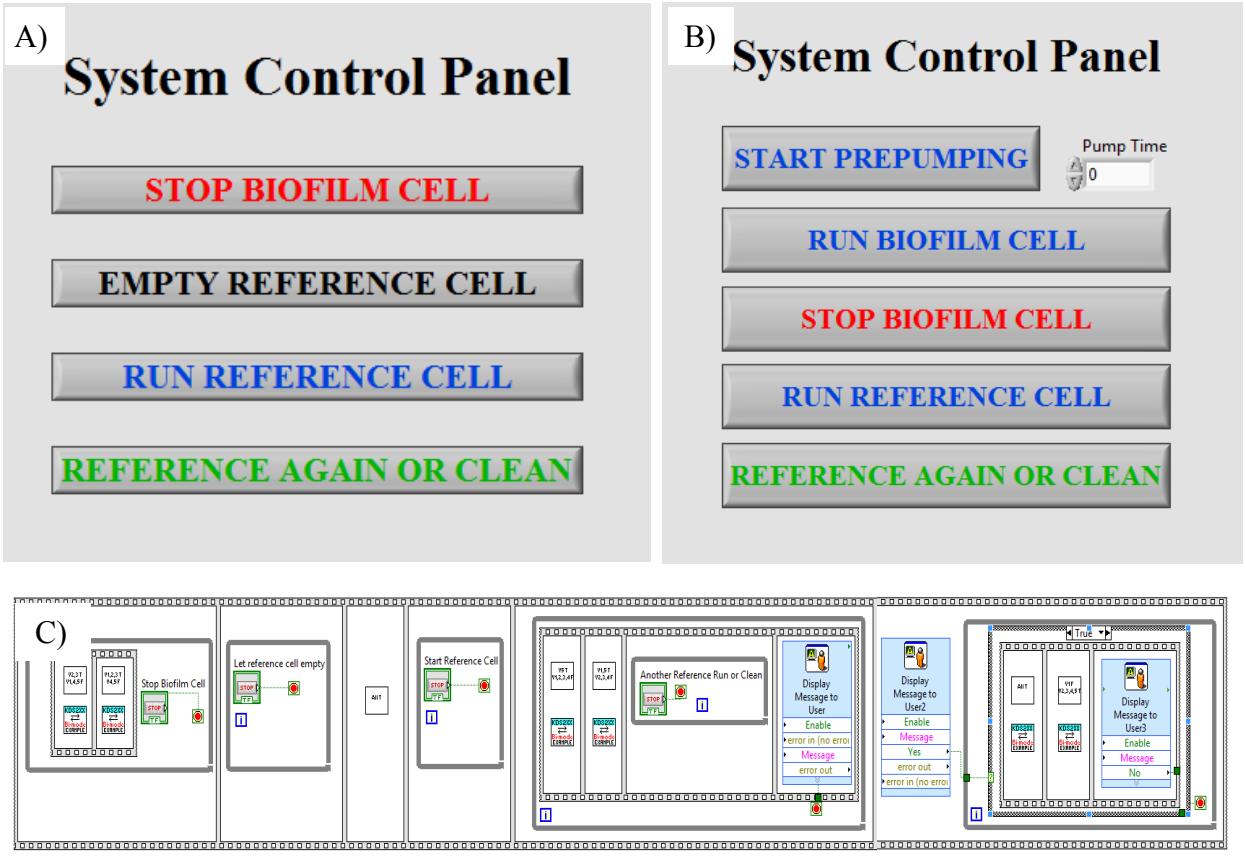

Figure 2.12. LabVIEW programs using sequence structure. A: Control panel for prototype 3. B: Control panel for prototype 5. C: Sequence structure for prototype 3.

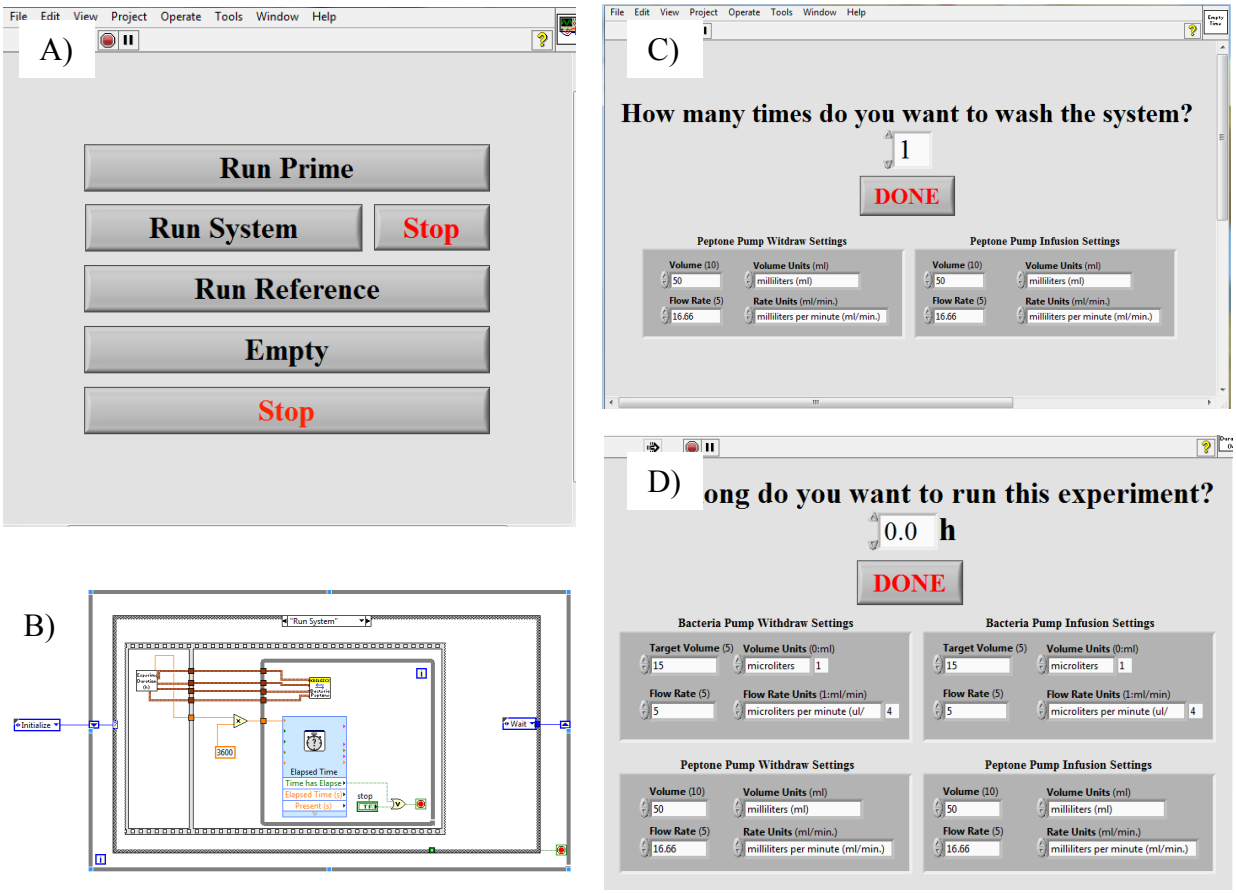

Figure 2.13. LabVIEW program using event structure. A: Control panel for prototype 6. B: Event structure. C: Wash time checking when clicking “Empty” button. D: Parameters checking when clicking “Run System” button.

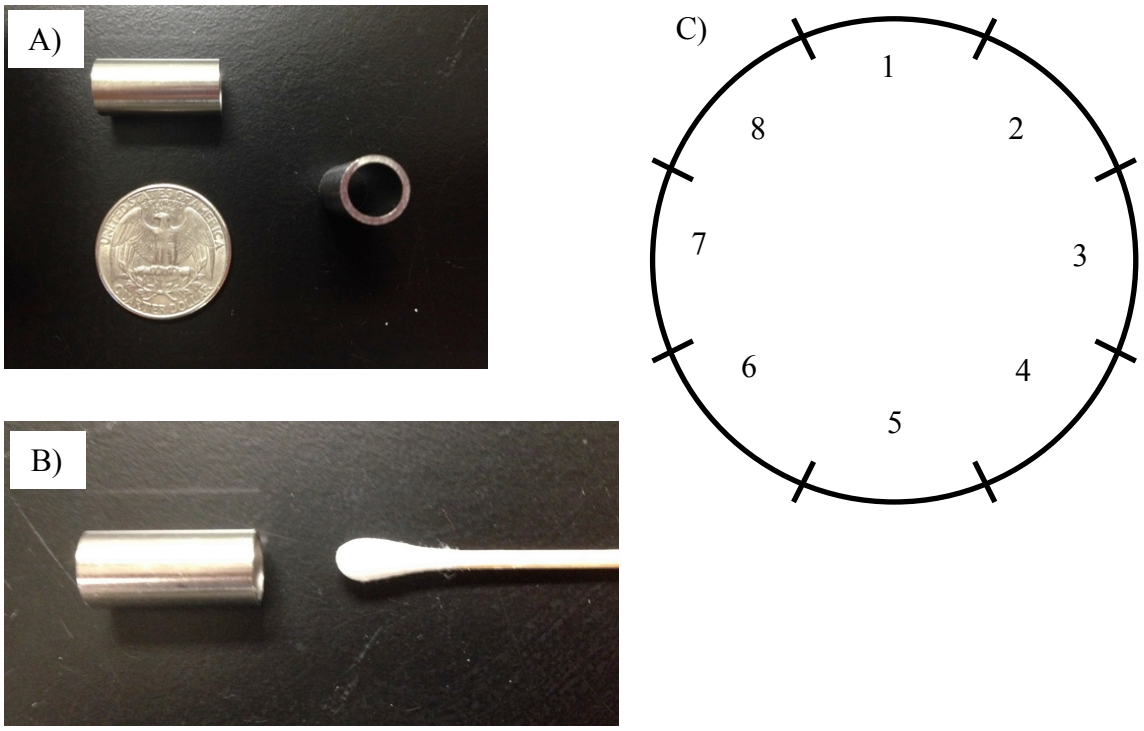

Figure 2.14. Stainless steel tube size and eight swabbing directions inside the tube. A: Tube placed horizontally and vertically compared to the size of a quarter coin. B: Tube and cotton tip used for swabbing. C: Eight swabbing directions on the inner surface of the tube sample.

Table 2.1. Comparison of inline mixers

Sample Number	Colony Count (CFU/ml)		
	4 Elements	8 Elements	12 Elements
1	$> 2.6 \times 10^5$ est.	$> 2.6 \times 10^5$ est.	1.0×10^5
2	$> 2.6 \times 10^5$ est.	1.6×10^5	1.0×10^5
3	7.6×10^4	$< 1.1 \times 10^4$ est.	2.4×10^5

Table 2.2. Data reproducibility of two different kinds of connectors and the reference electrode insert depth influence

Old Connector (0.1 M Potassium Phosphate Buffer)		New Connector (Peptone water)	
Reference Electrode	Z_{real} (kΩ)	Reference Electrode	Z_{real} (kΩ)
Position 1	9.4	Position 3	184.2
Position 2	8.6	Position 3	191.3
Position 3	7.3	Position 3	183.7
Position 4	7.4	Average +/- Standard Deviation	186.4 +/- 4.3
Position 5	7.4		
Position 3	7.3	Coefficient of Variation	2.2%
Average +/- Standard Deviation	7.9 +/- 0.9		
Coefficient of Variation	11.2%		

Position 3 is the place where reference electrode is at the inner surface of the connector shown in Figure 2.8. Position 1, 2 are inserted deeper and Position 4, 5 are inserted outer.

Table 2.3. Summary of prototype evolution

	Prototype 1	Prototype 2	Prototype 3	Prototype 4	Prototype 5	Prototype 6
Tube Direction	Horizontal	Vertical	Vertical	Vertical	Vertical	Vertical
Reference Cell Fluid Back to the System	Yes	Yes	No	No	No	No
Reference Cell Change Every Time	No	No	No	Yes	Yes	Yes
Reference Electrode Mounting	Unfixed	Unfixed	Unfixed	Fixed	Fixed	Fixed
Dilution Making	No	No	No	Yes	Yes	Yes
Filter Used	No	No	No	Yes	No	No
Large Peptone Carboy	No	No	No	No	Yes	Yes
Board Material	Wood	Wood	Wood	Wood	Wood	Stainless Steel
Board Number	1	1	1	1	1	2

CHAPTER 3

RESULTS AND DISCUSSION

3.1. Flow System

Six prototypes in total were built to ensure functionality, cost, and durability for future research.

3.1.1. Functionality

Good experiment result is always at the top of the priority when doing research. Prototype 2 placed the system vertically to solve the bubble problem in order to read EIS data. Prototype 3 discarded one tube piece to lower reference cell contamination risk. Including diluting procedure to slow biofilm growth speed, prototype 4 intended to observe impedance change with a new design.

3.1.2. Cost

Cost must be considered for any research whose final goal is for an application. Therefore, lower the cost should start from the experiment stage. When designing prototype 5, the costs of peptone and filter were compared. The much more expensive inline filter was discarded and a regular changed peptone carboy was replaced instead.

3.1.3. Durability

Similar to the cost, a system should last long if is designed as a potential product. Therefore, though having similar functions, prototype 6 was designed using stainless steel 316 to replace the wood used in prototype 5.

3.2. Microbial Counts

Original bacterial suspension and diluted suspension concentrations over 72 h are shown in Figure 3.1. Colony count (CFU/ml) was graphed on a log scale to better show the changing trend. Both suspensions' concentrations were stable. The original bacterial concentration stayed at 8.7 +/- 0.1 log CFU/ml for the whole 72-h test, while the diluted suspension stayed at 5.1 +/- 0.3 log CFU/ml starting from 4 h. Though having a 14.6% increase in the last 24 h, the diluted concentration was still within 10^5 CFU/ml. Therefore, the flow system dilution procedure was proved practical for at least 72 h.

The biofilm growth curve is shown in Figure 3.2. Colony count was calculated and shown in log CFU/swab. Each swab represented the whole tube piece inner surface area (10 cm^2). In the first 12 h, the count number was too small for TPC method to have an accurate calculation. Since the cotton tip was diluted in the 9-ml peptone and then 0.1 ml dilution was transferred onto TSA, the total dilution factor was 90. And the minimum accurate bacterial count is 25 on a plate. Therefore, the detection limit for TPC in this study was 2.3×10^3 CFU/swab. At 16 h, biofilm reached 3.9 log CFU/swab, which was the lowest detection counts for TPC in this experiment. In the 48 h that followed, the biofilm kept growing and then stayed 6.9 +/- 0.1 log CFU/swab for the last 8 h.

In other studies using EIS to monitor biofilms, the bacterial suspension concentration was seldom controlled. Common control methods include changing fresh culture medium regularly (Dheilly et al., 2008) and using a high initial concentration to run short-term experiments. One example for the latter one is Paredes et al. (2013) who used two different initial concentrations (10^5 CFU/ml and 10^7 CFU/ml) to run a 20-h experiment. It turned out that the higher initial concentration used, the faster the biofilm formed and the quicker EIS data started to change. This

was also pointed out by Yang et al. (2004b), indicating that EIS detection time highly relied on the initial bacterial concentration. In our study, the biofilm growth curve (Figure 3.3) clearly shows the number increase over a reasonable and relatively long-time range. It took 64 h to reach the maximum stable concentration (~7.0 log CFU/swab). Hence, our flow system enables EIS monitoring with controlled initial concentration and proper biofilm growth speed. In fact, in the industry, the bacterial suspension concentration is never constant or at such a high level (10^5 CFU/ml) as in our study. However, for this study, flow rate and microbial suspension concentration were adjusted to allow completing one entire biofilm formation time series replicate within one week at the most and show proof-of-concept.

For other flow systems already designed, Pires et al. (2013) used the "seeding and growth" strategy. Bacteria *Pseudomonas aeruginosa* (10^8 CFU/ml) was only introduced during the seeding step and some bacteria could attach the surface. Then, during the rest of the experiment, no fresh bacteria were used and the biofilm was grown from the already attached bacteria. Sterilized medium was used to flow through the system continuously when the biofilm was forming. Hence, biofilm growth speed was slowed, but how much attachment occurred was unknown and biofilm growth was unpredictable only using sterilized medium.

3.3. Electrochemical Impedance Spectroscopy

Unlike the other studies, our system used stainless steel tubes' inner surface as the biofilm attachment surface. We were able to use identical stainless steel tubes, as many others in the system for TPC sampling, as the working electrode and counter electrode. Among many similar studies, only Dheilly et al. (2008) chose metal surfaces to study biofilm attachment. Similar to the stainless steel 316 used in our flow system, they used stainless steel 304 but in the form of grids and coupons. They also used those grids and coupons as working electrodes. In our case,

the advantage of using stainless steel tubes as working and counter electrodes is that there is no need to insert extra electrodes into the system which lowered the inserted required electrode number to one, which is the reference electrode only. Considering stainless steel is the major material used in the food industry for most pipelines, using stainless steel tubes and fewer inserted electrodes make it easier to develop the real-time inline biofilm detector in the future.

Figures 3.3 and 3.4 are the Nyquist plots for the biofilm cell and the reference cell respectively from replication 3 as an example. Nyquist plots of the other replications are similar. Each one has 19 spectra measured in 72 h. These Nyquist plots all consist of a semicircle and a straight line, standing for an electron-transfer-limited process and a diffusion-limited process. Since the frequency increases from the right to the left, the reason why a portion of the semicircle is missing is that the equipment maximum frequency limit is 1 MHz. For the biofilm cell, the plots have a shift to the left and a semicircle diameter decrease, which means both Z_{real} and Z_{imag} decreased as biofilm grew. In contrast the reference cell curves also have the same change but not as big as the biofilm cell, which means medium impedance did change in the experiment. The maximal Z_{imag} is the diameter of the semicircle. It decreased by 39.9 +/- 2.6% for the biofilm cell and 15.9 +/- 4.9% for the reference cell.

Figure 3.5 gives a clearer look on the Z_{r0} change for both biofilm cell and reference cell. Z_{r0} is the Z_{real} at frequency 1 kHz and it is also where Z_{imag} is the minimum. For the first 24 h, the biofilm cell Z_{r0} stayed stable at 180.0 +/- 5.7 kΩ and then started to decrease after 28 h. It decreased steadily until 64 h and remained almost constant at 122.7 +/- 1.5 kΩ for the last 8 h. The total Z_{r0} decrease for biofilm cell was approximately 32.2%. On the contrary, the reference cell Z_{real} decreased from 182.6 kΩ to 155.3 kΩ, which was around 15.0%, much smaller than biofilm cell.

The impedance for the reference cell did have a minor decrease during the experiment. Though there must be metabolism occurring during the experiment, the reference cell impedance change probably means nothing but experiment error. The sterilized peptone Z_{r0} is around 180 kΩ and the 1/10 TSB Z_{r0} is around 8,000 kΩ. Since the flow system was making 10,000-fold dilution, the medium impedance change would not exceed 0.8 kΩ, which was much smaller than the actual impedance change (27.4 kΩ). Therefore, the variation detected by the reference cell may be due to changes in individual working electrodes and artifacts of cell manipulation during assembly and disassembly. Further experiments are needed to elucidate the sources of variability in the EIS response of the reference cell.

To study the actual biofilm impedance change, a corrected Z_{real} (Biofilm Cell Z_{r0} minus Reference Cell Z_{r0} at 0 h) was used. Figure 3.5 exhibits the corrected Z_{real} change through the 72-h biofilm growth period. After a 24-h stable phase (1.2 +/- 5.7 kΩ), it started to decrease at 28 h and stopped at 60 h. The total decrease was approximately -735.8%. For the last 8 h, the corrected Z_{real} remained constant (-56.0 +/- 1.5 kΩ).

Impedance decrease reported here is in agreement with the results of Bayoudh et al. (2008). It can be explained that transfer charges increase when negatively charged bacterial cells attach and have charge transfer to the electrode surface, resulting in the decrease of charge transfer resistance and impedance magnitude. Kim et al. (2012) also had a similar result with a Nyquist plot consisting of a semicircle with diameter decreasing as the biofilm grew. They explained that this was due to the charge transfer resistance decrease however only accounted for leakage current in their experiment.

Many studies reported opposite results to ours. Their impedance or electron transfer resistance increased as the biofilm grew. For example, using *Pseudomonas aeruginosa*, Dheilly

et al. (2008) observed that the resistance increased with the biofilm growth. They explained that this was because an electron-transfer barrier was formed between the redox probe and the electrode surface, resulting from the cells' attachment. Some of the others focused on explaining the results using capacitance change. Based on existing studies, double layer capacitance is increased by bacterial cell growth and decreased by bacterial attachment (Kim et al., 2012). Therefore, impedance change can be influenced by many different factors specifically in each experiment, including the medium used, temperature, bacterial strain, etc. The best impedance parameter to explain the change can also be different. Equivalent models will be built in the near future to better explain the impedance change in this study.

The smallest concentration that was detected in this study was 2.3×10^5 CFU/swab, which was approximately 10^4 CFU/cm^2 given that the inner surface area of each tube piece was 10 cm^2. This is similar to another biofilm monitoring study. Paredes et al. (2013) used interdigitated array microelectrode' to detect *Staphylococcus aureus* and *Staphylococcus epidermidis* biofilm growth in 96-well plates for 20 h. The initial bacterial concentration was 10^5 CFU/ml. It was observed that the impedance started to change at around 6 h and the corresponding biofilm was approximately 10^4 CFU/cm^2.

Biofilm detection limits using the EIS method are rarely discussed in current studies because it is a major disadvantage for label free electrode systems or biosensors. However, for bacterial suspension, the detection limit can be lowered to 10^2 CFU/ml with antibody-immobilized electrodes in magnetic fields (Dong et al., 2013; Nandakumar et al., 2008). However, unlike monitoring bacteria in suspension, biofilm detection is a relatively long-term process, especially when the bacterial concentration is low. Immobilizing antibodies to the

electrodes is no longer practical because damage is very likely to occur on the immobilized antibodies and influence the detection sensitivity and results (Paredes et al., 2013).

Nevertheless, Munoz-Berbel et al. (2008) claimed the correlation between the interface capacitance with different suspended bacterial concentration existed from 10^1 to 10^7 CFU/ml. They did the experiment within 1 min and focused on the biofilm pre-attachment stage. However, their finding has little use because it is more like monitoring the bacterial suspension instead of the biofilm. They did use a microscope to observe biofilms for comparison, but the optical results only provided biofilm images using bacterial suspension concentration starting from 10^3 CFU/ml. The real detection limit was difficult to determine and the capacitance change pattern was different after the short pre-attachment period (several minutes). What's more, the platinum electrodes they used continuously lost their capacity to measure the capacitance with more and more biofilm residue left on them.

In our study, Figure 3.7 is the combination of TPC and EIS test results. This is to look for any possible correlation between the corrected Z_{real} and biofilm colony count. Biofilm increased from 1.0×10^4 to 2.3×10^5 CFU/swab at 28 h, which was the point where corrected Z_{real} started to have a decrease as shown in Figure 3.7. From 28 h to 60 h, a straight line was fitted and showed a linear trend between corrected Z_{real} (Z_{rc}) and log biofilm colony counts (C). The line equation was $Z_{rc} = -23.3\ C + 100.9$ with $R^2 = 0.772$. This linear regression correlated biofilm microbial counts with a part of the impedance spectrum. It means when biofilm counts were within the range of 5.2 to 7.0 log CFU/swab, the corrected Z_{real} decreased 2.33 kΩ with every 0.1 log CFU/swab biofilm counts increase. In other words, the measurement sensitivity was 23.3 kΩ/(log CFU/swab) within the linear range. The detection limit for this regression fell between 4.0 to 5.0 log CFU/swab. This is the only linear relation among current similar studies. With this

correlation, *P. putida* biofilm growth can be predicted using the same controlled bacterial concentration. However, more experiments are required for confirmation.

Though very few studies including this have used EIS to monitor biofilm growth, this approach has a potential use in the food industries, especially in juice processing and water distribution systems. However, for high protein content food, the protein sediment attached to the surface can interfere impedance result and at least not suitable for impedance measurement used in this study.

3.4. Summary and Conclusions

With the ability to change syringe and pump parameters, this system allowed us to adjust the flow suspension concentration and hence change biofilm-growing speed. Therefore, this flow system has potential to make any growing speed biofilm with different microorganisms in a long experiment time. Impedance change was also observed as the biofilm grew and a linear regression was found to correlate biofilm microbial counts with a part of the impedance spectrum, indicating EIS can be used on this system to monitor biofilm growth.

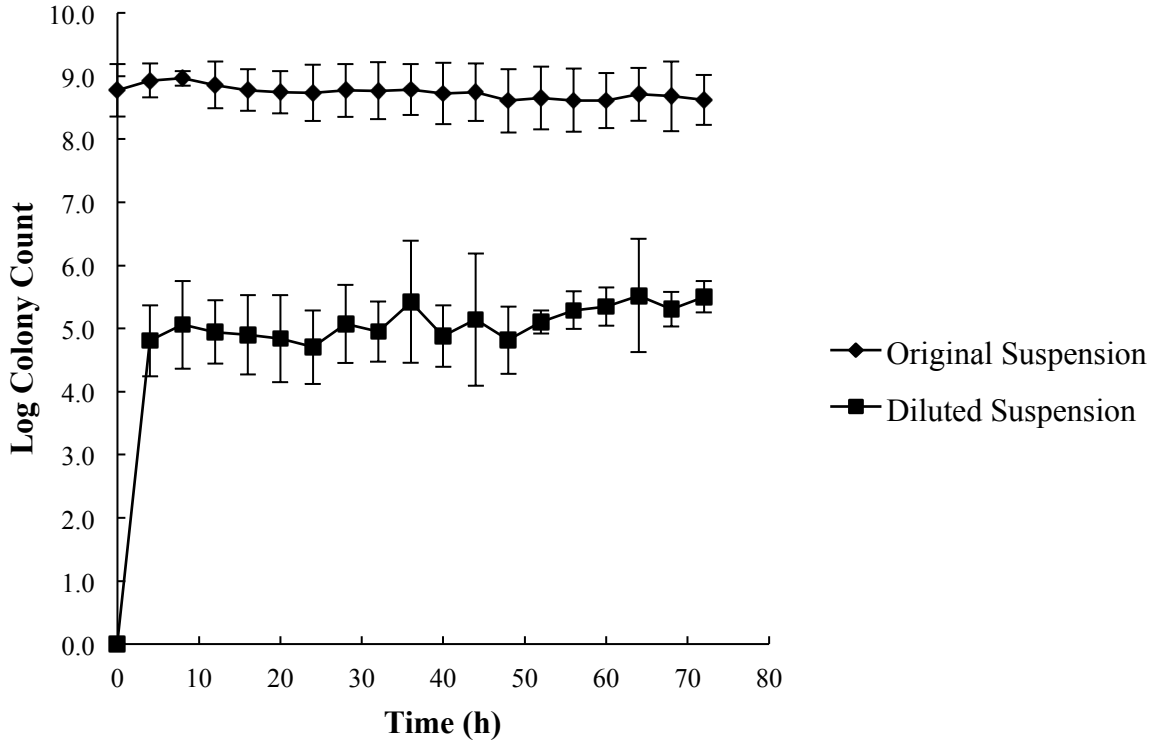

Figure 3.1. Original and diluted bacteria suspension concentration. Original suspension was sampled directly from the bacteria bottle; diluted suspension was sampled from the tube outlet. Both suspensions were sampled every 4 h in three 72-h tests. Error bars are the standard deviations.

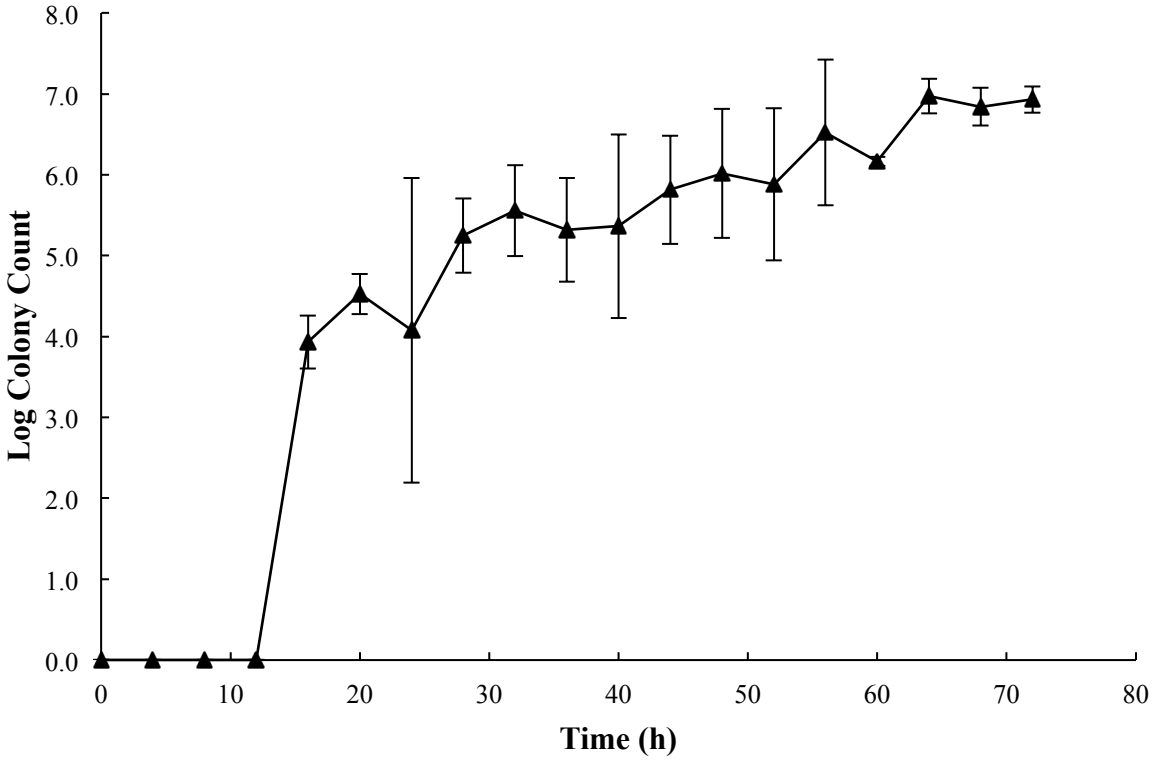

Figure 3.2. Biofilm growth curve. Tube was sampled every 4 h in three 72-h tests. Error bar is the standard deviation.

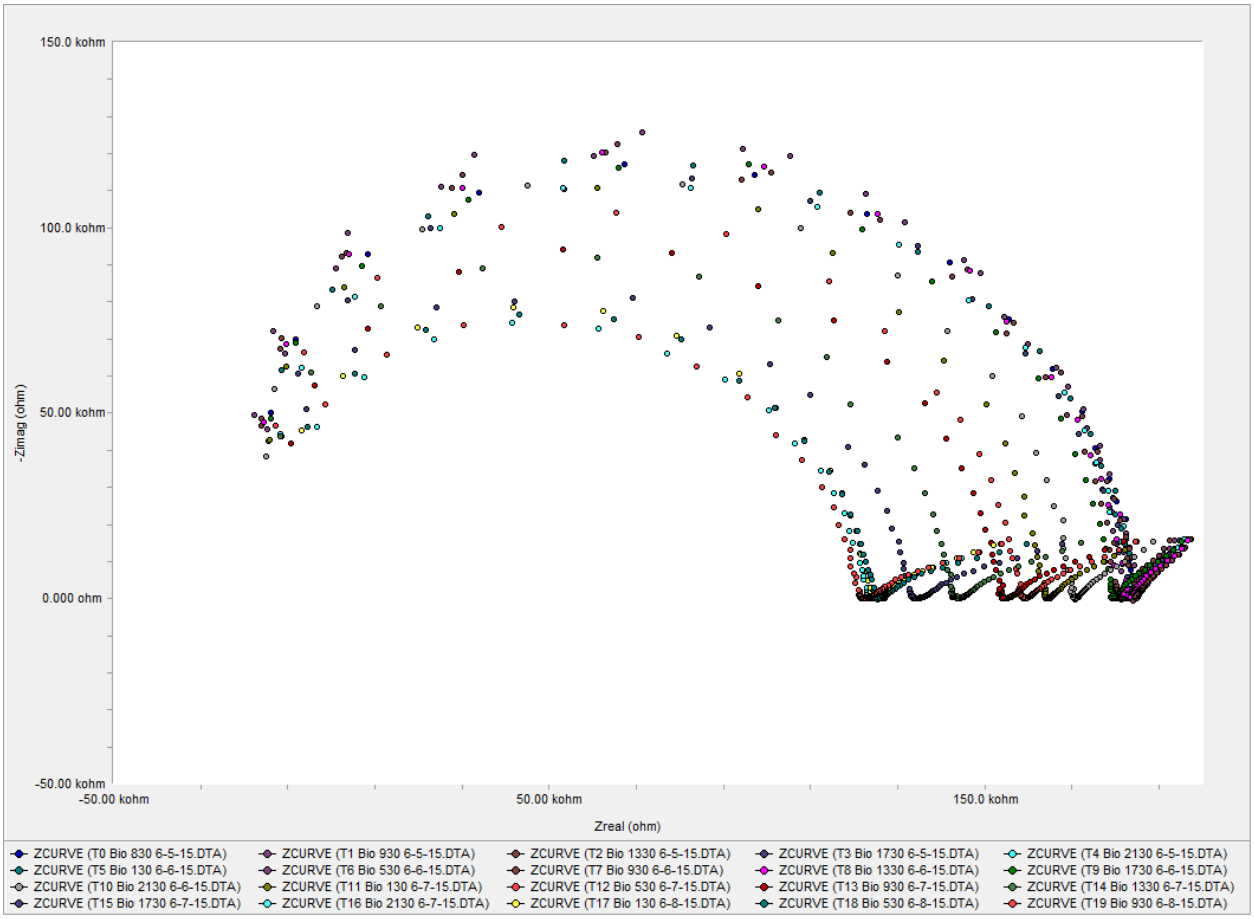

Figure 3.3. Biofilm cell Nyquist plots from replication 3. Produced by Gamry Echem Analyst software. Tested every 4 h for 72 h in total.

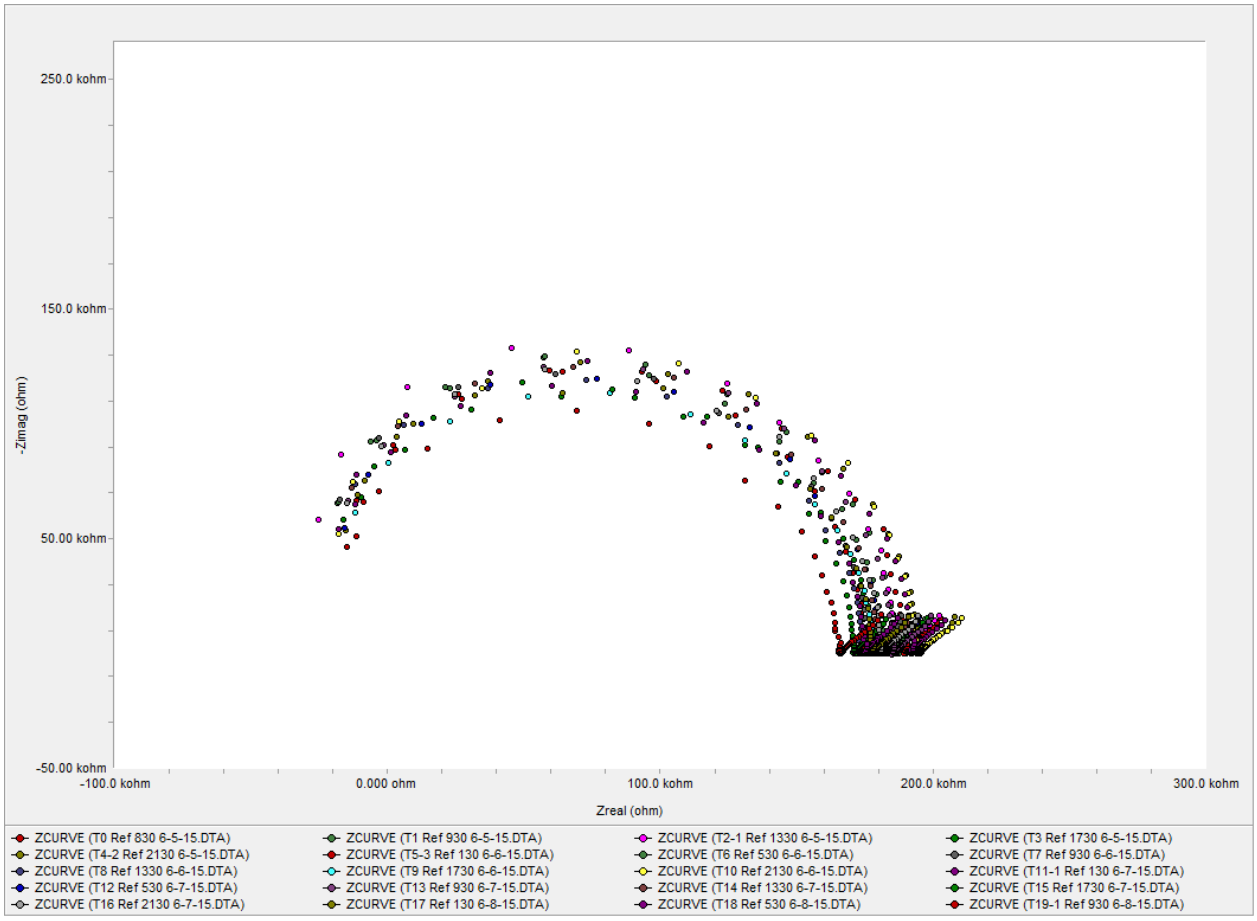

Figure 3.4. Reference cell Nyquist plots from replication 3. Produced by Gamry Echem Analyst software. Tested every 4 h for 72 h in total.

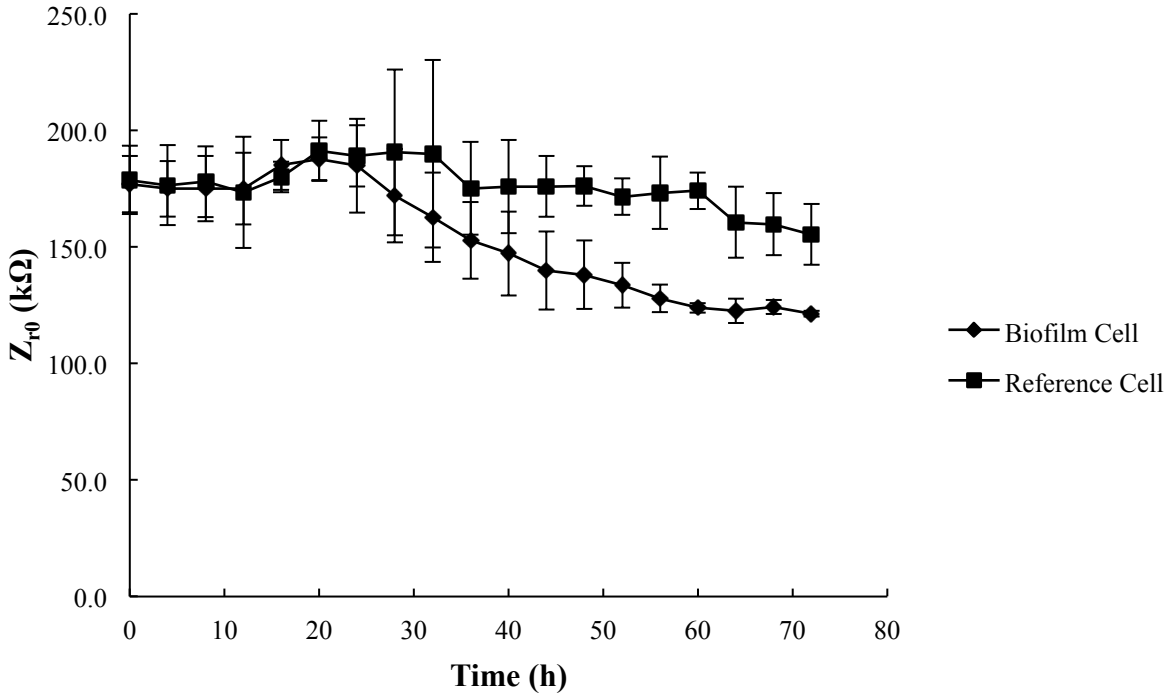

Figure 3.5. Z_{r0} changes of biofilm cell and reference cell, tested every 4 h for three 72-h tests. Error bar is the standard deviation.

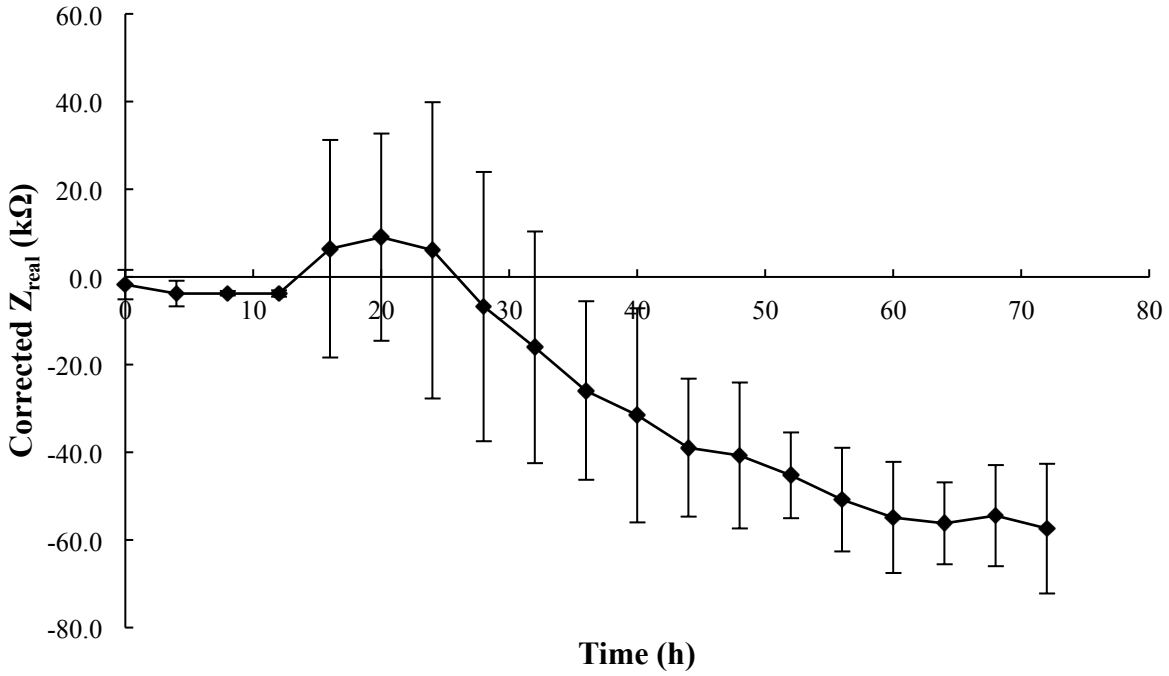

Figure 3.6. Corrected Z_{real} change during the 72-h tests. Corrected Z_{real} = biofilm cell Z_{r0} – reference cell Z_{r0} at 0 h (178.8 kΩ). Error bar is the standard deviation.

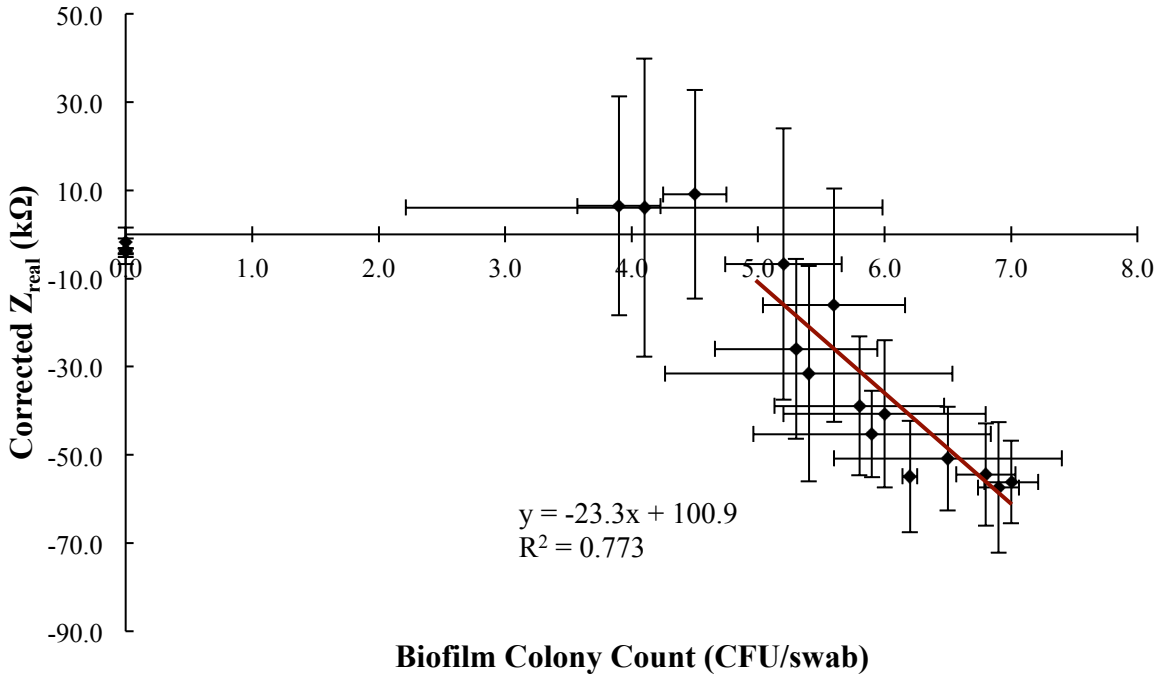

Figure 3.7. Correlation between corrected Z_{real} (y) and biofilm colony counts (x). X error bar is the standard deviation for biofilm colony count. Y error bar is the standard deviation for corrected Z_{real}.

CHAPTER 4

SUMMARY AND FUTURE WORK

A flow system was designed and constructed to monitor biofilm growth on the inner surface of stainless steel tubes over a wide range of time intervals (from minutes to days) with adjustable initial microbial populations, both by TPC and EIS methods. The system was tested using *P. putida* to grow biofilm for 72 h. *P. putida* was diluted from ~10^8 CFU/ml to ~10^5 CFU/ml and remained stable for the experiment period. Biofilm was detected by TPC after 16 h when it had reached 1.0×10^4 CFU/swab, while Z_{ro} started to decrease from 28 h when the biofilm was above 2.3×10^5 CFU/swab. The regression equation for the corrected Z_{real} (Z_{rc}) versus log biofilm colony counts (C, $5.2 < C < 7.0$) was $Z_{rc} = -23.3\ C + 100.9$ with $R^2 = 0.772$. It correlated biofilm microbial counts with a part of the impedance spectrum. Therefore, the designed flow system was proven to control *P. putida* biofilm growth well and suitable for EIS monitoring.

For future work, an EIS model must be built to fit the data first. The impedance change in the experiment cannot be further explained without it. It is also very important to understand how each parameter of the model is impacted by the biofilm formation. To better improve the flow system, peristaltic pumps should be considered to replace the syringe pumps for a more continuous pumping, and more experiments are needed to test the effectiveness of the reference cell.

Now with this flow system, the hypothesis that biofilms from single cultures specifically correlates to EIS can be tested. Different microorganisms can be tested under certain conditions.

With controlled bacterial suspension concentration, EIS monitoring performance difference under different biofilm growth speed can be studied. Long-term controlled biofilm growth is also possible now. If the hypothesis is supported, we can further test the hypothesis that EIS data of biofilm from mixtures of microorganisms correlates to the individual one.

REFERENCE

Arciola, C.R., Campoccia, D., Baldassarri, L., Donati, M.E., Pirini, V., Gamberini, S., Montanaro, L., (2006). Detection of biofilm formation in *Staphylococcus epidermidis* from implant infections. Comparison of a PCR-method that recognizes the presence of ica genes with two classic phenotypic methods. Journal of Biomedical Materials Research Part A 76A, 425-430.

Barreiros dos Santos, M., Agusil, J.P., Prieto-Simon, B., Sporer, C., Teixeira, V., Samitier, J., (2013). Highly sensitive detection of pathogen *Escherichia coli* O157:H7 by electrochemical impedance spectroscopy. Biosensors and Bioelectronics 45, 174-180.

Barreiros dos Santos, M., Sporer, C., Sanvicens, N., Pascual, N., Errachid, A., Martinez, E., Marco, M.P., Teixeira, V., Samiter, J., (2009). Detection of pathogenic bacteria by electrochemical impedance spectroscopy: influence of the immobilization strategies on the sensor performance. Procedia Chemistry 1, 1291-1294.

Bayoudh, S., Othmane, A., Ponsonnet, L., Ben Ouada, H., (2008). Electrical detection and characterization of bacterial adhesion using electrochemical impedance spectroscopy-based flow chamber. Colloids and Surfaces A: Physicochemical and Engineering Aspects 318, 291-300.

Ben-Yoav, H., Freeman, A., Sternheim, M., Shacham-Diamand, Y., (2011). An electrochemical impedance model for integrated bacterial biofilms. Electrochimica Acta 56, 7780-7786.

Chen, M.-Y., Chen, M.-J., Lee, P.-F., Cheng, L.-H., Huang, L.-J., Lai, C.-H., Huang, K.-H., (2010). Towards real-time observation of conditioning film and early biofilm formation under laminar flow conditions using a quartz crystal microbalance. Biochemical Engineering Journal 53, 121-130.

Chmielewski, R., Frank, J., (2003). Biofilm formation and control in food processing facilities. Comprehensive reviews in food science and food safety 2, 22-32.

Czaczyk, K., Myszka, K., (2007). Biosynthesis of extracellular polymeric substances (EPS) and its role in microbial biofilm formation. Polish Journal of Environmental Studies 16, 799.

Dheilly, A., Linossier, I., Darchen, A., Hadjiev, D., Corbel, C., Alonso, V., (2008). Monitoring of microbial adhesion and biofilm growth using electrochemical impedancemetry. Appl Microbiol Biotechnol 79, 157-164.

Dong, J., Zhao, H., Xu, M., Ma, Q., Ai, S., (2013). A label-free electrochemical impedance immunosensor based on AuNPs/PAMAM-MWCNT-Chi nanocomposite modified glassy carbon electrode for detection of Salmonella typhimurium in milk. Food Chem 141, 1980-1986.

Flemming, H.-C., Neu, T.R., Wozniak, D.J., (2007). The EPS matrix: the "house of biofilm cells". Journal of bacteriology 189, 7945-7947.

Fraga, D., Meulia, T., Fenster, S., (2008). Real‐Time PCR. Current Protocols Essential Laboratory Techniques, 10.13. 11-10.13. 40.

Garny, K., Neu, T., Horn, H., Volke, F., Manz, B., (2010). Combined application of 13C NMR spectroscopy and confocal laser scanning microscopy—Investigation on biofilm structure and physico-chemical properties. Chemical Engineering Science 65, 4691-4700.

Guilbaud, M., de Coppet, P., Bourion, F., Rachman, C., Prevost, H., Dousset, X., (2005). Quantitative detection of Listeria monocytogenes in biofilms by real-time PCR. Applied and Environmental Microbiology 71, 2190-2194.

Hernández-Gayosso, M.J., Zavala-Olivares, G., Ruiz-Ordaz, N., García-Esquivel, R., Mora-Mendoza, J.L., (2004). Microbial consortium influence upon steel corrosion rate, using the electrochemical impedance spectroscopy technique. Materials and Corrosion 55, 676-683.

ITRAMHIGIENE, retrieved on 7/6, 2015, from http://www.itramhigiene.com/en/biofilms.aspx

Jahid, I.K., Ha, S.-D., (2012). A review of microbial biofilms of produce: Future challenge to food safety. Food Science and Biotechnology 21, 299-316.

Janknecht, P., Melo, L.F., (2003). Online biofilm monitoring. Reviews in Environmental Science and Biotechnology 2, 269-283.

Juhna, T., Birzniece, D., Larsson, S., Zulenkovs, D., Sharipo, A., Azevedo, N.F., Menard-Szczebara, F., Castagnet, S., Feliers, C., Keevil, C.W., (2007). Detection of *Escherichia coli* in biofilms from pipe samples and coupons in drinking water distribution networks. Applied and Environmental Microbiology 73, 7456-7464.

Keevil, C., (2003). Rapid detection of biofilms and adherent pathogens using scanning confocal laser microscopy and episcopic differential interference contrast microscopy. Water Science & Technology 47, 105-116.

Kim, H., Ryu, J.-H., Beuchat, L.R., (2006). Attachment of and biofilm formation by *Enterobacter sakazakii* on stainless steel and enteral feeding tubes. Applied and Environmental Microbiology 72, 5846-5856.

Kim, S., Yu, G., Kim, T., Shin, K., Yoon, J., (2012). Rapid bacterial detection with an interdigitated array electrode by electrochemical impedance spectroscopy. Electrochimica Acta 82, 126-131.

Kim, T., Kang, J., Lee, J.H., Yoon, J., (2011). Influence of attached bacteria and biofilm on double-layer capacitance during biofilm monitoring by electrochemical impedance spectroscopy. Water Res 45, 4615-4622.

Kobayashi, H., Oethinger, M., Tuohy, M.J., Procop, G.W., Bauer, T.W., (2009). Improved detection of biofilm-formative bacteria by vortexing and sonication: a pilot study. Clinical

Orthopaedics and Related Research 467, 1360-1364.

Kujundzic, E., Cristina Fonseca, A., Evans, E.A., Peterson, M., Greenberg, A.R., Hernandez, M., (2007). Ultrasonic monitoring of earlystage biofilm growth on polymeric surfaces. Journal of Microbiological Methods 68, 458-467.

Linke, S., Lenz, J., Gemein, S., Exner, M., Gebel, J., (2010). Detection of *Helicobacter pylori* in biofilms by real-time PCR. International Journal of Hygiene and Environmental Health 213, 176-182.

Lu, L., Chee, G., Yamada, K., Jun, S., (2013). Electrochemical impedance spectroscopic technique with a functionalized microwire sensor for rapid detection of foodborne pathogens. Biosens Bioelectron 42, 492-495.

Meerpoel, L., Van Der Flaas, M.A.J., Van der Veken, L.J.E., Heeres, J., (2002). Biocidal benzylbiphenyl derivatives. Google Patents.

Muñoz-Berbel, X., García-Aljaro, C., Muñoz, F.J., (2008). Impedimetric approach for monitoring the formation of biofilms on metallic surfaces and the subsequent application to the detection of bacteriophages. Electrochimica Acta 53, 5739-5744.

Munoz-Berbel, X., Vigues, N., Jenkins, A.T., Mas, J., Munoz, F.J., (2008). Impedimetric approach for quantifying low bacteria concentrations based on the changes produced in the electrode-solution interface during the pre-attachment stage. Biosens Bioelectron 23, 1540-1546.

Muñoz-Berbel, X., Vigués, N., Mas, J., Jenkins, A.T.A., Muñoz, F.J., (2007). Impedimetric characterization of the changes produced in the electrode–solution interface by bacterial attachment. Electrochemistry Communications 9, 2654-2660.

Nandakumar, V., La Belle, J.T., Reed, J., Shah, M., Cochran, D., Joshi, L., Alford, T.L., (2008). A methodology for rapid detection of *Salmonella* Typhimurium using label-free electrochemical

impedance spectroscopy. Biosens Bioelectron 24, 1045-1048.

Orazem, M.E., Tribollet, B., (2011). *Electrochemical impedance spectroscopy*. John Wiley & Sons.

Paddock, S.W., (1999). Confocal laser scanning microscopy. Biotechniques 27, 992-1007.

Paredes, J., Becerro, S., Arana, S., (2014a). Comparison of real time impedance monitoring of bacterial biofilm cultures in different experimental setups mimicking real field environments. Sensors and Actuators B: Chemical 195, 667-676.

Paredes, J., Becerro, S., Arana, S., (2014b). Label-free interdigitated microelectrode based biosensors for bacterial biofilm growth monitoring using Petri dishes. J Microbiol Methods 100, 77-83.

Paredes, J., Becerro, S., Arizti, F., Aguinaga, A., Del Pozo, J.L., Arana, S., (2012). Real time monitoring of the impedance characteristics of *Staphylococcal* bacterial biofilm cultures with a modified CDC reactor system. Biosens Bioelectron 38, 226-232.

Paredes, J., Becerro, S., Arizti, F., Aguinaga, A., Del Pozo, J.L., Arana, S., (2013). Interdigitated microelectrode biosensor for bacterial biofilm growth monitoring by impedance spectroscopy technique in 96-well microtiter plates. Sensors and Actuators B: Chemical 178, 663-670.

PI, retrieved on 7/6, 2015, from http://www.processinstruments.co.uk/products/water-analysers/biofilm-monitor/

Pires, L., Sachsenheimer, K., Kleintschek, T., Waldbaur, A., Schwartz, T., Rapp, B.E., (2013). Online monitoring of biofilm growth and activity using a combined multi-channel impedimetric and amperometric sensor. Biosens Bioelectron 47, 157-163.

Potera, C., (1999). Forging a link between biofilms and disease. Science 283, 1837-1839.

Pulcini, E., (2001). Bacterial biofilms: a review of current research. Nephrologie 22, 439-441.

Randviir, E.P., Banks, C.E., (2013). Electrochemical impedance spectroscopy: an overview of bioanalytical applications. Analytical Methods 5, 1098-1115.

REALCO, retrieved on 7/6, 2015, from http://blog.realco.be/realcos-biofilm-detection-kit/

Reipa, V., Almeida, J., Cole, K.D., (2006). Long-term monitoring of biofilm growth and disinfection using a quartz crystal microbalance and reflectance measurements. J Microbiol Methods 66, 449-459.

Ruan, C., Yang, L., Li, Y., (2002). Immunobiosensor chips for detection of *Escherichia coli* O157: H7 using electrochemical impedance spectroscopy. Analytical Chemistry 74, 4814-4820.

Saravanan, V., Sreekrishnan, T., (2006). Modelling anaerobic biofilm reactors—A review. Journal of Environmental Management 81, 1-18.

Scallan, E., Hoekstra, R.M., Angulo, F.J., Tauxe, R.V., Widdowson, M.-A., Roy, S.L., Jones, J.L., Griffin, P.M., (2011). Foodborne illness acquired in the United States—major pathogens. Emerg Infect Dis 17.

Schofield, A.L., Rudd, T.R., Martin, D.S., Fernig, D.G., Edwards, C., (2007). Real-time monitoring of the development and stability of biofilms of *Streptococcus mutans* using the quartz crystal microbalance with dissipation monitoring. Biosens Bioelectron 23, 407-413.

Schwartz, T., Kalmbach, S., Hoffmann, S., Szewzyk, U., Obst, U., (1998). PCR-based detection of mycobacteria in biofilms from a drinking water distribution system. Journal of Microbiological Methods 34, 113-123.

Schwartz, T., Kohnen, W., Jansen, B., Obst, U., (2003). Detection of antibiotic-resistant bacteria and their resistance genes in wastewater, surface water, and drinking water biofilms. Fems Microbiology Ecology 43, 325-335.

Shi, X., Zhu, X., (2009). Biofilm formation and food safety in food industries. Trends in Food

Science & Technology 20, 407-413.

Sim, S., Suwarno, S., Chong, T., Krantz, W.B., Fane, A.G., (2013). Monitoring membrane biofouling via ultrasonic time-domain reflectometry enhanced by silica dosing. Journal of Membrane Science 428, 24-37.

Simões, M., Simões, L.C., Vieira, M.J., (2010). A review of current and emergent biofilm control strategies. LWT-Food Science and Technology 43, 573-583.

Srey, S., Jahid, I.K., Ha, S.-D., (2013). Biofilm formation in food industries: A food safety concern. Food Control 31, 572-585.

Standard, A., (2005). Standard specification for chemical passivation treatments for stainless steel parts. ASTM International A 967 - 05, 7.

Stepanović, S., Ćirković, I., Ranin, L., (2004). Biofilm formation by Salmonella spp. and Listeria monocytogenes on plastic surface. Letters in Applied Microbiology 38, 428-432.

Swaminathan, B., Feng, P., (1994). Rapid Detection of Food-Borne Pathogenic Bacteria. Annual Review of Microbiology 48, 401-426.

Van Houdt, R., Michiels, C.W., (2010). Biofilm formation and the food industry, a focus on the bacterial outer surface. Journal of Applied Microbiology 109, 1117-1131.

Varshney, M., Li, Y., (2008). Double interdigitated array microelectrode-based impedance biosensor for detection of viable *Escherichia coli* O157:H7 in growth medium. Talanta 74, 518-525.

Varshney, M., Li, Y., Srinivasan, B., Tung, S., (2007). A label-free, microfluidics and interdigitated array microelectrode-based impedance biosensor in combination with nanoparticles immunoseparation for detection of *Escherichia coli* O157:H7 in food samples. Sensors and Actuators B: Chemical 128, 99-107.

Wagner, M., Ivleva, N.P., Haisch, C., Niessner, R., Horn, H., (2009). Combined use of confocal laser scanning microscopy (CLSM) and Raman microscopy (RM): investigations on EPS–matrix. Water research 43, 63-76.

Ward, A.C., Connolly, P., Tucker, N.P., (2014). *Pseudomonas aeruginosa* can be detected in a polymicrobial competition model using impedance spectroscopy with a novel biosensor. PLoS One 9, e91732.

Warner, J., Rothwell, S., Keevil, C., (2008). Use of episcopic differential interference contrast microscopy to identify bacterial biofilms on salad leaves and track colonization by *Salmonella* Thompson. Environmental microbiology 10, 918-925.

Yang, L., (2008). Electrical impedance spectroscopy for detection of bacterial cells in suspensions using interdigitated microelectrodes. Talanta 74, 1621-1629.

Yang, L., Bashir, R., (2008). Electrical/electrochemical impedance for rapid detection of foodborne pathogenic bacteria. Biotechnology Advances 26, 135-150.

Yang, L., Li, Y., Erf, G.F., (2004a). Interdigitated Array Microelectrode-Based Electrochemical Impedance Immunosensor for Detection of *Escherichia coli* O157: H7. Analytical Chemistry 76, 1107-1113.

Yang, L., Li, Y., Griffis, C.L., Johnson, M.G., (2004b). Interdigitated microelectrode (IME) impedance sensor for the detection of viable *Salmonella* Typhimurium. Biosensors and Bioelectronics 19, 1139-1147.

Zwietering, M., Jongenburger, I., Rombouts, F., Van't Riet, K., (1990). Modeling of the bacterial growth curve. Applied and Environmental Microbiology 56, 1875-1881.

APPENDICES

A. LabVIEW Program

This LabVIEW program was designed under the guidance of Dr. Reyes, and the syringe pump program was modified from the example downloaded from National Instruments website.

1. Whole System Front Panel

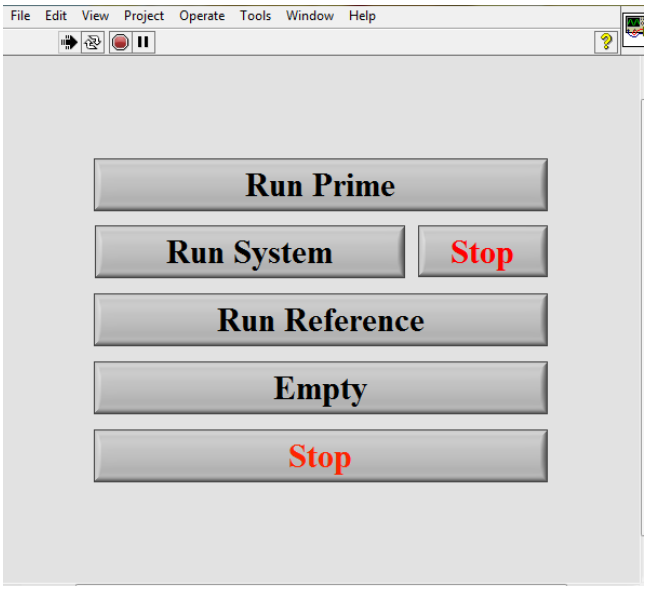

2. “Prime”

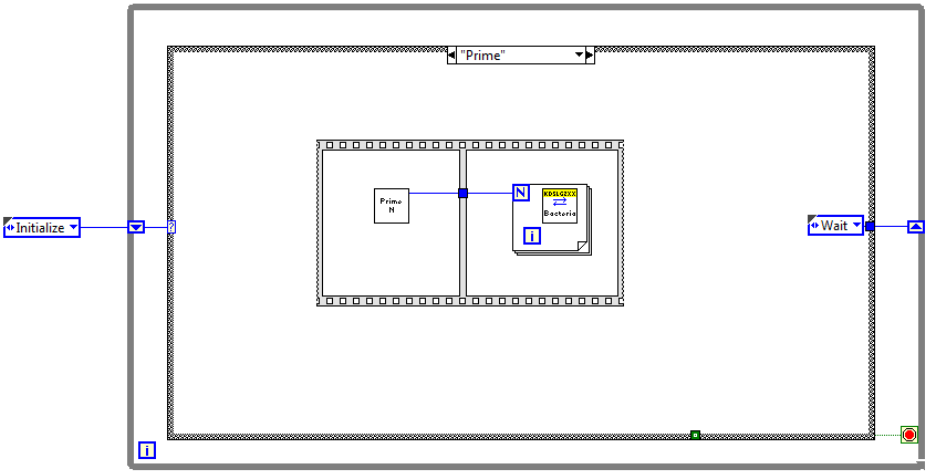

Icon Front Panel

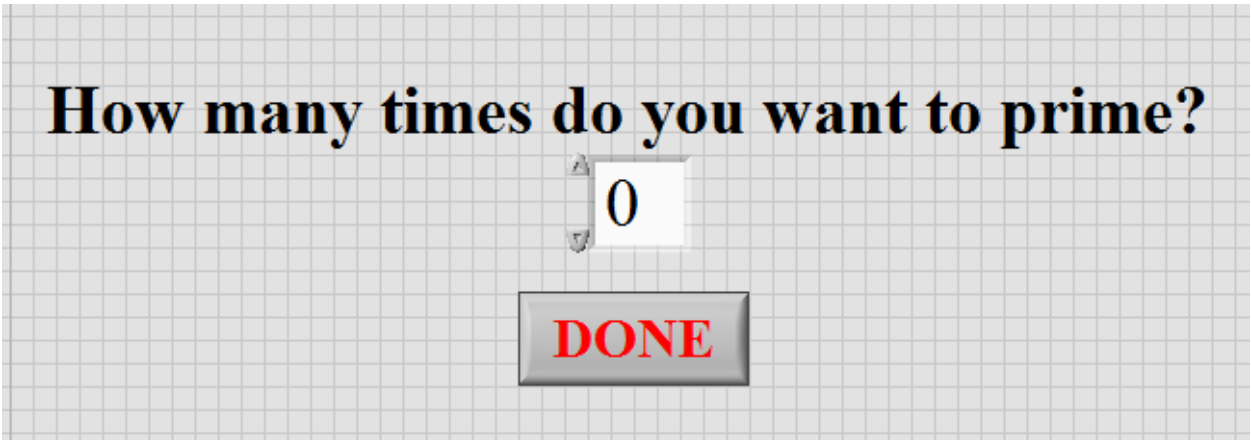

Icon Block Diagram

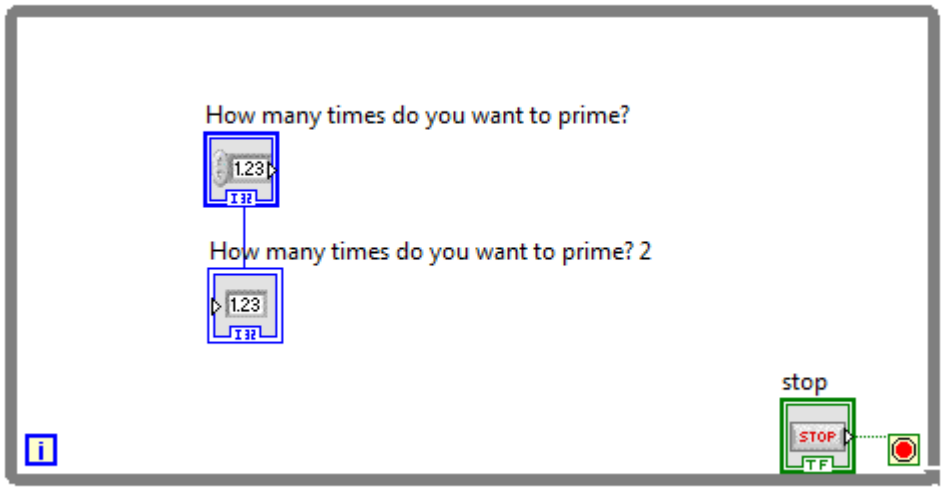

Icon Front Panel

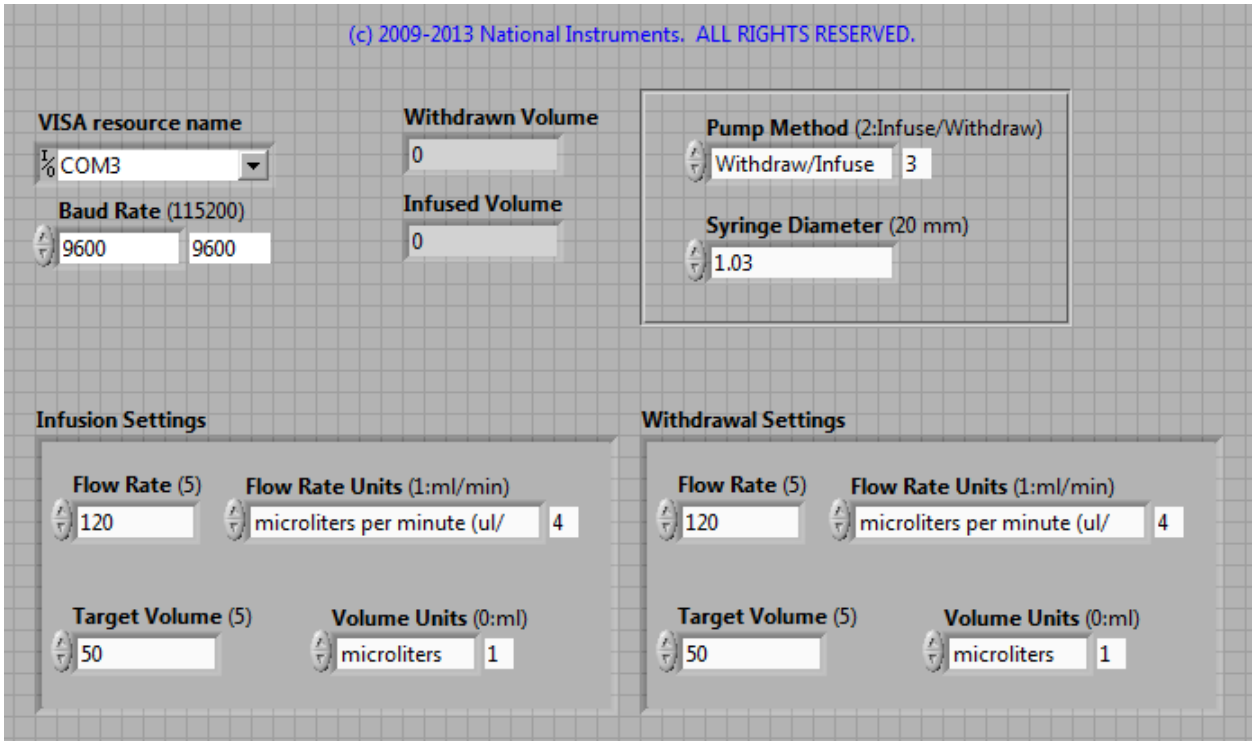

Icon Block Diagram

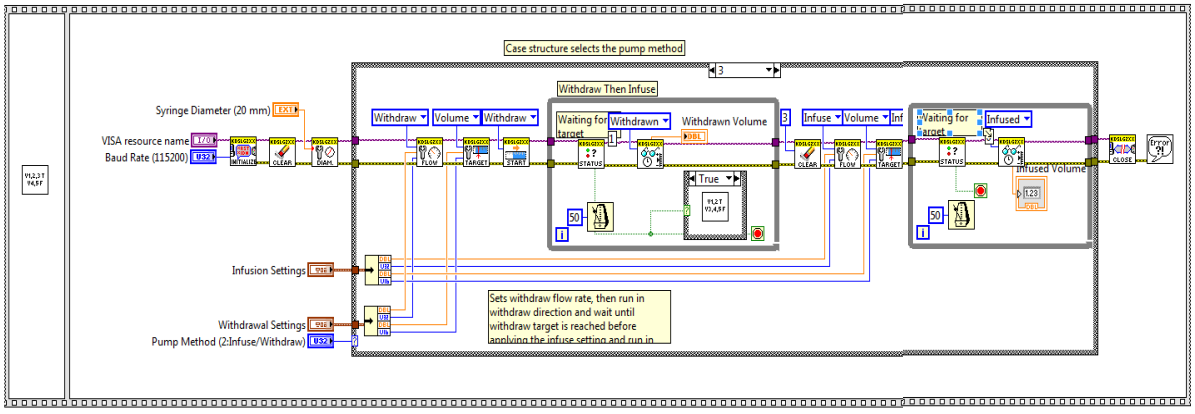

3. “Run System”

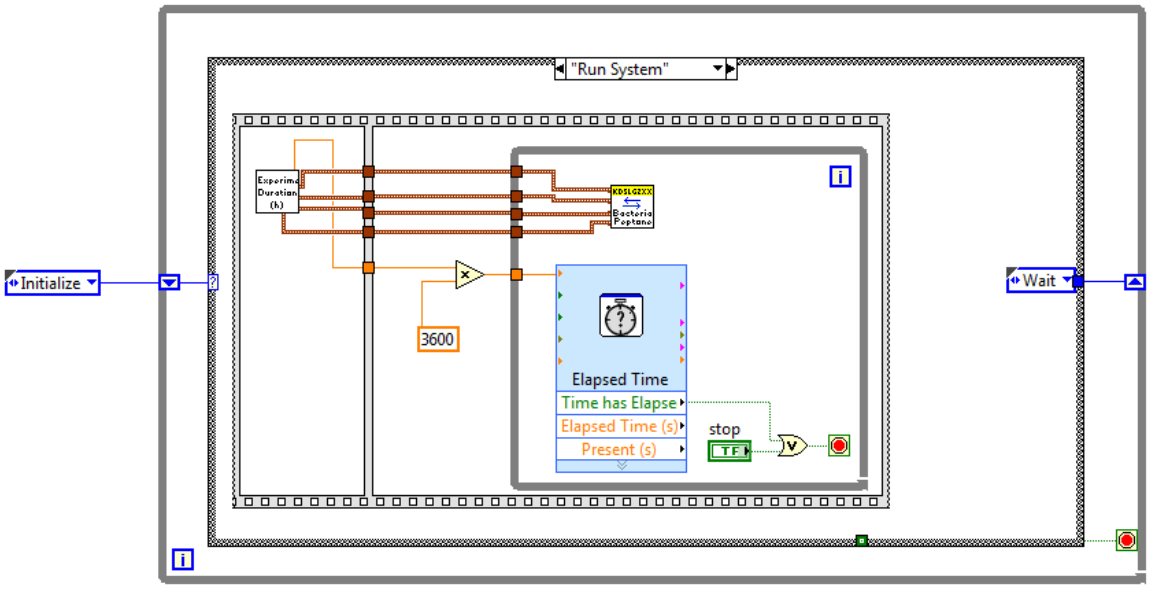
"Run System"
Initialize
Wait
3600
Elapsed Time
Time has Elapse
Elapsed Time (s)
Present (s)
stop
TF

Icon Front Panel

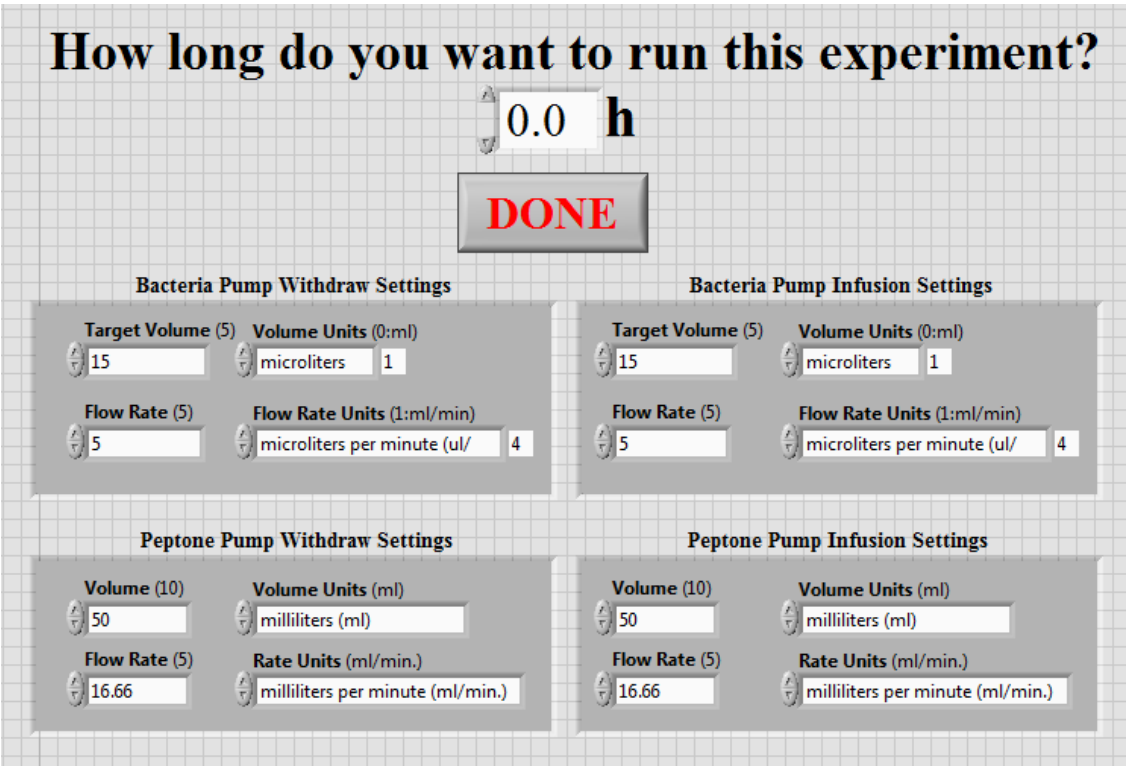

Icon Block Diagram

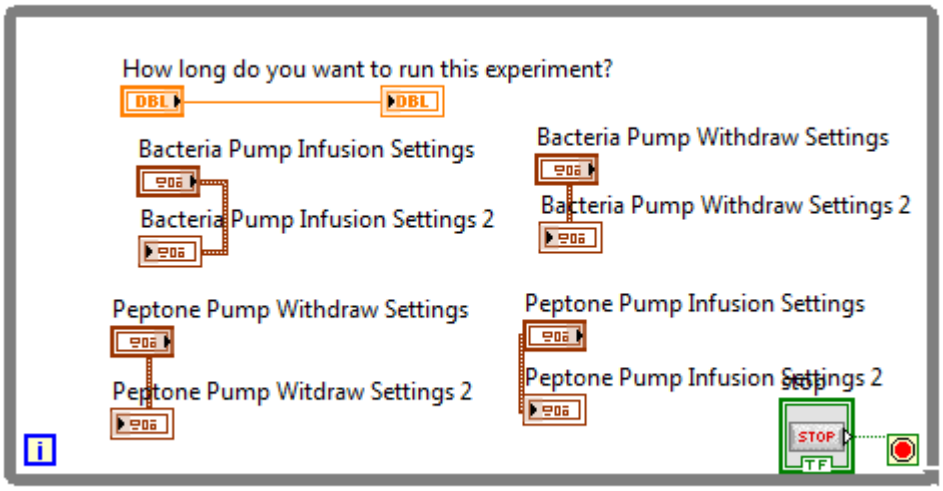

Icon Front Panel

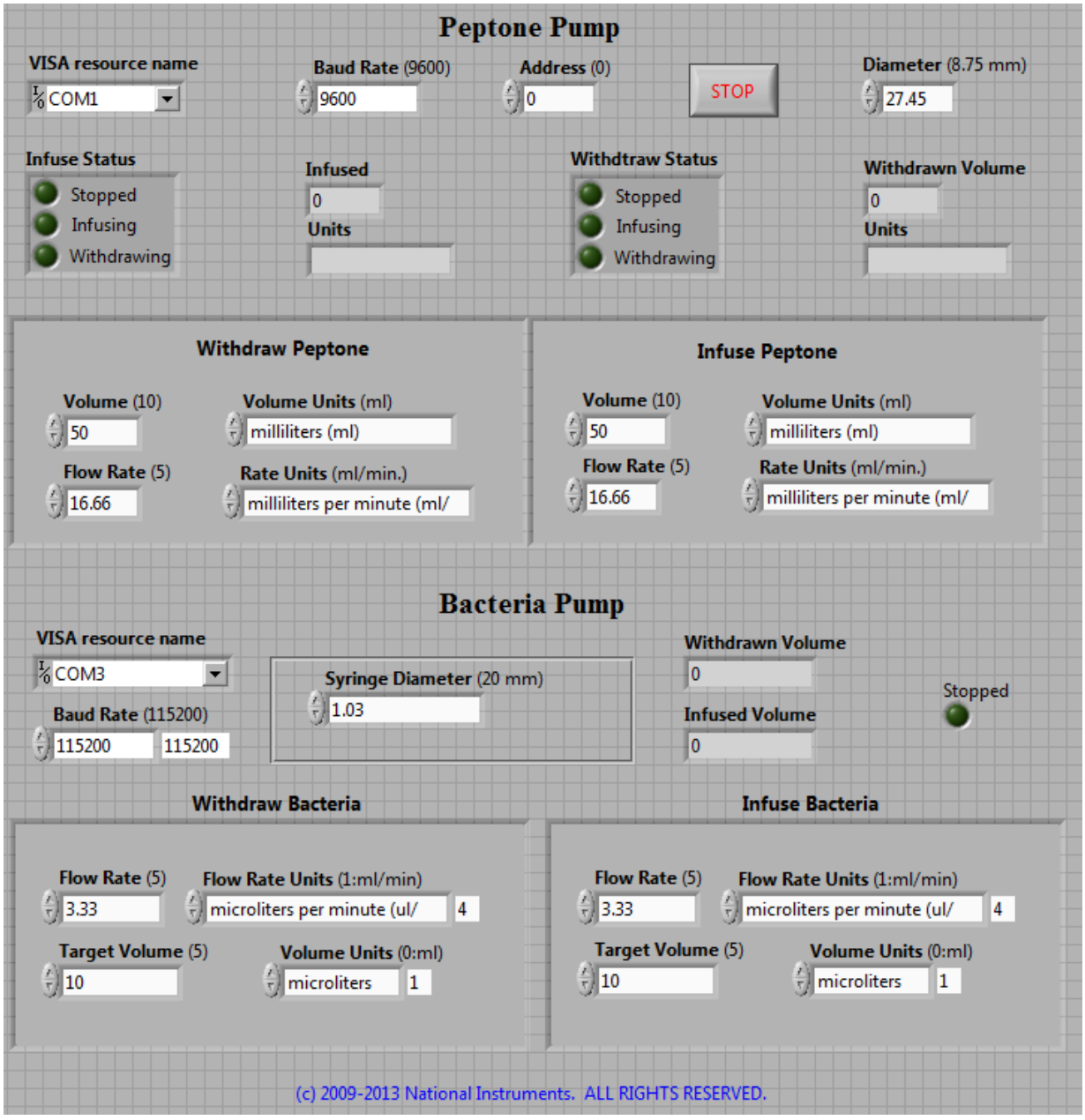

Icon Block Diagram

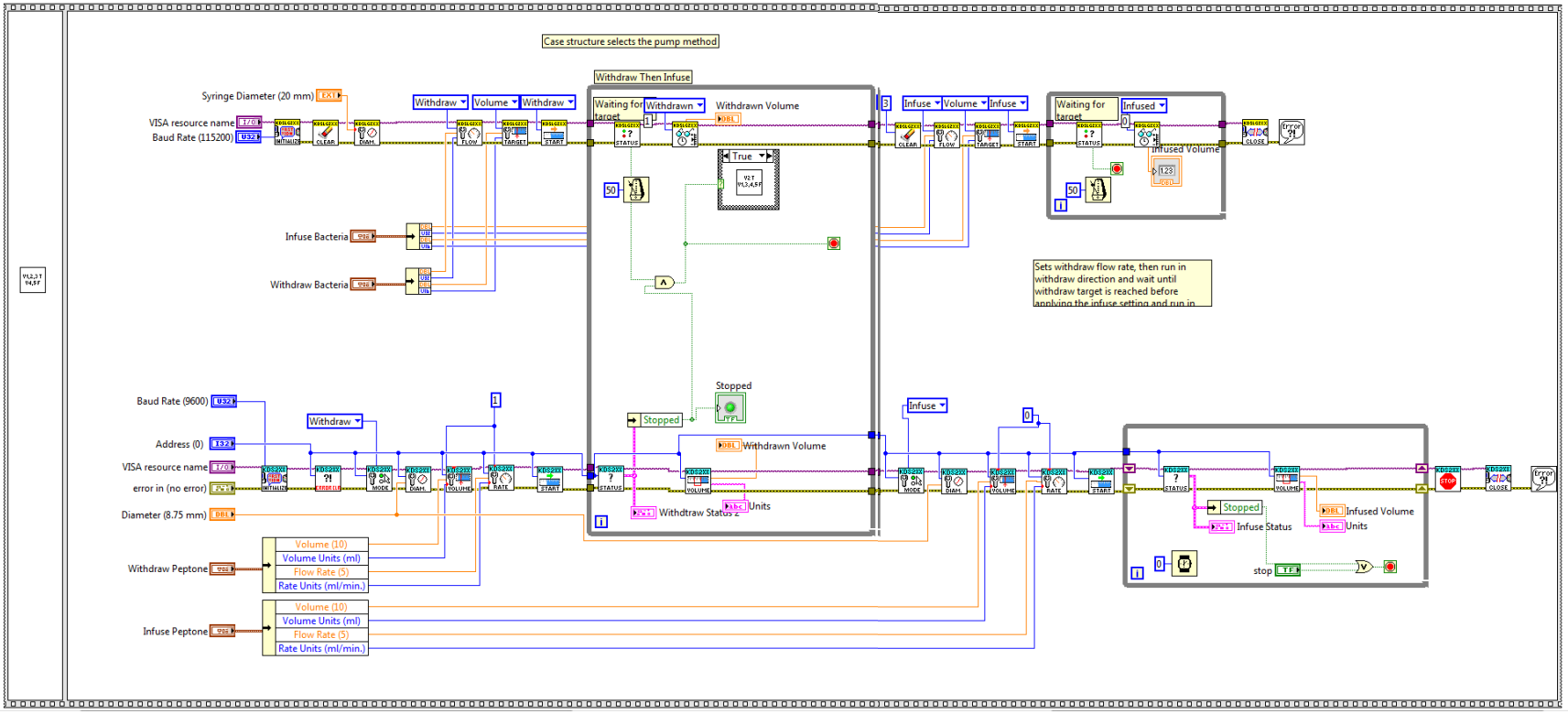

4. “Run Reference”

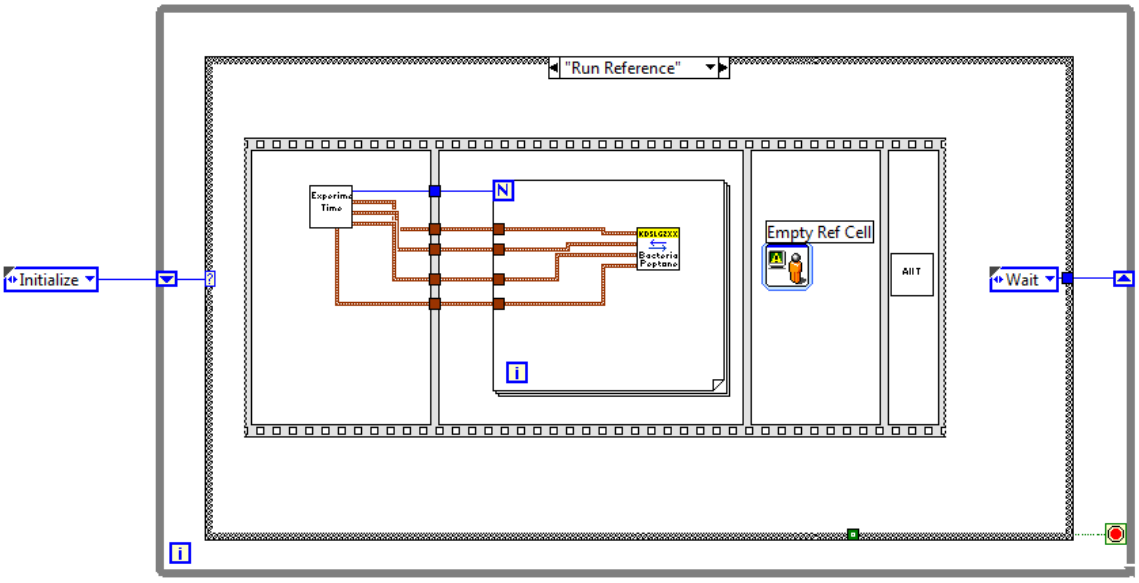

Icon Front Panel

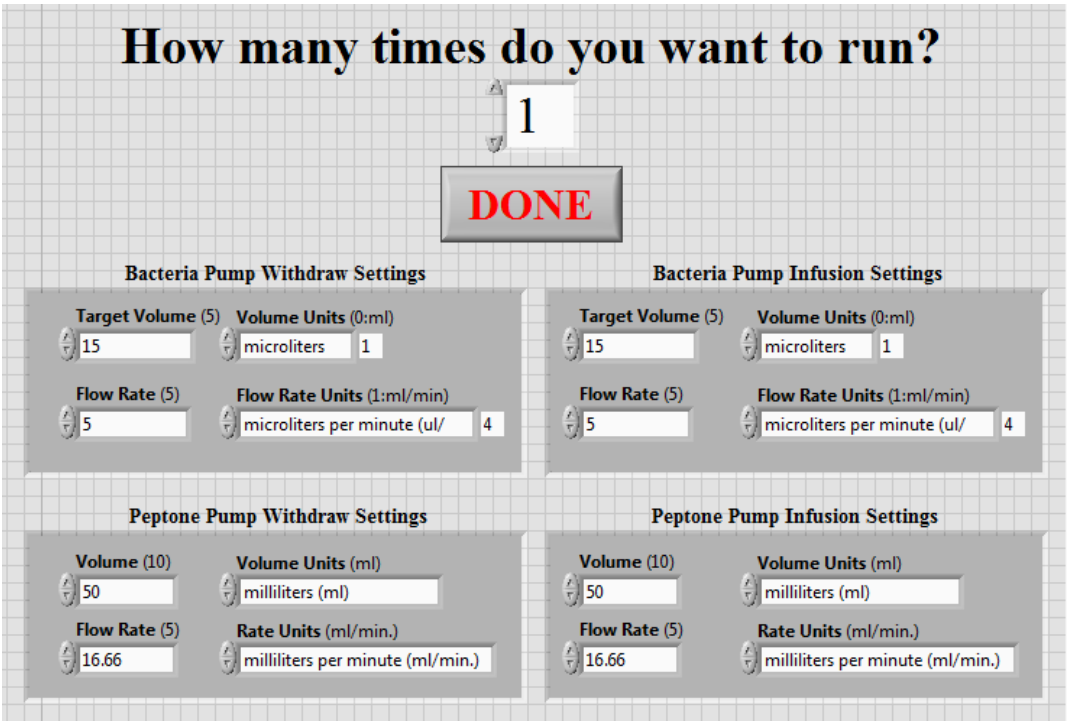

Icon Block Diagram

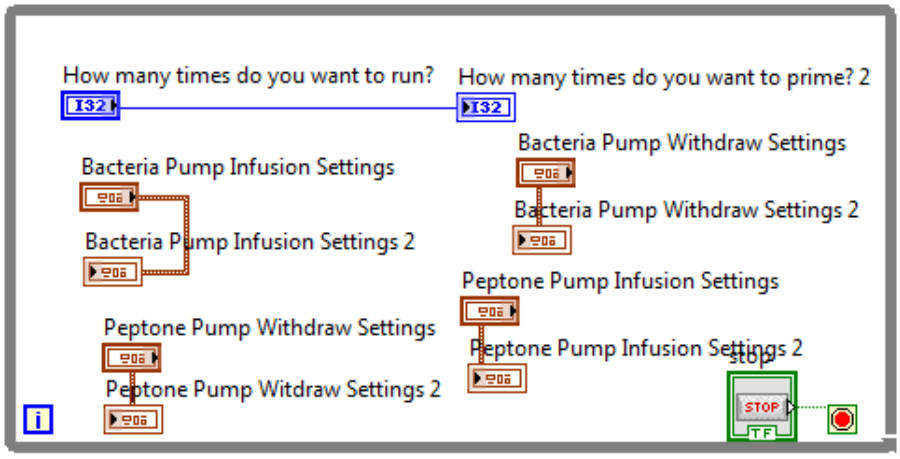

Icon Front Panel

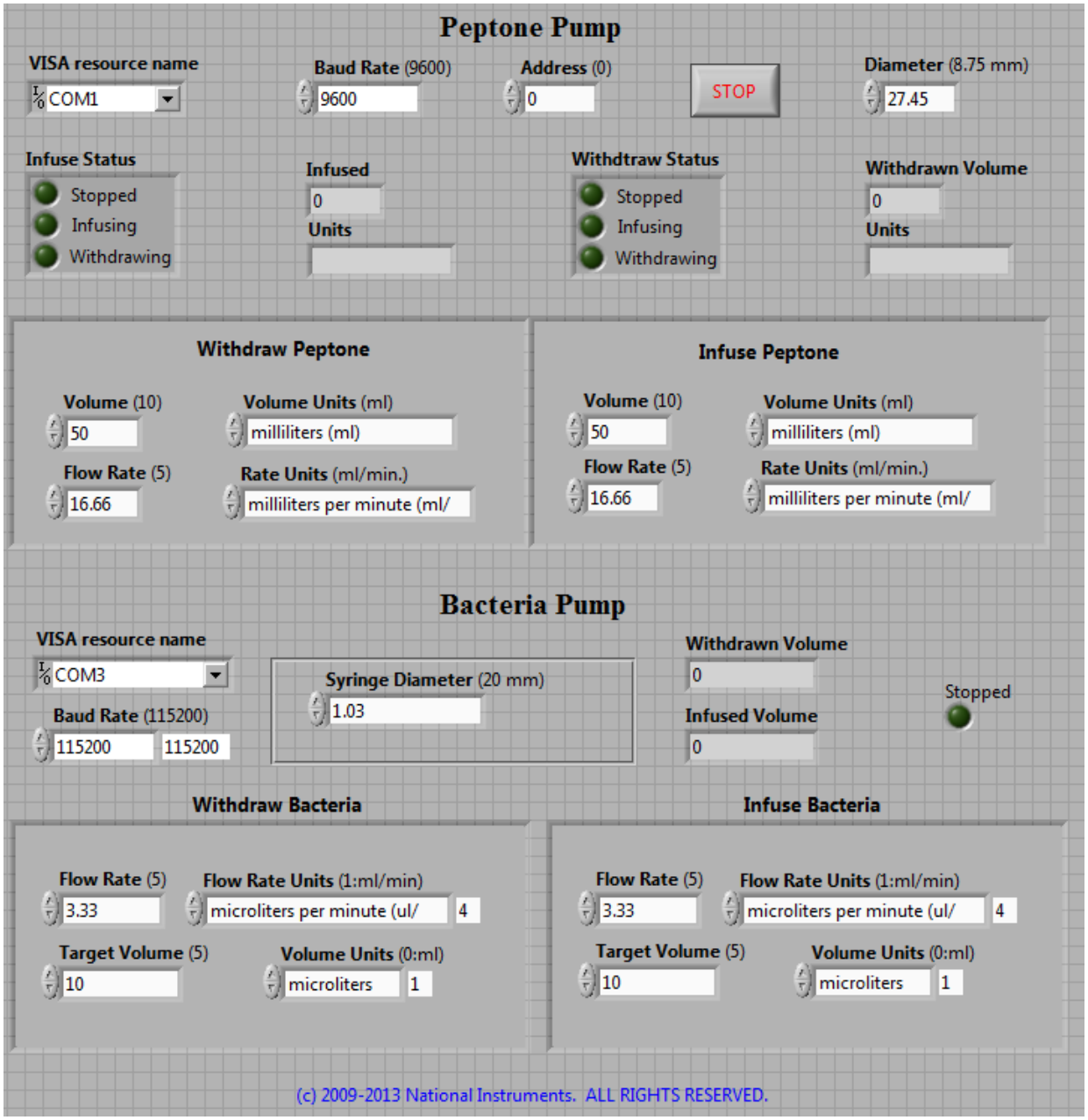

Icon Block Diagram

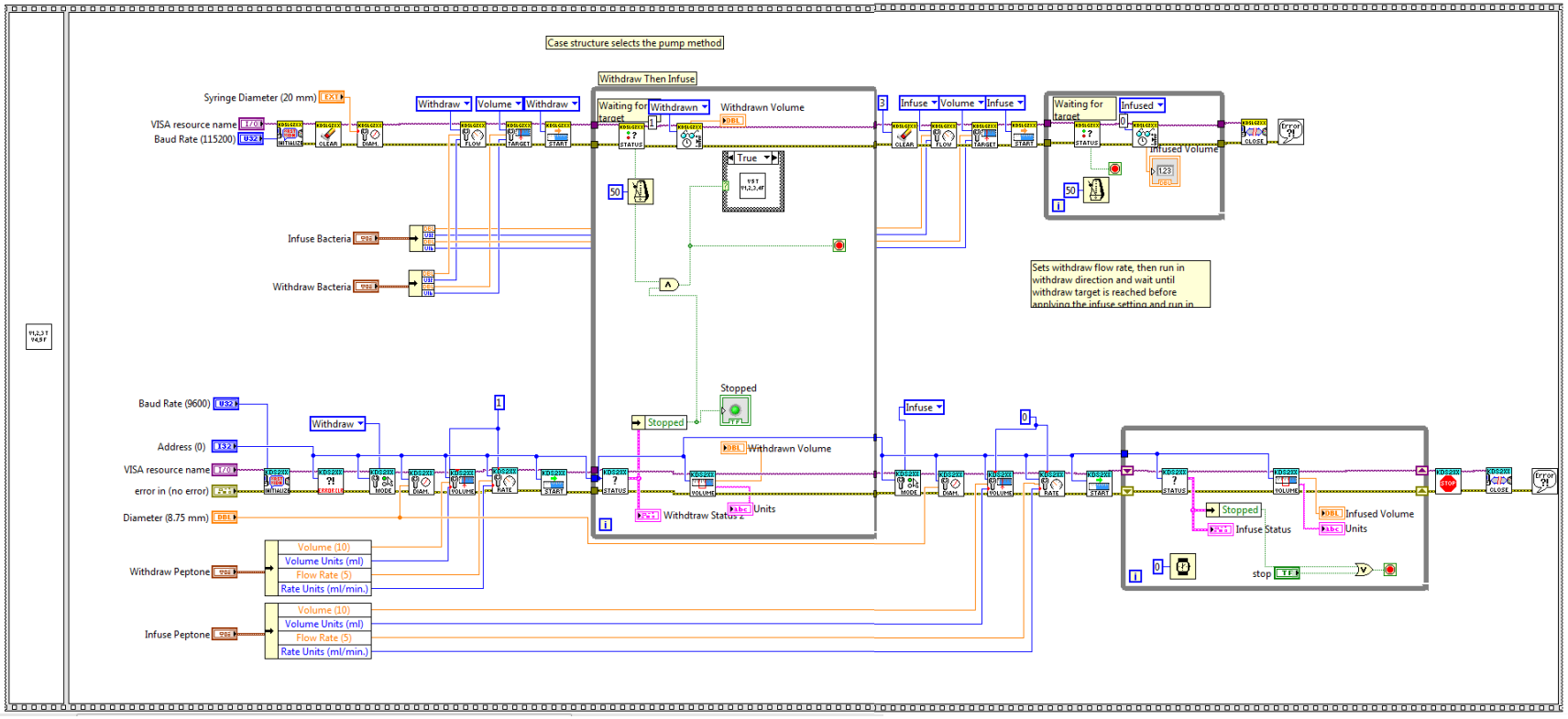

5. “Empty”

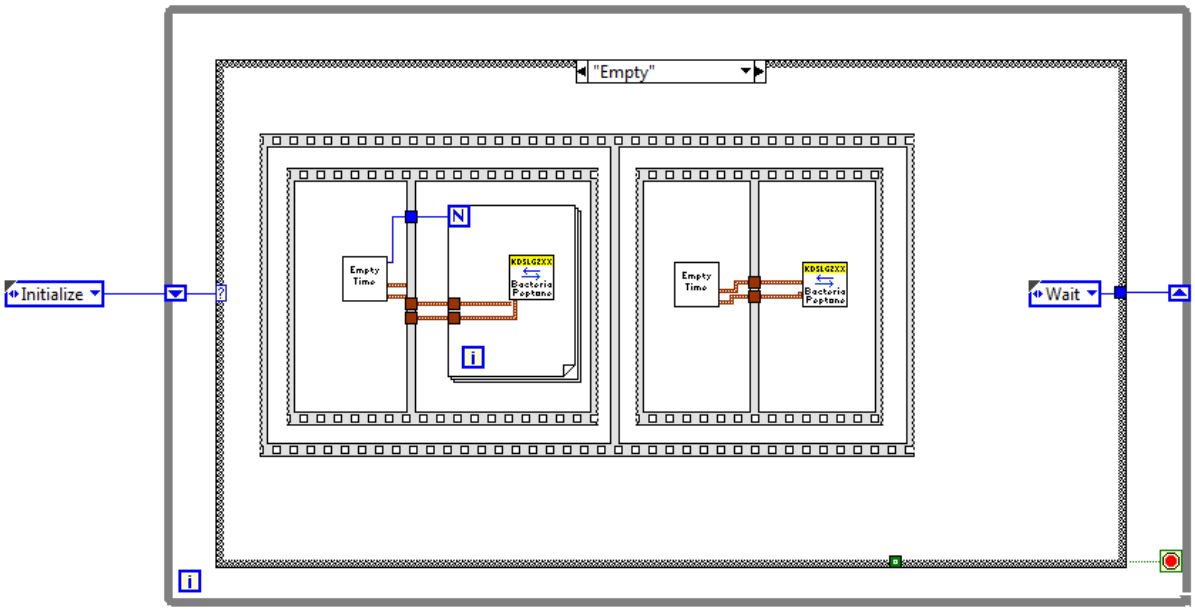
"Empty"
Initialize
Wait
Empty Time
KDSLGEXX
Bacteria Peptone
N
i

Icon Front Panel

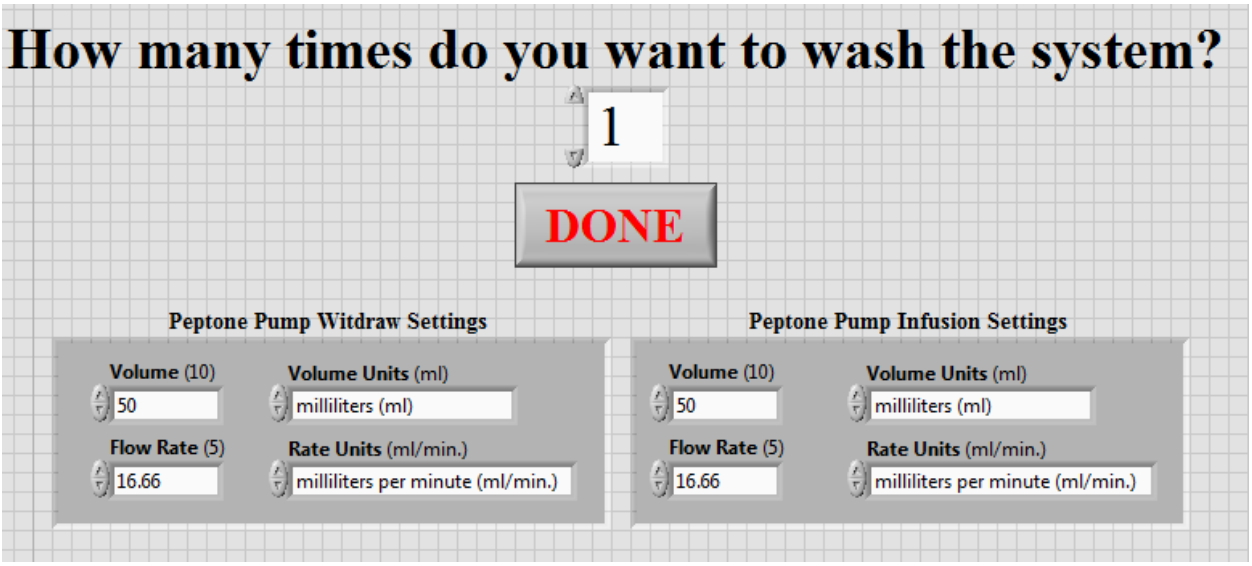

Icon Block Diagram

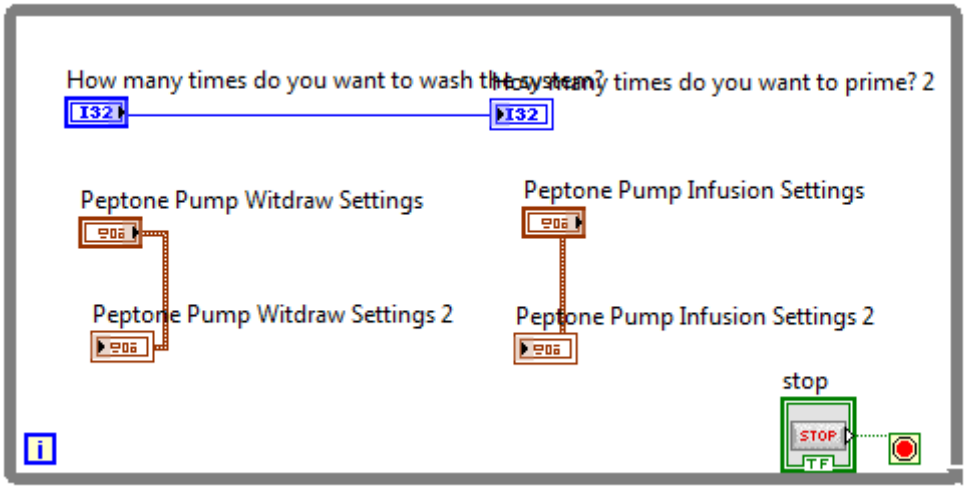

Icon Front Panel

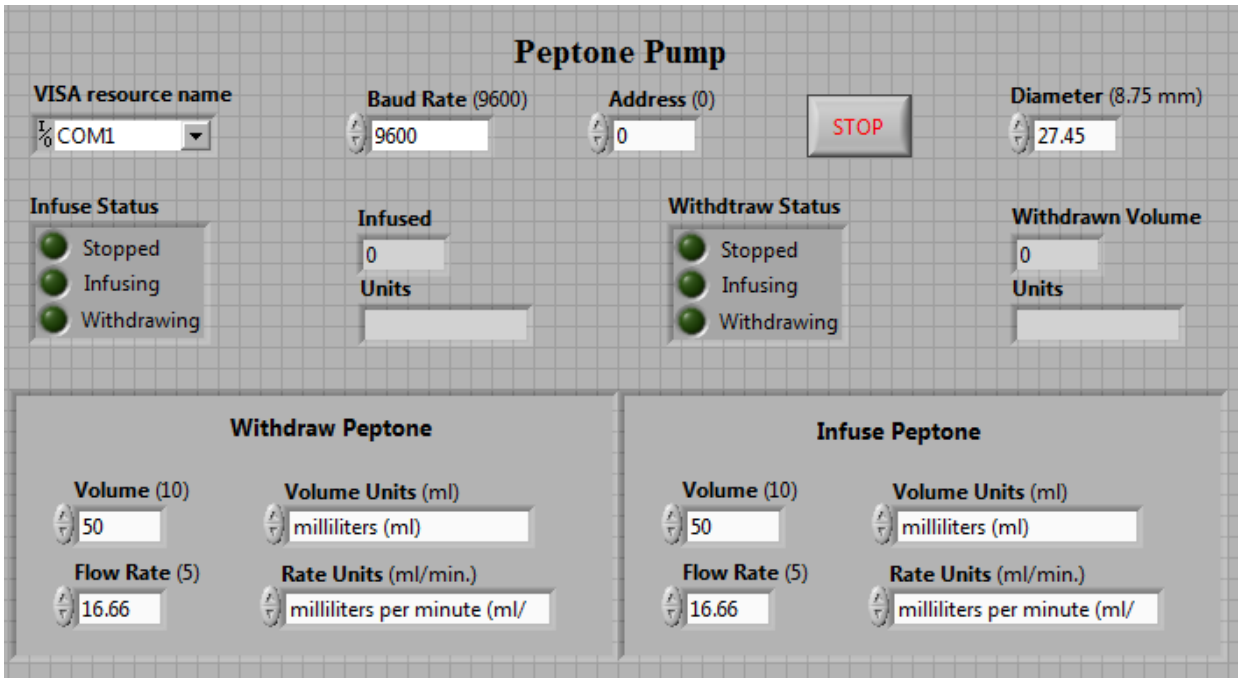

Icon Block Diagram

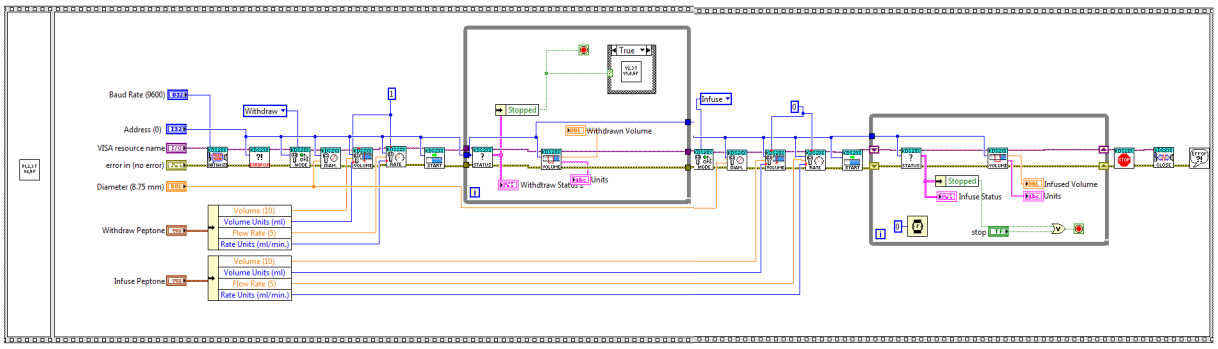

Icon Front Panel

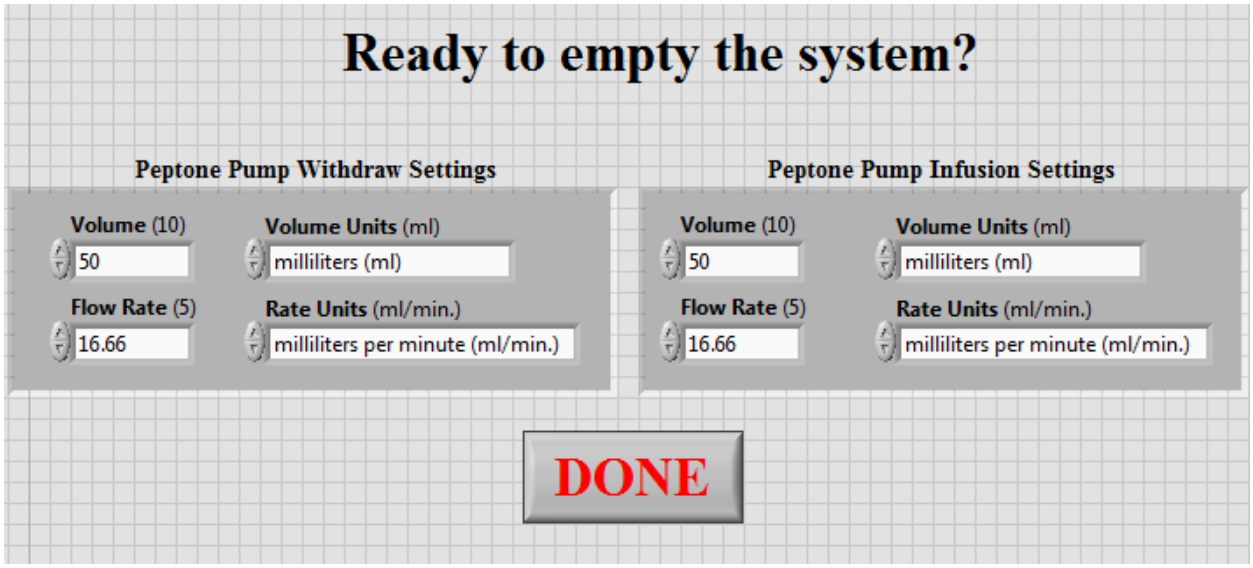

Icon Block Diagram

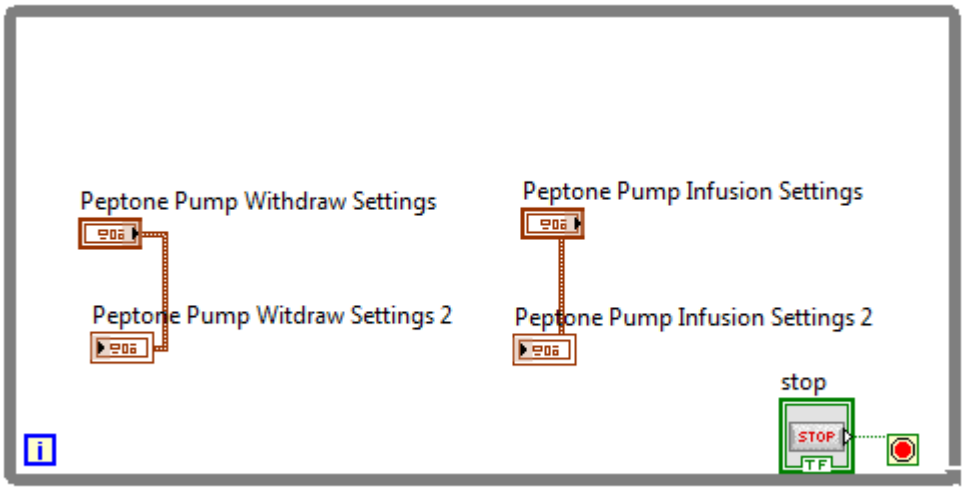

Icon Front Panel

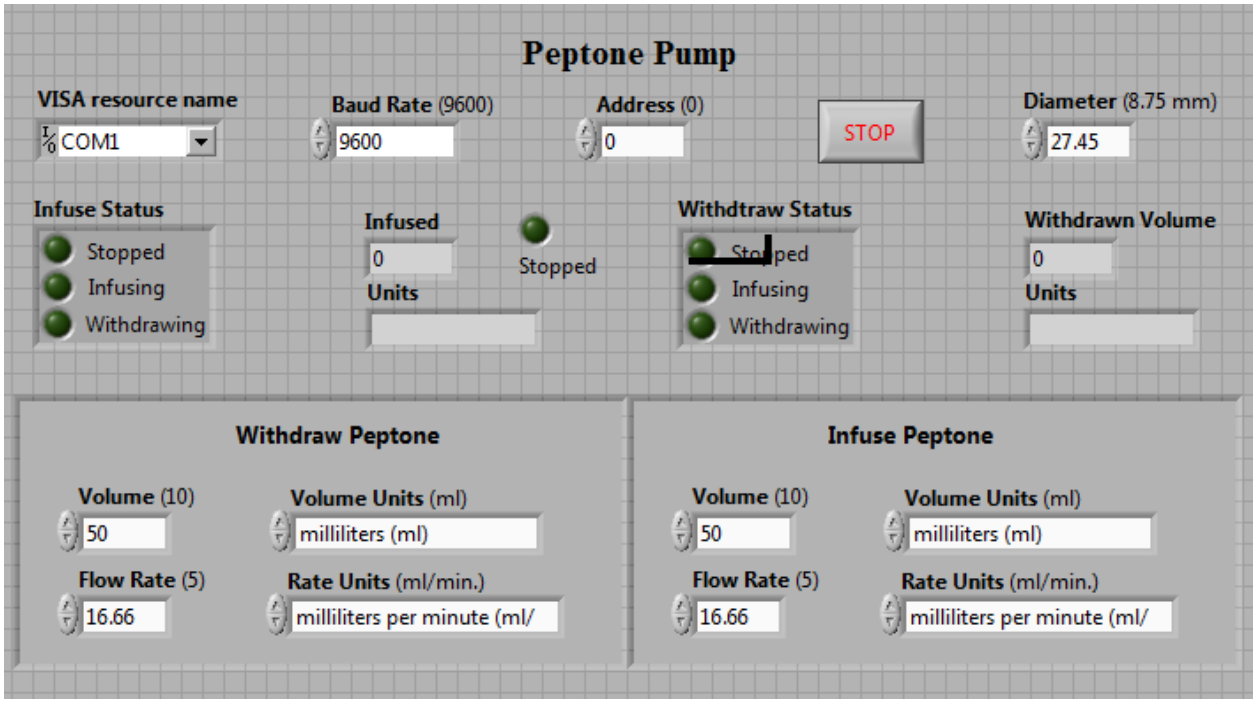

Icon Block Diagram

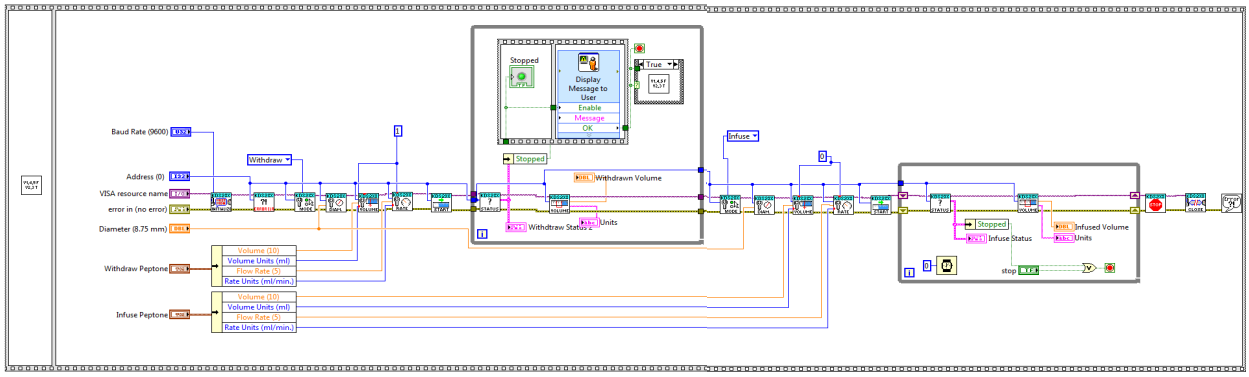

6. “Stop”

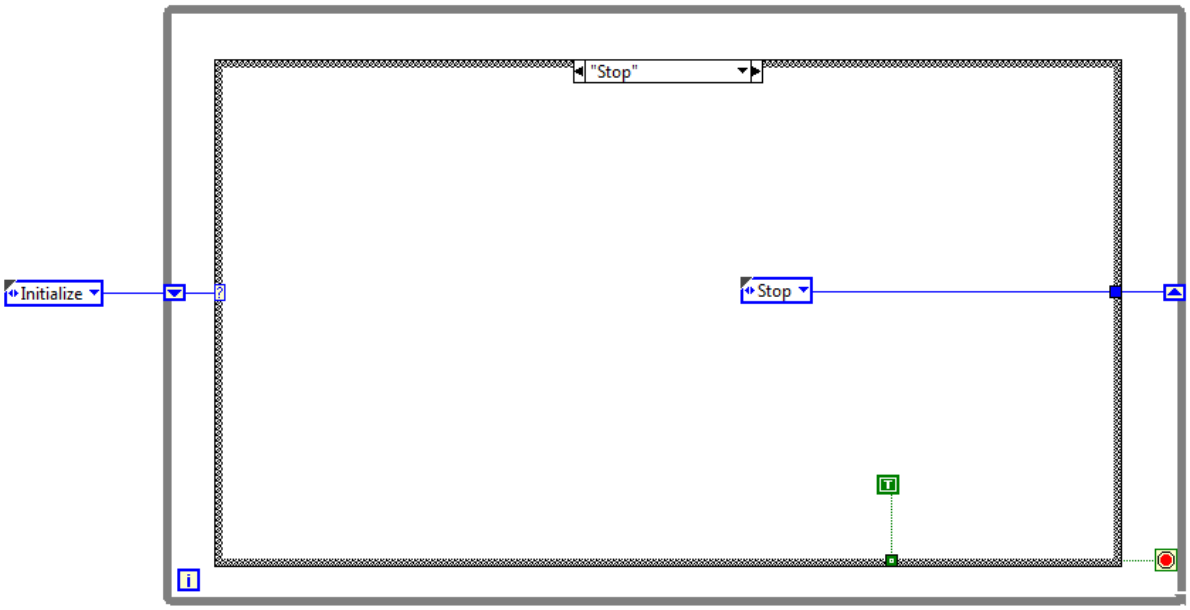
"Stop"
Initialize
Stop

7. “Wait”

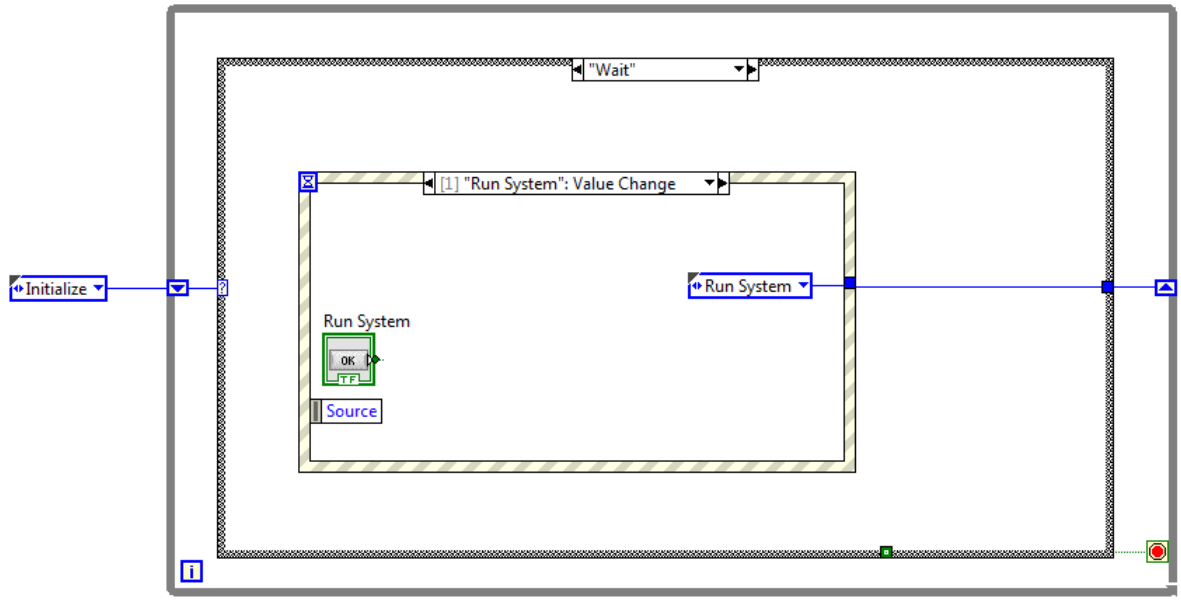
"Wait"
[1] "Run System": Value Change
Initialize
Run System
Run System
OK
TF
Source

B. Experiment Timeline

72 h Experiment Plan (Test Every Four Hours)

Time	Day 0	Day 1	Day 2	Day 3	Day 4	Day 5
12:30			Ref Cell Preparation (4)			
1:30			Test 5	Test 11	Test 17	
2:30						
3:30						
4:30						
5:30			Test 6	Test 12	Test 18	
6:30		Lab Preparation				
7:30	Bacteria Innoculation	System Assmbling				
8:30	Reference Electrode Checking	Peptone Testing & Prime				
9:30	EIS Calibration	Test 1	Test 7	Test 13	Test 19	
10:30	System Autoclaving		Peptone Water Changing	Peptone Water Changing	Autoclave Waste and Clean the System	
11:30						
12:30						
13:30		Test 2	Test 8	Test 14		
14:30				Autoclave Waste and Used Ref Cell (5)		
15:30	Materials Needed to Prepare: 371 Plates; 19 Stainless Steel Tubes; 266 9 ml Peptone Water; 19 60 ml Peptone Water; One Bottle Steriled DI Water; 4 Carboy Peptone Water (13 L Each); 19 Washing Tubes Set			Ref Cell Preparation (5)		
16:30						
17:30		Test 3	Test 9	Test 15		
18:30			Autoclave Waste and Used Ref Cell (5)			
19:30			Ref Cell Preparation (5)			
20:30			Day 1 Plate Counting	Day 2 Plate Counting	Day 3 Plate Counting	Day 4 Plate Counting
21:30		Test 4	Test 10	Test 16		
22:30		Autoclave Waste and Used Ref Cell (4) / Peptone Water Changing	Peptone Water Changing	Peptone Water Changing		
23:30						